

The Implementation and Evaluation of Stormwater Control  
Measures in Series

By  
Cara Elizabeth Lyons

A Thesis Submitted to  
Department of Civil and Environmental Engineering  
College of Engineering  
in partial fulfillment of the requirements  
for the degree of

Master of Science in  
Civil Engineering  
May 2013

Villanova University  
Villanova, Pennsylvania

**Copyright © 2013**

Cara Elizabeth Lyons

All Rights Reserved

# The Implementation and Evaluation of Stormwater Control Measures in Series

By

Cara Elizabeth Lyons

---

Robert G. Traver, Ph.D., P.E. , D. WRE Date  
Professor, Department of Civil and Environmental Engineering  
Advisor

---

Bridget Wadzuk, Ph.D. Date  
Associate Professor, Department of Civil and Environmental Engineering  
Advisor

---

Ronald Chadderton, Ph.D., P.E. Date  
Chairman and Professor, Department of Civil and Environmental Engineering

---

Gary A. Gabriele, Ph.D. Date  
Dean, College of Engineering

A copy of this thesis is available for research purposes at Falvey Memorial Library

### Statement by Author

This dissertation has been submitted in partial fulfillment of requirements for an advanced degree at the Villanova University and is deposited in the University Library to be made available to borrowers under rules of the Library.

Brief quotations from this dissertation are allowable without special permission, provided that accurate acknowledgment of source is made. Requests for permission for extended quotation from or reproduction of this manuscript in whole or in part may be granted by the head of the major department or the Associate Dean for Graduate Studies and Research of the College of Engineering when in his or her judgment the proposed use of the material is in the interests of scholarship. In all other instances, however, permission must be obtained from the author.

## **Acknowledgements**

The completion of this thesis would not be possible without the generous support of the Pennsylvania Department of Environmental Protection Growing Greener Grant. The funding provided through this grant allowed for the construction and monitoring of the treatment train. The Villanova Urban Stormwater Partnership has also provided significant support for the success of this project and the Villanova Stormwater Control Research and Demonstration Park. In addition, many thanks are owed to Villanova University Facilities Department for their cooperation in site construction and continued maintenance.

Special thanks to Dr. Robert Traver, Dr. Bridget Wadzuk, and Dr. Andrea Welker for their support and guidance throughout work on this project. I am very grateful for the opportunity provided by these advisors to attend Villanova University and be a part of such a well-established stormwater community. I would also like to thank my fellow graduate students for always lending a hand and helping establish the treatment train.

Finally, I would like to thank my parents. Without their continuous love, support, and sacrifice, I would never have had the opportunities my education has provided.

## **Abstract**

The objective of this research was to evaluate the construction, implementation, and monitoring of stormwater control measures (SCMs) in series. The series of SCMs, known as the Villanova Treatment Train, was constructed in October 2011 and monitoring began in July 2012. There is a need for quantifying the hydrologic and water quality effects of installing SCMs in a series, as they are typically categorized as single entities. The treatment train, which includes a swale, two rain gardens in series, and an infiltration trench, provides a means of studying not only the effects of the entire system, but also the performance of each individual SCM. The treatment train is intended to provide pre-treatment prior to other SCMs to increase longevity and decrease maintenance. The infiltration trench is to be specifically monitored and compared to an infiltration trench nearby for its longevity and maintenance needs.

The treatment train collects water from an adjacent parking deck and was designed for a 2.54 cm (1 in) storm event. Through a quantity analysis including data from the infiltration trench, the system appears to function better than designed; the treatment train captured at least 95% of every storm event analyzed from July 2012 to March 2013. The analysis includes a focus on storm volume, duration, and intensity as it relates to the volume into the treatment train, volume to the infiltration trench, and overflow volume. The analysis includes 30 storm events totaling to 75 cm of rainfall; 668 m<sup>3</sup> of rainfall entered the treatment with approximately 185 m<sup>3</sup> entering the infiltration trench and only 8.5 m<sup>3</sup> of rainfall determined to overflow from the system. Further research will provide insight as to how the individual SCMs perform and what types of rainfall influence the system performance.

## Table of Contents

Acknowledgements.....	i
Abstract .....	ii
List of Tables .....	vi
List of Figures .....	viii
Chapter 1 Introduction.....	1
1.1. Stormwater Control Measures.....	1
1.2. Site Description .....	2
1.3. Climate .....	3
1.4. Research Goals and Objectives .....	7
Chapter 2 Literature Review.....	9
2.1. Treatment Trains in Environmental Engineering.....	9
2.1.1. Traditional WWTP.....	9
2.1.2. Living Machine.....	9
2.2. Stormwater and Treatment Trains.....	10
2.2.1. Current Research and Applications .....	11
2.2.2. State BMP Manuals and SCMs in Series.....	13
2.2.3. Water Environmental Federation and SCMs .....	18
2.3. SCMs as Single Entities .....	19
2.3.1. Swales .....	19
2.3.2. Rain Gardens (Bioinfiltration) .....	21
2.3.3. Infiltration Trenches.....	23
Chapter 3 Site Design and Construction.....	26
3.1. Treatment Train Design .....	26
3.1.1. Weir Box.....	26
3.1.2. Swale.....	30
3.1.3. Rain Gardens.....	31
3.1.4. Infiltration Trench.....	32
3.1.5. Design Summary.....	33
3.2. Construction .....	34
3.2.1. Construction Timeline .....	35
3.2.2. Construction Conclusions .....	46
3.3. Soil Analysis .....	48
Chapter 4 Methods.....	51

4.1.	Instrumentation and Monitoring Equipment .....	51
4.1.1.	Water Level and Flow .....	51
4.1.2.	Instrumentation Success and Challenges .....	62
4.2.	Rainfall .....	63
4.2.1.	Rainfall Measurements .....	63
4.3.	Water Quantity Measurements .....	66
4.3.1.	Infiltration Trench Recession Rate Calculations .....	67
4.3.2.	Infiltration Trench Infiltration Rate Calculations .....	68
4.3.3.	Statistical Analyses .....	68
4.3.4.	Treatment Train Inflow .....	70
4.3.5.	Infiltration Trench Inflow .....	71
4.3.6.	Infiltration Trench Overflow .....	71
4.3.7.	Calculation Examples .....	72
4.3.8.	Old Infiltration Trench .....	78
4.4.	Water Quality Measurements .....	78
4.4.1.	Water Quality Collection Procedures .....	79
4.4.2.	Water Quality Testing Procedures .....	80
Chapter 5	Water Quantity Analysis .....	81
5.1.	Water Quantity Research Goals .....	81
5.2.	Infiltration Trench Data .....	81
5.2.1.	Infiltration Trench Recession Rates .....	82
5.2.2.	Infiltration Trench Infiltration Rates .....	87
5.2.3.	Recession and Infiltration Rates and Temperature .....	91
5.2.4.	Volumes in Treatment Train and Infiltration Trench .....	94
5.2.5.	Infiltration Trench Comparison .....	99
5.2.6.	Infiltration Trench Data Conclusions .....	104
5.3.	Infiltration Trench and the Treatment Train Performance .....	105
5.3.1.	Rainfall Data .....	105
5.3.2.	Infiltration Trench Overflow .....	110
5.3.3.	Treatment Train Performance and Rainfall .....	115
5.4.	Summary and Recommendations .....	120
Chapter 6	Summary and Future Research .....	122
6.1.	Project Summary .....	122
6.2.	Future Research .....	123

6.2.1. Water Quantity Future Research.....	123
6.2.2. Water Quality Future Research.....	125
6.2.3. Longevity and Maintenance.....	125
References.....	127
Appendices.....	132
Appendix A: Construction Cost Breakdown .....	132
Appendix B: Plant List.....	133
Appendix C: Unused Survey Data.....	134
Appendix D-1: CR1000 Programming Code for Data Recording.....	135
Appendix D-2: Wiring for Pressure Transducers and Sensors in CR1000.....	139
Appendix E: XT-1000 Calibration Method .....	140
Appendix F-1: Infiltration Trench Individual Storm Graphs.....	143
Appendix F-2: Rainfall and Time before Depth Occurs in IT.....	158
Appendix F-3: Recession and Infiltration Rate Raw Data Table and Calculations.....	159
Appendix G: Inflow, Overflow, and Capture Volumes.....	162
Appendix H: Volume into the Treatment Train and Infiltration Trench .....	163
Appendix I: Storm Durations and Volumes.....	164
Appendix J: Rainfall Intensities ( $i_{1,2,3}$ ) vs. Rainfall Volumes .....	165

## List of Tables

Table 2.1 - Example Removal Efficiencies from the PA BMP Manual (PADEP 2006)..	14
Table 3.1 - Weir plate dimensions .....	29
Table 3.2 - ACF Environmental R-Tank dimensions .....	33
Table 3.3 - SCM design summary and capture volumes .....	34
Table 3.4 - Water content of soils samples collected during construction .....	48
Table 3.5 - Percent gravel, sand, silt, and clay for each soil sample and the classifications .....	50
Table 3.6 - Summary of results from the nuclear density gauge test (in-situ values).....	50
Table 4.1 - Survey data for pressure transducers and sensors (top value in metric, bottom in English units) .....	56
Table 4.2 - Pressure transducer information .....	59
Table 4.3 - Recession rates for August 14, 2012 storm event .....	74
Table 4.4 - Recession rates from August 14, 2012 converted to infiltration rates .....	75
Table 5.1 - Mean, median, and first and third quartiles of recession rate box and whisker plot .....	85
Table 5.2 - T-test p-values for the recession rate depth range comparisons.....	86
Table 5.3 - Mean, median, and first and third quartiles of infiltration rate box and whisker plot .....	90
Table 5.4 - T-test p-values for the infiltration rate depth range comparisons.....	91
Table 5.5 - Slope (m), R-squared, correlation coefficients, and t-test results for comparing recession and infiltration rates to temperature .....	94
Table 5.6 - Estimated recession rates for the first and second year of monitoring for OIT (Note: this data is converted to cm/hr from the graph in in/hr) .....	102
Table 5.7 - Storm durations and volumes summary .....	107
Table 5.8 - Storm intensities ( $i_1$ , $i_2$ , $i_3$ ) .....	109
Table 5.9 - Intensity t-test p-values.....	110
Table 5.10 - Summary of events with overflow .....	115

Table A.1 - Treatment train construction costs.....	132
Table B.1 - List of plants at the treatment train .....	133
Table C.1 - July 10, 2012 survey data .....	134
Table C.2 - July 11, 2012 survey data .....	134
Table C.3 - July 18, 2012 survey data .....	134
Table C.4 - August 17, 2012 survey data.....	134
Table D.1 - Treatment train CR1000 wiring list.....	139
Table F.1 - Rainfall volume and amount of time before IT depth occurs .....	158
Table F.2 - Recession and infiltration rates and data.....	159
Table G.1 - Rainfall volume, duration and intensity, and treatment train inflow, overflow, and capture volumes .....	162
Table H.1 - Rainfall characteristics and volume of stormwater to the TT and into the IT .....	163
Table I.1 - Rainfall volumes and storm durations.....	164

## List of Figures

Figure 1.1 - Aerial of the treatment train.....	3
Figure 1.2 – Philadelphia rainfall event frequency: Event rainfall volume – 24 hr minimum interval time .....	4
Figure 1.3 - Pie chart displaying Philadelphia rainfall event frequencies as a percentage of total historic rainfall events.....	5
Figure 1.4 - Percent storm by volume and percent capture by volume using the Philadelphia Airport Gage 24 hour rainfall data (1948-2011).....	6
Figure 3.1 – Plan view of the weir box.....	27
Figure 3.2 - Side view of the weir box.....	27
Figure 3.3 - Conduits inside the weir box which exit and turn toward the parking garage .....	28
Figure 3.4 - Conduits reaching the garage .....	28
Figure 3.5 - Weir plate sketch.....	29
Figure 3.6 - Leveling of weir plates during construction.....	30
Figure 3.7 - Swale sketch.....	31
Figure 3.8 - Rain garden sketch .....	32
Figure 3.9 - R-Tank.....	33
Figure 3.10 - Stripping of topsoil day one of construction.....	35
Figure 3.11 - Infiltration trench layers of stone and geotextile before inserting R-Tanks	36
Figure 3.12 - Transition piece following 2nd rain garden .....	37
Figure 3.13 - Pipe going into IT.....	37
Figure 3.14 - Basket to catch debris prior to infiltration trench.....	37
Figure 3.15 - Installation of 4 in PVC in center R-Tank for instrumentation.....	38
Figure 3.16 - Tee fittings which allow conduit to exit IT.....	39
Figure 3.17 - Conduit from IT for instrumentation wires.....	39
Figure 3.18 - Infiltration trench before topsoil .....	40

Figure 3.19 - Infiltration trench near completion.....	40
Figure 3.20 - Weir plate installed with concrete.....	41
Figure 3.21 – Example of splash pads used to prevent erosion .....	41
Figure 3.22 - Rain gardens at October, 2011 planting.....	42
Figure 3.23 - Swale planting in October, 2011 .....	42
Figure 3.24 - Weir box completed – outflow end with weir plate and splash pad .....	44
Figure 3.25 - Inside weir box – perforated pipes and second baffle plate .....	44
Figure 3.26 - Erosion control mat with topsoil along the swale .....	45
Figure 3.27 - Beginning of the swale following June 7, 2012 planting.....	45
Figure 3.28 - Weir box and beginning of the swale on October 29, 2012.....	46
Figure 3.29 - First rain garden on October 29, 2012 .....	46
Figure 3.30 - Wash sieve grain size analysis .....	49
Figure 4.1 - CS450-L .....	52
Figure 4.2 - Pressure transducer casing in the laboratory.....	53
Figure 4.3 – Pressure transducer casing in the field .....	54
Figure 4.4 - Survey calculation diagram.....	56
Figure 4.5 - Weir box calculation diagram .....	57
Figure 4.6 - Diagram of pressure transducer and sensor conduit to data logger .....	58
Figure 4.7 - Optical level switch.....	61
Figure 4.8 - Cap installed to block sunlight.....	61
Figure 4.9 - Gems XT-1000.....	63
Figure 4.10 - Tipping bucket rain gage on the parking garage adjacent to the treatment train .....	64
Figure 4.11 - Ponding and runoff on the pervious pavers at the IT (May 2012) .....	67
Figure 4.12 - August 14, 2012 IT pressure transducer depth and rainfall .....	74
Figure 4.13 - September 2, 2012 infiltration trench storm data.....	76

Figure 4.14 - September 4, 2012 infiltration trench storm data.....	77
Figure 4.15 - Aerial image of the treatment train (yellow) and old infiltration trench (red) .....	78
Figure 5.1 - Recession rates (cm/hr) per depth increment for each storm event .....	84
Figure 5.2 - Box and whisker plot of recession rates.....	85
Figure 5.3 - Infiltration rates (cm/hr) per depth increment.....	89
Figure 5.4 - Box and whisker plot of infiltration rates .....	90
Figure 5.5 - Recession rates as a function of the average storm temperature.....	93
Figure 5.6 - Infiltration rates as a function of the average storm temperature.....	93
Figure 5.7 - Volumes into the IT compared to the volume entering the treatment train ..	96
Figure 5.8 - Infiltration volume to treatment train volume ratio vs. rainfall volume .....	98
Figure 5.9 – Volume of overflow as a fraction of the volume entering the IT.....	99
Figure 5.10 – OIT recession rates (in/hr) for the first three years of data collection .....	100
Figure 5.11 - Philadelphia historical event frequency vs. recent data frequency .....	107
Figure 5.12 - Hurricane Sandy infiltration trench pressure transducer and rainfall data (red and yellow circles indicate periods of possible overflow, areas to zoom into).....	111
Figure 5.13a - Hurricane Sandy (October 29, 2012) overflow duration (10/29/12).....	112
Figure 5.13b - Hurricane Sandy (October 29, 2012) overflow duration (10/29/12).....	114
Figure 5.14 - Total intensity (cm/hr) vs. rainfall volume (cm).....	116
Figure 5.15 - Rainfall volume and storm duration.....	117
Figure 5.16 - Overflow percentage vs. storm duration .....	118
Figure 5.17 - Expected capture performance vs. actual capture as a percentage of inflow and outflow volumes.....	119
Figure 5.18 - Ponding on the pervious pavers at the IT after a March 12, 2013 storm event.....	120
Figure F.1 - July 16, 2012 pressure transducer data .....	143
Figure F.2 - July 20, 2012 pressure transducer data .....	143

Figure F.3 - July 28, 2012 pressure transducer data .....	144
Figure F.4 - August 5, 2012 pressure transducer data .....	144
Figure F.5 - August 10, 2012 pressure transducer data .....	145
Figure F.6 - August 14, 2012 pressure transducer data .....	145
Figure F.7 - August 18, 2012 pressure transducer data .....	146
Figure F.8 - August 27, 2012 pressure transducer data .....	146
Figure F.9 - September 2, 2012 pressure transducer data.....	147
Figure F.10 - September 4, 2012 pressure transducer data.....	147
Figure F.11 - September 8, 2012 pressure transducer data.....	148
Figure F.12 - September 18, 2012 pressure transducer data.....	148
Figure F.13 - October 2, 2012 pressure transducer data .....	149
Figure F.14 - October 28, 2012 pressure transducer data .....	149
Figure F.15 - November 7, 2012 pressure transducer data .....	150
Figure F.16 - November 13, 2012 pressure transducer data .....	150
Figure F.17 - November 27, 2012 pressure transducer data .....	151
Figure F.18 - December 8, 2012 pressure transducer data .....	151
Figure F.19 - December 9, 2012 pressure transducer data .....	152
Figure F.20 - December 11, 2012 pressure transducer data .....	152
Figure F.21 - December 18, 2012 pressure transducer data .....	153
Figure F.22 - December 20, 2012 pressure transducer data .....	153
Figure F.23 - December 26, 2012 pressure transducer data .....	154
Figure F.24 - January 11, 2013 pressure transducer data .....	154
Figure F.25 - January 14, 2013 pressure transducer data .....	155
Figure F.26 - January 30, 2013 pressure transducer data .....	155
Figure F.27 - February 11, 2013 pressure transducer data .....	156

Figure F.28 - February 26, 2013 pressure transducer data .....	156
Figure F.29 - March 12, 2013 pressure transducer data .....	157
Figure J.1 - Rainfall intensity ( $i_1$ ) vs. rainfall for each storm .....	165
Figure J.2 – Intensity ( $i_2$ ) vs. rainfall for each storm .....	165
Figure J.3 - Intensity ( $i_3$ ) vs. rainfall for each storm.....	166

# **Chapter 1 Introduction**

## **1.1. Stormwater Control Measures**

Development in urban areas alters the watershed's landscape and changes the hydrologic balance. With increased impervious area, stormwater runoff quantity increases and its quality decreases, while infiltration and evapotranspiration also decrease. For these reasons, stormwater runoff has become a growing concern across the United States; agencies, such as the U.S. Environmental Protection Agency (EPA), are developing methods to better manage stormwater runoff and its pollutants (NRC 2009; PADEP 2006). According to the EPA, the primary method to control stormwater is the use of stormwater control measures (SCMs) (also known as best management practices, BMPs) (NRC 2009). Stormwater controls aim to reduce runoff volumes and peak flows to predevelopment conditions (WEF 2012). In addition to water quantity, controls are also intended to reduce pollutant loads through evapotranspiration, infiltration, and natural chemical and biological processes (WEF 2012). Stormwater control measures include rain gardens (bioretention), trenches, constructed wetlands, and swales. These measures have been implemented over the past decade and are typically installed as individual entities. Thus, the benefits of applying multiple SCMs in series are not well understood.

At Villanova University in southeastern Pennsylvania, many SCMs have been installed and monitored over a number of years for their quantity and quality effects on stormwater runoff. However, not yet has a system of SCMs in series been implemented and analyzed, nor is there abundant evidence of SCMs in series in literature. Therefore, a new research site, the Villanova treatment train, was constructed to monitor the effects of

multiple SCMs combined in series. The concept, similar to a wastewater treatment plant, is intended to utilize the benefits of each individual entity in order to achieve ideal water quantity reductions and water quality improvements throughout the system. In addition to these characteristics, the system is designed to increase the longevity and reduce typical maintenance procedures of each individual SCM, as well as the system as a whole.

## **1.2. Site Description**

The Villanova treatment train is located on the University's campus in southeastern Pennsylvania, a suburban area approximately 13 miles west of center city Philadelphia. It is in the Mill Creek watershed, a contributor to the Schuylkill River. As of 2012, the treatment train is the newest addition to the Villanova Stormwater SCM Demonstration and Research Park. The specific site of the Villanova treatment train was formerly a grassed area bordering a parking garage. There is a natural downhill slope from the point of loading to the point of overflow at the final SCM. Stormwater is collected from an area of about 930 m<sup>2</sup> (10,000 ft<sup>2</sup>) on the top deck of a two-story parking garage and drainage pipes were re-routed to deliver stormwater to the treatment train. The garage is used year round, providing pollutant-laden stormwater, which is representative of runoff from an urban setting due to the daily vehicle traffic. *Figure 1.1* displays an aerial photo adapted from Google Earth of the site's contributing area and the approximate location of each SCM and monitoring points.

The design of the Villanova treatment train utilizes three types of SCMs. It begins with a vegetated swale, followed by two rain gardens in series. The final SCM is an underground infiltration trench. In *Figure 1.1*, the swale, rain gardens, and infiltration

trench are noted by the green, yellow, and red arrows, respectively. The six monitoring and sample collection sites are represented by white arrows. In total, the site was designed for a 2.54 cm (1 in) storm with approximately one third of the total volume being controlled by each type of SCM. The site was constructed in the fall of 2011 and continues to be monitored.



**Figure 1.1 - Aerial of the treatment train (Adapted from Google Earth)** Green, yellow, and red arrows signify the swale, rain gardens, and infiltration trench, respectively. White arrows indicate monitoring and sampling points.

### 1.3. Climate

The Philadelphia area receives approximately 96.52 cm (38 in) of rainfall annually and a majority of this rainfall are in small storm events (2.54 cm (1 in) or less), as noted in the frequency analysis of events based on the historical data (*Figure 1.2*; PWD 2013). From

the frequency distribution, the rainfall volumes and their percentage of occurrence were determined (Figure 1.3); 77% of storms are 2.54 cm (1 in) or less and over 95% of storms are 5.08 cm (2 in) or less. The treatment train was designed to capture and treat the volume from a 2.54 cm (1 in) storm over the contributing watershed, controlling approximately 77% of annual rain events.

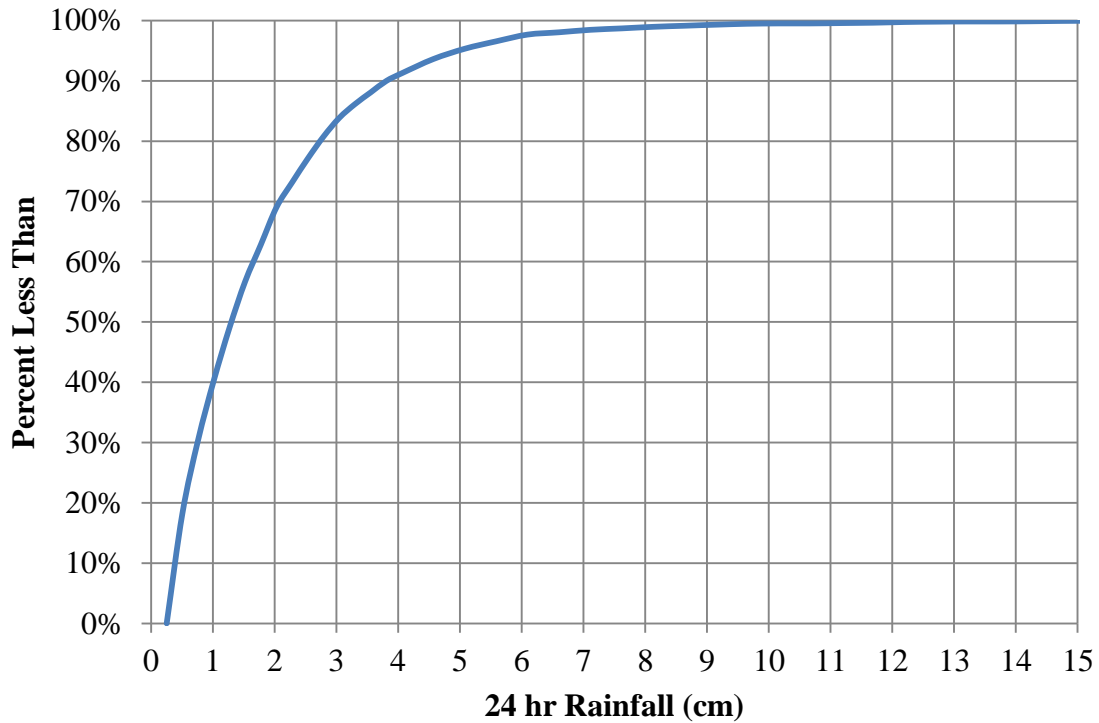


**Figure 1.2 – Philadelphia rainfall event frequency: Event rainfall volume – 24 hr minimum interval time (PWD 2013)** This graph, a cumulative rainfall distribution chart, includes data from the Philadelphia International Airport from 1948-2011.

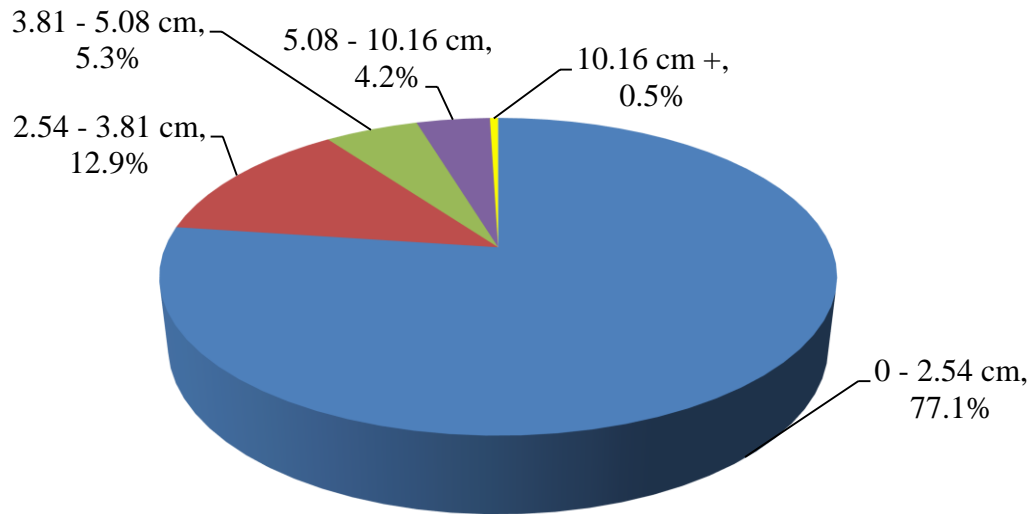


**Figure 1.3 - Pie chart displaying Philadelphia rainfall event frequencies as a percentage of total historic rainfall events**

While a majority of precipitation events are 2.54 cm (1 in) or less and by design the treatment train is intended to control these events, it is important to examine the potential of each individual SCM and the volume of rainfall capture from events larger than the 2.54 cm (1 in) design storm. The graph of *Figure 1.4* shows the percentage of total rainfall volume that each storm event contributes (red line) along with the percentage of total annual rainfall volume captured at each rainfall depth (blue line). For each rainfall depth, this includes any storm up to that depth but also the first part of the rainfall up to that depth for larger storms. This is demonstrated by the three SCMs at the treatment train.

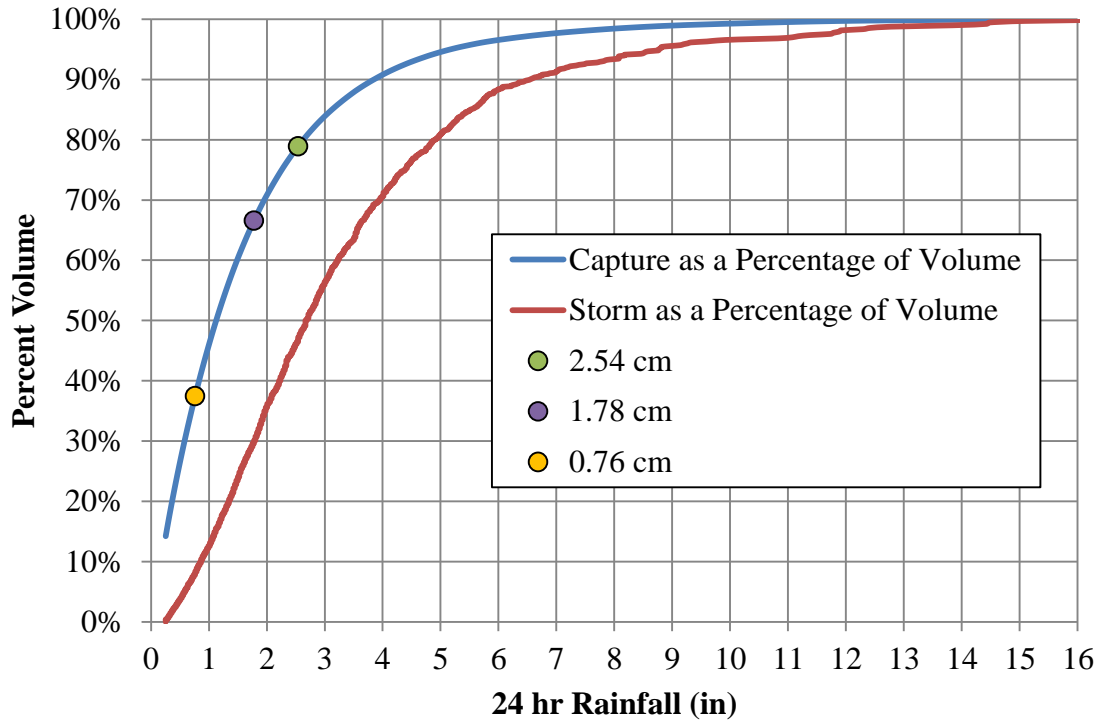


**Figure 1.4 - Percent storm by volume and percent capture by volume using the Philadelphia Airport Gage 24 hour rainfall data (1948-2011)**

By design, the total treatment train should capture a 1 inch storm. In *Figure 1.4*, events that are 2.54 cm (1 in) or less account for almost 50% of the total rainfall volume annually (red line). However, represented by the green point, is the nearly 80% of rainfall captured as it includes not just events that are 2.54 cm (1 in) or less but also the first 2.54 cm (1 in) of any event larger than 2.54 cm (1 in). Excluding the infiltration trench, the rain gardens and swale are design for 1.78 cm (0.7 in) of rainfall. Storms of 1.78 cm (0.7 in) or less contribute to 30% of annual rainfall volume, but nearly 67% of annual volume can be captured by the swale and rain gardens. This represents all events 1.78 cm (0.7 in) or less and the first 1.78 cm (0.7 in) of any event larger. Finally, the swale as a single entity is designed for 0.76 cm (0.3 in) of rainfall. As shown in *Figure 1.4*, events of 0.76 cm (0.3 in) make up 8% of annual volume (red line). The orange

point shows 37% of annual volume, by design, can be captured by the swale alone. Once again, this indicates that 37% of annual rainfall volume includes events 0.76 cm (0.3 in) or less and the first 0.73 cm (0.3 in) of events larger.

It is important to identify that these capture volume percentages are related only to design and are simply expectations of the treatment train. These values do not reflect variables, such as infiltration during the storm event and rain patterns, that will be analyzed for its potential to exceed design. In addition, the historic rainfall event frequency curve will be compared to rainfall data collected at the research site for comparison. Although significantly fewer data points will be used for comparison to historical data, analyzing expected rainfall against actual rainfall will be helpful for research purposes. Design capture volumes and actual capture volumes will also be analyzed through this research.

#### **1.4. Research Goals and Objectives**

The goals of this entire research project consist of the following:

- To examine water quality benefits of the vegetated swale
- To explore the water quality benefits of two rain gardens in series
- To discover the water quality effects of an infiltration trench with pre-treatment
- To examine water quality effects through the entire treatment train
- To examine the water quantity effects of SCMs in a series, specifically stormwater volume and peak flows
- To determine if applying SCMs in a series decreases maintenance needs and increases system longevity

This thesis is a first phase of work to achieve the aforementioned goals. The specific objectives detailed in this thesis include the following:

- To evaluate the construction and monitoring setup of the treatment train as a research site
- To assess the water quantity at the inflow and outflow of the treatment train
- To evaluate the rainfall events causing overflow of the treatment train
- To model the treatment train using SWMM

## **Chapter 2 Literature Review**

### **2.1. Treatment Trains in Environmental Engineering**

The concept of a treatment train for engineering purposes is certainly not unfamiliar. It has been applied for decades in the environmental engineering field, particularly in relation to water and wastewater treatment. The combined effect of multiple treatments in a series provides the most ideal output by utilizing individual processes in an efficient and effective order. This idea serves as the basis for analyzing the potential effects of applying stormwater control measures in a series to best utilize each individual part for the highest quality of effluent possible while maintaining the longevity of the system.

#### **2.1.1. Traditional WWTP**

Waste water treatment plants (WWTP) are an ideal example of applying a series of physical, chemical, and biological processes to remove contaminants and produce cleaner effluent. Primary and secondary treatments are common processes in most WWTP, and often there are even tertiary treatment processes. The combination of numerous processes in a specific order allows for maximum contaminant removal and ultimately an environmentally sound effluent. Despite the development of treatment trains for use in wastewater and water treatment plants, there is little research and literature available on the use of treatment trains for stormwater.

#### **2.1.2. Living Machine**

While the treatment train concept has been applied in traditional water and wastewater treatment plants for years, a new process, the Living Machine, is an innovative application of a treatment train. The Living Machine provides a transition in thinking

from wastewater to stormwater treatment trains because of the application of natural processes with the ultimate goal of a cleaner effluent. In order to recycle wastewater, the Living Machine System recreates the ecology of natural coastal wetlands. The series of treatment includes a primary filtration stage followed by a turbo-charged wetland simulation (Living Machine 2012). The wetland cells, which include gravel-filled planters, are flooded to create tidal cycles in which micro-ecosystems efficiently remove nutrients and solids. The high quality effluent moves to the final stage where it is filtered and disinfected and ready for reuse (Living Machine 2012). This type of treatment train is significant to the development of SCMs in series because it demonstrates the potential of natural systems to filter out pollutants and to continue to improve water quality with additional processes. While the SCMs will not be manipulated to the extent of a Living Machine System since they are treating runoff and not wastewater, identifying an ideal order and loading rate will contribute to their success and efficiency in treating stormwater runoff.

## **2.2. Stormwater and Treatment Trains**

Installing SCMs in series to form a treatment train is a relatively new concept. There is mention of SCMs in series in some state BMP manuals (e.g. PADEP 2006; MDE 2009) and a few research studies have been completed (Hathaway and Hunt 2010; Brown et al. 2012). However, specific design details as well as the efficiency of constructing SCMs in series are not well defined. There is a need to understand the effects of applying SCMs in a treatment train as demonstrated by the minimal amount of literature and resources currently available.

### **2.2.1. Current Research and Applications**

There is very limited research on the application of stormwater management treatment trains. While this provides a challenge for design, implementation, and monitoring, it also demonstrates the need for such research. Very few sites with multiple SCMs in a series have been monitored, especially containing the specific SCMs installed at the Villanova University treatment train. As noted by Brown et al. (2012), aligning different treatment mechanisms is intended to increase groundwater recharge, improve water quality, and reduce pollutant export. The current literature related to SCMs in series includes research on pervious concrete with bioretention and a system of wetlands. Using these studies as a basis for research, it is clear there are many gaps in the knowledge of the effectiveness of constructing stormwater treatment trains.

In one study in North Carolina, Hathaway and Hunt (2010) analyzed three constructed wetlands in a series. Connected by plastic or concrete pipes, the wetlands were examined for water quality improvements. After analyzing results, the only cell to provide statistically significant reductions for all pollutants was the first one of the series. The second two cells also contributed to reductions in most pollutants, but 80% of the total concentration changes for all pollutants took place within the first cell (Hathaway and Hunt 2010). This study demonstrated the concept of an irreducible minimum concentration as well as the ineffectiveness in terms of water quality performance for placing similar SCMs in a series. However, there are still volume reductions and peak flow control by applying the wetlands in series, although no statistical information was presented on water quantity effects (Hathaway and Hunt 2010).

While Hathaway and Hunt (2010) showed that three identical SCMs in a series may not be effective for water quality improvement, the system may be useful from a maintenance perspective. Perhaps if the first wetland becomes less productive over time, the second wetland may become increasingly effective in improving water quality and treating water quantity (Hathaway and Hunt 2010). This aspect of applying the SCMs in a series becomes important in examining the longevity of the individual pieces of the series as well as the system as a whole. Hathaway and Hunt only were able to monitor their site for a short period, and were unable to examine the potential effects over the lifetime of the system. This is an area of SCM research that should be considered for the future.

A second study in North Carolina involved pervious concrete and a bioretention cell in series (abbreviated as PC-B). The pervious concrete parking lot, which was installed over a gravel subsurface storage basin, was designed so that overflow from storms greater than 2.54 cm (1 in) would drain to the bioretention rain garden. Brown, et al. (2012) analyzed the two infiltrating SCMs over 17 months for water quality and quantity effects. The PC-B system was found to be successful in reducing runoff volume, peak flow, and duration of high outflow rates (Brown et al. 2012). Water quality measurements from this site were difficult since it was constructed in an area with a high water table. With groundwater draining through the bioretention cell, many nutrients were increased from inflow to outflow (Brown, et al. 2012). The lesson learned was to avoid constructing infiltrating SCMs in high water table areas.

### **2.2.2. State BMP Manuals and SCMs in Series**

Many state BMP manuals, including Pennsylvania's, provide very limited information in regards to the design and efficiency of applying SCMs in series. Throughout the Pennsylvania BMP (PA BMP) Manual (2006), specifically Chapter 6: Structural BMPs, there are mentions of utilizing multiple SCMs, and chapter eight provides equations for calculating removal efficiencies of SCMs installed in series. It is suggested to use a vegetative element, such as a vegetative filter or grassed swale, to reduce sediment as a form of pre-treatment for an infiltration trench. It also describes the potential use for a vegetated swale as a pre-treatment for other structural SCMs, and in particular for roadway runoff, to increase system longevity and removal efficiency. A vegetated swale allows for some of the heavier sediments to settle out which prevents those particles from reaching the rest of the system (PADEP 2006). As discussed later, in the PA BMP Manual, the efficiency of a system is assumed to be related to the number of SCMs in a series. Adding an SCM, such as a vegetated swale, will act as pretreatment to the rain gardens and infiltration trench, allowing those SCMs to become even more efficient and function properly for a longer period of time. A third recommendation of using a pre-treatment in the PA BMP (2006) manual is applying a vegetated buffer strip, cleanout, or water quality inlet before a rain garden. These are only brief notes on applying SCMs in a series, but do not give practical knowledge for implementation.

In chapter eight: Stormwater Calculations and Methodology, of the PA BMP manual (2006), there is a small section, 8.6.2 "Analysis of Water Quality Benefits from BMPs," which describes how to estimate the efficiency of applying SCMs in a series. There is an equation provided to compute the removal efficiency of SCMs connected in series or in

parallel, although little evidence supporting the use and application of these equations is apparent. The equation to determine the total removal efficiency for SCMs in series is  $R = 1 - \prod_{i=1}^n (1 - r_i)$  where R is the removal efficiency of n SCMs in series and  $r_i$  is the removal efficiency of SCM<sub>i</sub> (PADEP 2006). The PA BMP method is based on suggested values of SCM removal efficiencies. Recommended removal efficiency values for individual SCM types are included in tables in the PA BMP Manual and are drawn from literature. *Table 2.1* displays some of the removal efficiencies for the SCMs at the Villanova treatment train. The bottom row of *Table 2.1* displays what the treatment train estimated removal efficiencies are using this method; almost 100% removal for total suspended solids (TSS) and total phosphorus (TP) seem high, but these values will be tested at the site. The nitrate (NO<sub>3</sub>) is lower but still could be an overestimate for the SCMs. These efficiencies are summarized in the description of each SCM in Chapter 6 of the manual, but the tables in Appendix A of the manual provide a wide range of efficiencies for each type of SCM.

**Table 2.1 - Example Removal Efficiencies from the PA BMP Manual (PADEP 2006)**

SCM	TSS	TP	NO <sub>3</sub>
Vegetated Swale	50%	50%	20%
Rain Garden	85%	85%	30%
Infiltration Trench	85%	85%	30%
VU Treatment Train	99.8%	99.8%	72.6%

While these values are presented as the summary of removal efficiencies, there is a wide range of performance estimated for each SCM and each pollutant. This range may result in the system over or underperforming. For example, infiltration trench TSS removal efficiency ranges from 50-90% and TP ranges from 4.5-100% (PADEP 2006). It is unlikely the treatment train will perform to the standards the equation in the BMP Manual

provides for SCMs in series, but research will allow for this concept to be analyzed and is intended to provide a better estimate of SCM performance in series.

The presented efficiencies may be from literature, but the PA BMP Manual, is from 2006. There has been a considerable amount of research in the stormwater field completed since 2006, making some of the PA BMP Manual suggestions likely out of date. Not only are the specific values for removal efficiencies difficult to define as evident by the large ranges presented in Appendix A of the PA BMP Manual, they are skewed to the incoming flow values, as previous studies such as Strecker et al. (2001) suggest. Pollutant percentage removal efficiencies are not an ideal metric to determine SCM effectiveness which is why Li and Davis (2009) emphasize the use of other water quality metrics such as event mean concentrations (EMC). The negative implications of using percent removal as a representative of SCM efficiency identify the need to consider a method to better analyze SCMs (Strecker et al. 2001, Li and Davis 2009).

Maryland (MD) has been a pioneer in stormwater management and in the design and application of SCMs. The MD Stormwater Design Manual, most recently revised in May 2009, includes detailed descriptions of performance and design criteria for various types of SCMs in chapters three and four. Differing from the PA BMP Manual, chapter three of the MD manual describes pretreatment requirements for SCMs, such as the infiltration trench, to prevent clogging (MDE 2009). Requirements for pretreatment of an infiltration trench include a minimum 25% of the water quality volume ( $WQ_v$ ) pretreated prior to entry, and three techniques to protect long term integrity of the individual system (MDE 2009). The  $WQ_v$  (acre-feet) is defined as  $(P \cdot R_v \cdot A) / 12$  where P is the rainfall depth of 1 inch,  $R_v$  is the volumetric runoff coefficient, and A is the site area in acres. Choices for

the three techniques of pretreatment include a grass channel, grass filter strip, bottom sand layer, upper sand layer, or the use of washed bank run gravel as aggregate (MDE 2009). This concept of pretreatment is similar to the idea for a treatment train to reduce the sediment and improve longevity of not just the infiltration trench, but each individual SCM installed.

The infiltration trench has extensive pretreatment requirements in the MD Stormwater Manual, but there are also pretreatment criteria for stormwater filtering systems, which includes rain gardens or bioinfiltration sites. Once again, it involves treating at least 25% of the computed  $WQ_v$ , which is typically provided for bioretention systems with a grass filter strip or sand filter layer, a gravel diaphragm, and a mulch layer (MDE 2009). As for a swale, the pretreatment requirements include storage of 0.1 inches of runoff per impervious acre, which is usually provided by check dams (MDE 2009).

The Minnesota Stormwater Manual (MSM) thoroughly describes the process for choosing and designing SCMs and notes four important factors: (1) the characteristics of the resource to be protected, (2) the feasibility of implementation, (3) public demands and (4) governmental requirements (MSSC 2008). Other emphasis is placed on aesthetics, physical suitability, cost effectiveness, and maintenance requirements. While there is no direct mention of SCMs in series, pretreatment is mentioned as means to remove sediment (MSSC 2008). For bioretention, there is a portion of the design description dedicated to pretreatment. Other manuals only briefly mention the use of pretreatment, but in the MSM, it is stated as a requirement to reduce maintenance needs and reduce potential clogging effects (MSSC 2008). Different types of pretreatment are suggested for the project type; for example, for sheet flow runoff grass filter strips are

recommended (MSSC 2008). Other types of pretreatment recommended include a grass channel, gravel diaphragms, mulch layer, or forebay (MSSC 2008). The Minnesota Stormwater Manual does not, however, mention the use of a combination of SCMs to maximize runoff treatment.

Pretreatment is also recommended in the Minnesota Stormwater Manual for vegetated swales. For a concentrated flow site, similar to the Villanova treatment train, pretreatment in the form of a plunge pool is recommended and additional measures may include parking lot sweeping to prevent suspended solids from entering the system (MSSC 2008). In the MSM, the infiltration trench is noted to function as the end of a treatment train to reduce pollutants, increase groundwater recharge, decrease peak flow rate and volume, and reduce thermal impacts of runoff (MSSC 2008). Pretreatment for an infiltration trench is also required in Minnesota and suggestions include a plunge pool, sump pit, filter strip, sedimentation basin, grass channel, or a combination (MSSC 2008). Water quality effects are estimated from pollutant removal efficiencies in literature such as the International BMP Database (MSSC 2008).

Most state BMP manuals, such as those of Pennsylvania, Maryland, and Minnesota, estimate water quality effects of stormwater control measures through pollutant removal efficiencies found in literature. While these values have been determined from extensive research, they may not be ideal in predicting the efficiency of SCMs. Percent removal, while easy to understand, has significant shortcomings (WWEGC 2007). As suggested by the International Stormwater BMP Database, approaches which focus on the volume of runoff treated, volume reduced, statistical differences between influent and effluent

quality, and how the BMP functions to reduce peak runoff rates during small, frequent events may better analyses of stormwater control measure performance (WWEGC 2007).

### **2.2.3. Water Environmental Federation and SCMs**

The Water Environmental Federation's manual, *Design of Urban Stormwater Controls*, includes all aspects of SCM design criteria, and maintenance procedures. In the manual, swales, bioinfiltration systems, and infiltration trenches are thoroughly explained, along with limitations and recommendations. Applying SCMs in a series is not directly referenced, but forms of pre-treatment are described for nearly every stormwater control.

Swales may provide some peak flow attenuation, especially during smaller events, but in terms of water quality, the primary process involves sedimentation (WEF 2012). While swales are not particularly effective in reducing dissolved particles, they can improve water quality by reducing sediment particles greater than 6 to 15 um (WEF 2012). In addition to allowing particles to settle, pollutants attached to the particles may also be reduced (WEF 2012). Pretreatment suggestions include a sump unit for contributing areas, which are high in total suspended solids (TSS) (WEF 2012).

Bioretention filters, similar to the rain gardens at Villanova, are described by the WEF as an expanded filter strip. They provide runoff quantity control through infiltration and evapotranspiration and incorporate water quality benefits through biological process from ponding, sorption, and filtration (WEF 2012). Pretreatment in the form of forebays or filter strips are suggested for bioretention units (WEF 2012). These forms of pretreatment can remove larger debris and extend the infiltration life of the bioretention surface (WEF 2012).

Infiltration trenches provide significant volume reduction and peak attenuation through storage, and water quality benefits mainly relate to sorption and filtration methods (WEF 2012). However, since infiltration trenches are subjected to clogging from sediments, pretreatment is highly recommended in the WEF manual. Swales or filters strips are recommended along with sand layers (WEF 2012). This form of pretreatment is similar to the treatment train at Villanova since the swale and the rain gardens are intended to remove particles prior to the runoff reaching the infiltration trench.

### **2.3. SCMs as Single Entities**

While there is only limited research, there is great potential for applying SCMs in a series to improve water quality and reduce water quantity. The system at Villanova University, which includes a vegetated swale, two rain gardens in series, and an infiltration trench, is difficult to compare to current literature due its unique design and construction. Therefore, it is important to recognize research on individual stormwater control measures to evaluate their potential in a series system. Perhaps their maintenance needs and reasons for failure will be compensated for if applied in the correct order as a treatment train. In order to further analyze this idea, each SCM has been researched for its general design and purpose, as well as reasons for success and failure.

#### **2.3.1. Swales**

Research on the application of swales for stormwater treatment is limited with the exception of highway runoff treatment. Roadside filter strips have been monitored in Virginia, North Carolina, and Texas, and research has shown that most contribute to pollutant reduction (Kaighn and Yu 1996; Winston et al. 2011; Barrett et al. 1998). Most of these swales showed concentration reductions in total suspended solids (TSS), zinc

(Zn), total phosphorus (TP), and total Kjeldahl nitrogen (TKN). Research has also determined that pollutant removal typically increases as a function of swale length (Barrett et al. 1998; Yousef et al. 1985; Yu et al. 2001). In addition to swale length, Yu et al. (2001) and Kaighn and Yu (1996) found that check dams contributed to increased retention time and therefore increased pollutant removal. Many variables, including swale length, longitudinal slope, presence of check dams, cross-sectional shape, vegetative density, grass stiffness, soil infiltration rate, design flow depth, and design flow rate, are important in pollutant removal (Yu et al. 2001; Bäckström 2002).

Winston et al. (2012) analyzed four swales for their quantity and quality impacts on highway runoff in eastern North Carolina. In order to determine if wetland characteristics in swales are more effective for nutrient removal, two dry swales with vegetated filter strips (VFS) and two swales with wetland characteristics were used in the study. The VFS had poor pollutant reduction efficiencies, which were possibly due to their design and maintenance (Winston et al. 2012). Low vegetated cover and relatively steep slopes may have contributed to the minimal pollutant reductions or pollutant concentration increases. Additionally, these strips received runoff which was at or near “irreducible” concentrations for TSS and particulate-bound pollutants (Winston et al. 2012). As for the swale comparison, nitrogen concentration effluents were typically lower in the wetland swales than in the dry swales, and TP and TSS were similar in all four swales with the exception of one. One of the dry swales had significantly higher TSS effluent likely due to soil compaction in the filter strip along with a head cut at the swale inlet which was causing erosion (Winston et al. 2012). The results of this study

signify the importance of design, construction, and maintenance in the efficiency of swales as SCMs.

### **2.3.2. Rain Gardens (Bioinfiltration)**

Bioinfiltration facilities, also known as rain gardens, are SCMs with planted landscapes intended to collect, store, filter, and treat runoff (Davis 2005). As this form of SCM has become increasingly adopted in LID practices, there have been many studies to verify their benefits. Over the past decade, researchers have demonstrated the effectiveness of water quality improvements and water quantity impacts on local hydrology (Li and Davis 2009). While a main focus of applying bioretention is to treat pollutants in stormwater runoff, they are also beneficial in their ability to significantly reduce stormwater volumes through both infiltration and evapotranspiration (Roy-Poirier et al. 2010). This implies a benefit of using rain gardens in an urban setting in an attempt to counteract stormwater volume increases from urban development (Roy-Poirier et al. 2010).

Rain gardens have proven to be effective in treating stormwater runoff. As shown by Li and Davis (2009), there is a varying capacity to manage different pollutants, but data indicated bioretention can effectively reduce total suspended solids (TSS), chromium (Cr), lead (Pb), and zinc (Zn) concentrations in runoff. Box experiments by Davis et al. (2006) also demonstrated water quality improvements. In these tests, total phosphorus (TP) removal efficiencies ranged from 70 to 85% and total kjeldahl nitrogen (TKN) removal efficiencies ranged from 55-65% (Davis et al. 2006). Tests were also performed to demonstrate varying runoff durations and intensities. Results showed reductions in nutrient removal due to increasing flow rates through the bioretention media (Davis et al. 2006).

As for water quantity effects, a few studies of rain gardens, including those by Davis (2008), Hunt et al. (2006), and Dietz and Clausen (2005) have demonstrated hydrologic benefits. Davis (2008) studied over 49 storms at two bioretention facilities (located parallel to each other but not connected) at the University of Maryland. Of the monitored events, there was no outflow for 18% of them and mean peak flow reductions of the cells were 49 and 58% (Davis 2008). In addition, time to peak significantly increased, which is desirable for LID practices and attempting to mimic pre-development hydrologic conditions. Hunt et al. (2006) studied a rain garden in North Carolina over 12 months and estimated the annual average ratio of outflow volume to estimated runoff volume to be 0.22 for the cell. However, some seasonal differences were present, with a lower mean ratio in the summer (0.07) and a higher mean ratio (0.54) during winter months. Dietz and Clausen (2005) reported on their study of two rain gardens in Connecticut that overflow occurred for just 0.8% of the total inflow volumes. Since their study included a cold winter, Dietz and Clausen (2005) also concluded that infiltration can effectively occur in bioretention cells even under freeze-thaw conditions.

Despite many benefits to the implementation of rain gardens as SCMs, Roy-Poirier et al. (2010) have found some problems with bioinfiltration application. A major factor in the success of a bioinfiltration system is its construction. Since many contractors are unfamiliar with construction of SCMs and rain gardens specifically, poor construction can lead to many issues (Roy-Poirier et al. 2010). Infiltration rates may be affected by the presence of preferential flow paths due to construction techniques or soil mixtures. This type of system failure can be avoided with proper construction and using correct media proportions. According to Roy-Poirier et al. (2010), the issue of system ownership

may also lead to failure due to lack of maintenance. In addition to these concerns, there have been reports of varying nutrient removal efficiencies, and as Roy-Poirier et al. (2010) suggests, more research is required to identify the ideal design of rain gardens to optimize their hydrologic and water quality effects on stormwater.

### **2.3.3. Infiltration Trenches**

As an SCM, infiltration trenches are designed and implemented to not only enable infiltration into the underlying soil and store runoff volume (Akan 2002), but also to provide groundwater recharge (Shaver 1986) and offer water quality benefits (Barraud et al. 2005; Birch et al. 2005; Siriwardene et al. 2007). An infiltration trench often concentrates a large volume of runoff into a small area, which can inhibit the natural hydraulic functions of the surrounding soil (Emerson et al. 2010). Therefore, proper design of an infiltration trench, which accounts for the role of influent solids by minimizing contributing area and installing a form of pretreatment, is necessary to extend the functioning life of this particular SCM (Emerson et al. 2010). Some studies have demonstrated the efficiency of using an infiltration trench as way to control and treat stormwater, while others have discovered the potential faults in its application.

Infiltration trenches are able to maintain the ability to not only control water quantity, but also water quality (Birch et al. 2005; Emerson et al. 2010; Siriwardene et al. 2007; Scholz and Yazdi 2008). The primary pollutant considered for infiltration trenches is total suspended solids due its potential to clog pore spaces and reduce the lifespan of the SCM (Siriwardene et al. 2007). Suspended solids are not only a primary pollutant removed, but due to their potential for clogging, they are also a concern to the longevity of an infiltration trench (Emerson et al. 2010; Siriwardene et al. 2007). For instance, the

infiltration trench at Villanova University in Pennsylvania, studied by Emerson et al. 2010, while intentionally undersized to accelerate long-term loading effects, removed TSS at a 36% removal rate. It also demonstrated a decrease in the ability to infiltrate stormwater runoff volumes over time, most likely attributed to clogging of the bottom layer (Emerson et al. 2010). A changing infiltration rate is not unlikely as solids clog the bottom layer of the infiltration trench, so it is recommended to add pretreatment in order to attempt to remove some of the sediment that decreases a trench's efficiency (Emerson et al. 2010; Duchene et al. 1994).

Despite the potential for infiltration rates into the surrounding soil to decrease, the infiltration trench typically provides a means for runoff water quality improvement. A study by Birch et al. (2005) evaluated the weighted average concentration reductions for TSS, nutrients, trace metals, and pesticides and fecal coliforms. Several contaminants, including TSS, Cu, Pb, and Zn were reduced 50%, 68%, 93%, and 52%, respectively. Nutrients TP and TKN were reduced by 51% and 65%, respectively, and the infiltration trench removed 96% of fecal coliforms. However, other pollutants, such as total nitrogen (TN), chromium (Cr), iron (Fe), manganese (Mn), and nickel (Ni) were either similar in concentration or higher in concentration when comparing the inflow to the outflow (Birch et al. 2005).

In a modeling study of a gravel and sand filter combined with a subsurface detention and infiltration unit, both water quantity and quality impacts were observed (Scholz 2008). Volume reductions averaged 70% and mean peak flow reductions of 90% were achieved. Pollutant removal efficiencies for biochemical oxygen demand (BOD), TSS, nitrate-nitrogen, and orthophosphate-phosphorus were 77%, 83%, 32%, and 47%, respectively

(Scholz 2008). If used effectively, an infiltration trench has the ability to manage runoff volume and improve runoff quality (Akan 2002; Barraud et al. 2005; Birch et al. 2005; Siriwardene et al. 2007). Their potential for failure from the impact of large amounts of sediment loading should be considered in design and construction and adding pretreatment to create a type of treatment train is likely to extend the functioning life (Emerson et al. 2010; Duchene et al. 1994).

## **Chapter 3 Site Design and Construction**

### **3.1. Treatment Train Design**

The treatment train at Villanova University, which contains a dry vegetated swale, two rain gardens in series, and an infiltration trench, was designed to capture and treat a one inch storm. Stormwater runoff is collected from a 930 square meter (10,000 ft<sup>2</sup>) area of a parking garage adjacent to the site. The garage drainage pipes route runoff to the treatment train which begins at the weir box and then the water flows through the system; there is a weir and pressure transducer to monitor flow from the drainage area to the treatment train over time.

#### **3.1.1. Weir Box**

The weir box is the first piece of the treatment train as it serves as a collection point for the stormwater from the contributing area. The box, as shown in the sketches of *Figures 3.1* and *3.2*, is 2.03 m (6.67 ft) long, 0.91 m (3 ft) wide, and 0.91 m (3 ft) deep. The inflow is through a 15.24 cm (6 in) diameter PVC and the top of the pipe is approximately 15.24 cm (6 in) from the top of the box. There are then two baffles plates, which are designed to steady the flow for the instrumentation at the downstream end of the weir box. The first baffle plate comes down from the top of the box 20.32 cm (8 in) about 25.4 cm (10 in) from the back of the weir box. The second baffle plate comes up from the bottom of the box 68.58 cm (2.25 ft) and is 25.4 cm (10 in) further downstream from the first baffle plate.

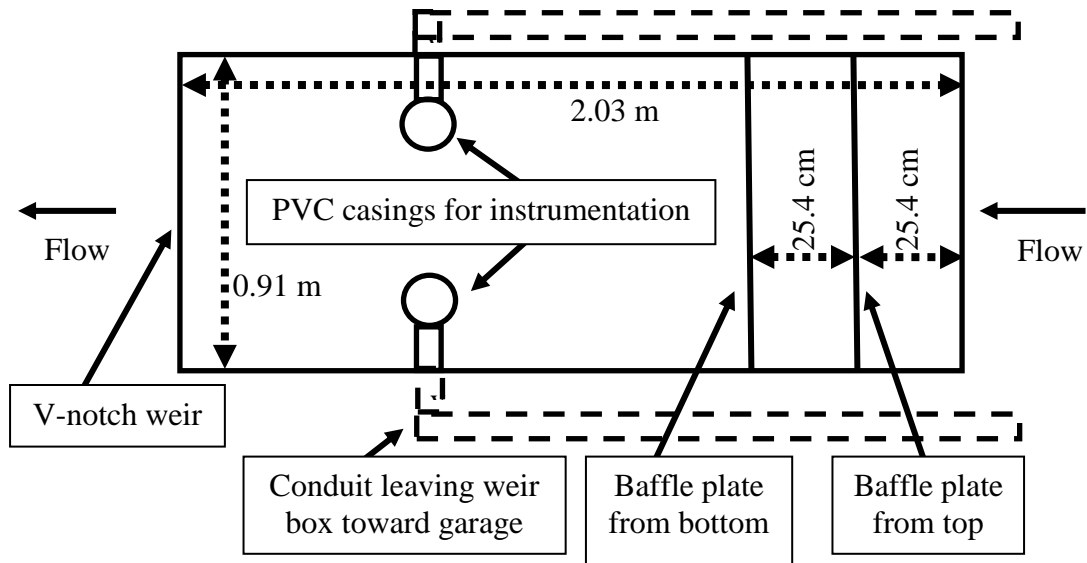


Figure 3.1 – Plan view of the weir box

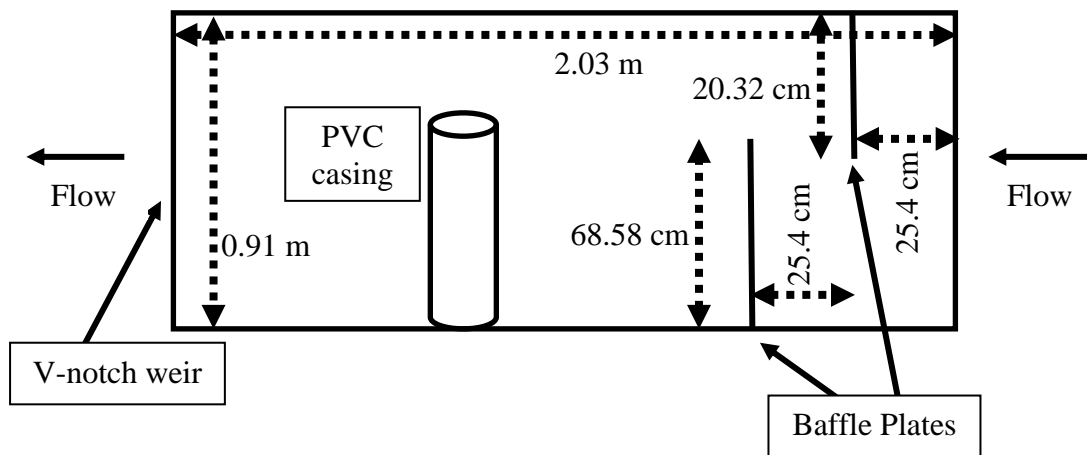


Figure 3.2 - Side view of the weir box

The weir box is also designed to contain instrumentation for water quantity and quality measurements. Two 10.16 cm (4 in) diameter perforated pipes were designed to store and protect instrumentation. Attached to these two major pipes is 3.18 cm (1.25 in) diameter conduit which allows instrumentation wires to reach the data logger inside the garage. The conduit exits the box on each side, makes a 90° turn toward the garage, and ends near the concrete wall of the garage. *Figure 3.3* shows the smaller conduit going

out of the weir box from both larger pipes, and *Figure 3.4* shows where that 3.18 cm (1.25 in) PVC reaches the garage. This was included in the design to ensure protection of any wires and making installation and removal simple and repeatable. The design included an access door to allow for entry and monitoring of the inside of the box.



**Figure 3.3 - Conduits inside the weir box which exit and turn toward the parking garage**



**Figure 3.4 - Conduits reaching the garage**

The first of five v-notch weirs throughout the system (W1) is attached at the downstream end of the box. There is a v-notch weir halfway through the swale, at the end of the swale, and one following each rain garden. The weirs were purchased from Rickly

Hydrological Co.; a sketch is shown in *Figure 3.5* with dimensions in *Table 3.1*. The aluminum, 90° v-notch weirs are designed to USGS standards and the flow can be calculated with the equation  $Q = 2.49h^{2.48}$  where h is the head of water over the v-notch in feet (USBR 2001). These plates were attached to wooden 10.16 cm by 10.16 cm (4 in by 4 in) posts and installed and leveled during construction, as seen in *Figure 3.6*. For further reference, weir plates were named based on their position in the system with weir 1 (W1) referring to the weir box weir. W2 and W3 are the middle of the swale and end of the swale; W4 and W5 are the weirs following the first and second rain gardens.

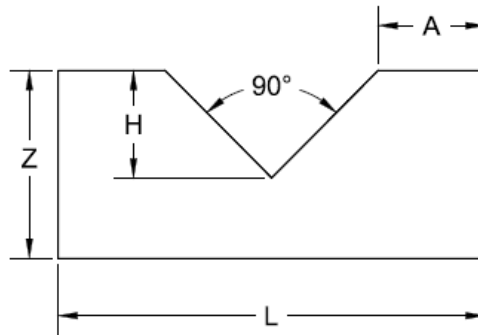


**Figure 3.5 - Weir plate sketch**

**Table 3.1 - Weir plate dimensions**

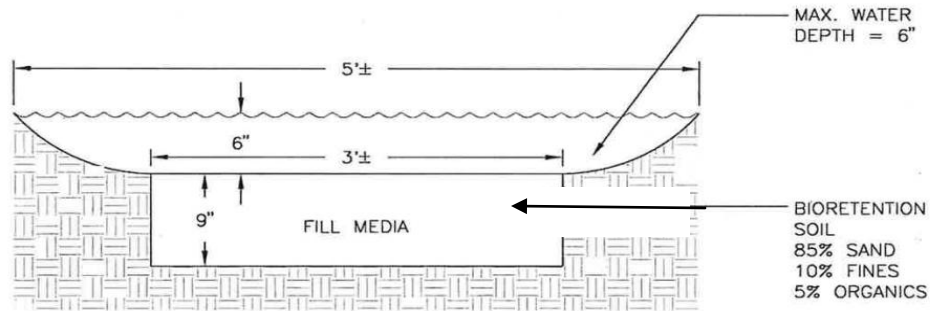
	<b>Z</b>	<b>H</b>	<b>L</b>	<b>A</b>
<i>Feet</i>	1.75	1	4	1
<i>Meters</i>	0.5334	0.3048	1.2192	0.3048



**Figure 3.6 - Leveling of weir plates during construction**

### **3.1.2. Swale**

The vegetated swale is the first SCM in the series at the Villanova treatment train. The swale begins at the weir box and is approximately 37 meters (120 ft) long and manages 0.76 cm (0.3 in) of rain by design. The design is about 23 cm (9 in) of an engineered media in the swale and a ponding depth of about 15 cm (6 in) (*Figure 3.7*). As noted in the sketch, the engineering media is designed to be 85% sand, 10% fines, and 5% organics. This media was designed for both the swale and the rain gardens. An analysis of the actual media collected during construction is included in Section 3.3. The bottom width of the swale is approximately 1 m (3 ft) and side slopes are at a 2:1 ratio. Design capture volume is based only on bowl depth and channel shape. Soil capacity is considered minimal and is a source of additional capture potential. There is a weir plate halfway through the swale and at the end of the swale to measure flow and serve as locations for water quality grab samples; additionally these weir plates acts a bit like a check dam to slow flow through the swale.



TYPICAL SWALES (QTY:2) (S)

NOTE: ADD BERM ON DOWNHILL SIDE IF NECESSARY TO FACILITATE 6" HORIZONTAL SWALE DEPTH.

CAUTION: DO NOT COMPACT SWALE SUB-BASE SOIL.

Figure 3.7 - Swale sketch

### 3.1.3. Rain Gardens

Following the vegetated swale are two rain gardens in series. Elliptical in shape, the rain gardens longer lengths run in the direction of flow. The rain gardens have a bottom width of one meter (3 ft) and bottom length of 1.83 meters (6 ft) (*Figure 3.8*). The engineered media (specifics in *Figure 3.8*) fill depth is about 46 cm (18 in) with an additional 46 cm of ponding depth available. Side slopes are the same as the swale at 2:1. Each rain garden is designed to capture 0.51 cm (0.2 in) of rain, totaling to 0.7 inches of rain through the system up to the second rain garden. As with the swale, the rain garden capture design volume is based only on storage above the soil surface as estimated 0.25 soil porosity provides minimal storage. There are weir plates at the end of each rain garden, which are intended for flow measurement as well as water quality grab sample points.

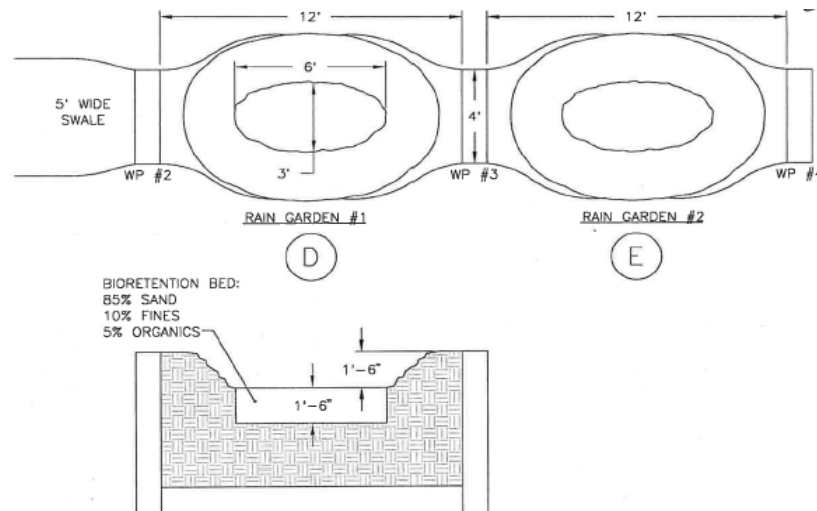


**Figure 3.8 - Rain garden sketch**

### 3.1.4. Infiltration Trench

The infiltration trench serves as the final SCM in the treatment train. Formed from crates known as R-Tanks by the manufacturer ACF Environmental, the infiltration trench covers an area of approximately 2.00 m by 2.86 m (6.56 ft by 9.38 ft) and is just over 1.28 m (4.20 ft) deep. The R-Tanks, as pictured in *Figure 3.9*, have 95% porosity and are designed to store the final 0.76 cm (0.3 in) of a 2.54 cm (1 in) storm. The dimensions of each individual tank are in *Table 3.2*; a total of 20 R-Tanks were used in the Villanova treatment train infiltration trench. They were placed five by four with the total depth being 2.86 m (9.38 ft) and the width being 2.00 m (6.56 ft), resulting in a total area of 5.43 m<sup>2</sup> (58.50 ft<sup>2</sup>). The area also accounts for the 95% porosity. The design of the infiltration trench intentionally does not include an under drain or an overflow system. The trench is designed with 30 Xeripave pervious pavers with a flow rate over 1 gallon per second per square foot at the surface to serve as the overflow. Each paver is 40 cm x 40 cm in surface area and 50 mm high deep (15.75 in x 15.75 in x 1.97 in). When the IT is filled, water simply flows through the pavers and over the downstream curb to the

sewer system and is ultimately routed to another SCM at Villanova, the constructed wetland.



Figure 3.9 - R-Tank

Table 3.2 – ACF Environmental R-Tank dimensions

Depth	Width	Height	Top/Bottom Surface Area
0.40 m (15.75 in)	0.72 m (28.15 in)	1.28 m (50.39 in)	5.43 m <sup>2</sup> (58.50 ft <sup>2</sup> )

### 3.1.5. Design Summary

The treatment train is designed to capture and control a 2.54 cm (1 in) storm over the 930 m<sup>2</sup> (10,000 ft<sup>2</sup>) contributing area. The ratio of the contributing area to the SCM area is approximately 7.5 (930 m<sup>2</sup> : 124 m<sup>2</sup>). Each component, the swale, rain gardens, and infiltration trench, by design, are expected to capture approximately one third of the total design volume. *Table 3.3* summarizes the capture volume as cm (in) of rainfall and the capture volume as m<sup>3</sup> (ft<sup>3</sup>) for each SCM. The total design capture volume, 22.45 m<sup>3</sup> (825 ft<sup>3</sup>) is nearly identical to the design storm over the contributing impervious

watershed (23.38 m<sup>3</sup> (826 ft<sup>3</sup>)). As previously mentioned, the site was constructed to analyze the water quantity and quality effects of SCMs in series along with maintenance and longevity benefits. Most storms (77%) in the Philadelphia area are 2.54 cm (1 in) or less so the system is expected to overflow only a few times per year. In addition, since approximately 63% of storms are 1.78 cm (0.7 in) or less, over half of the storms should be controlled by the swale and rain gardens alone. This concept of the design is intended to increase longevity of the infiltration trench. These design expectations of treatment volumes will be compared to actual percent capture during rainfall events.

SCM	Purpose	Rainfall (in)/[cm]	Volume Captured (ft <sup>3</sup> )/[m <sup>3</sup> ]
Vegetated Swale	Slow flow with check dams, volume retention, and pollution capture	0.3 in / 0.76 cm	240 ft <sup>3</sup> / 6.80 m <sup>3</sup>
Rain Gardens	Retain water for infiltration, pollution capture	0.4 in / 1.02 cm	340 ft <sup>3</sup> / 8.70 m <sup>3</sup>
Infiltration Trench	Hold volumes from larger storms (> 0.7 in)	0.3 in / 0.76 cm	245 ft <sup>3</sup> / 6.95 m <sup>3</sup>
<b>Totals</b>		<b>1 in / 2.54 cm</b>	<b>825 ft<sup>3</sup> / 22.45 m<sup>3</sup></b>

Table 3.3 - SCM design summary and capture volumes

### 3.2. Construction

Construction of the Villanova treatment train took place from September 30 – November 4, 2011. Mayfield Site Contractors, Inc of King of Prussia, PA completed the construction at a total cost of \$64,787, which included excavation, media fill, infiltration trench and weir box assembly, and the re-piping of the garage drainage system. A breakdown of construction costs is included in *Appendix A*.

### 3.2.1. Construction Timeline

Once the general path of the swale and locations of the rain gardens and infiltration trench were staked out, excavation began. The first day included installation of construction and silt fences, and the stripping of the topsoil approximately five feet wide along the path of the system from the garage through the second rain garden, as displayed in *Figure 3.10*. The next few days were focused on the infiltration trench. Once excavated, a layer of geotextile was placed followed by a bottom layer of stone with approximately 40% void space. With the bottom layer of stone leveled, another layer of geotextile was positioned to ultimately wrap the crates, as seen in *Figure 3.11*. The 20 crates were placed in the infiltration trench and wrapped in the second layer of geotextile. As recommended by the manufacturer's installation guide, there was a minimum of 0.30 m (1 ft) of space on all four sides of the crates to allow for a stone backfill. At this site there was 0.30 m to 1 m (1 ft to 3 ft) of stone around the outside of the crates to allow for more storage and infiltration, although this is not considered in the design storage.



**Figure 3.10 - Stripping of topsoil day one of construction**



**Figure 3.11 - Infiltration trench layers of stone and geotextile before inserting R-Tanks**

Water from the second rain garden is transported to the infiltration trench through a 0.30 m (12 inch) PVC pipe. A prefabricated transition piece, as designed and built by the contractor, collects stormwater from the final weir plate and directs it through the pipe to the infiltration trench. *Figures 3.12* and *3.13* display the transition piece and pipe from the second rain garden to the infiltration trench. The pipe was placed flush with the R-Tanks and surrounded by stone to keep it secure. The placement of the 0.30 m (12 in) corrugated pipe is approximately in the middle of one of the R-Tanks to allow for a sufficient slope following the transition piece. As seen in *Figure 3.12*, the transition piece does not prevent objects from entering the pipe to the infiltration trench. Due to the potential for leaves, mulch, and plant debris moving through the system, a basket was designed and built to fit in the semi-circle transition piece. The basket can be removed and cleaned out as necessary. An image of this basket is in *Figure 3.14*. The basket is made of stainless steel mesh purchased from Edward J. Darby & Son, Inc. of Philadelphia, PA. A 2.13 m by 1.22 m (7 ft by 4 ft) sheet with mesh size 28 and 0.46 mm (0.018 in) diameter wire resulting in 24.6% open area was purchased. The pieces were

cut and essentially sewn together with a stainless steel wire purchased at Home Depot. Once in the transition piece, the v-notch was also cut out to allow water to flow freely into the basket.



**Figure 3.12 - Transition piece following 2nd rain garden**



**Figure 3.13 - Pipe going into IT**



**Figure 3.14 - Basket to catch debris prior to infiltration trench**

In addition to installing the crates with the geotextile and stone as the installation guide advised, pipes were required to serve as a conduit for instrumentation and wires. One crate, as designed by the manufacturer, contained a 0.30 m (1 ft) diameter hole in order to vacuum out sediment if needed for maintenance of the infiltration trench. Since this large hole also allows for visibility in the trench, this crate was chosen to be used for further

holes and PVC pipe inserts to serve as conduits. The contractor cut out four 10.16 cm (4 in) diameter holes for the additional four pipes to contain and protect instrumentation as seen in *Figure 3.15*. Two 10.16 cm (4 in) pipes on each side of the larger 0.30 m (1 ft) hole were connected with 3.81 cm (1.5 in) PVC. In order to provide access from the infiltration trench to the instrumentation box, the conduits from each pair of 10.16 cm (4 in) pipes continued through the crates, stone, and soil and extended to the garage wall. *Figures 3.16* and *3.17* show the use of the PVC tee fittings and the extension of the conduit to the garage.



**Figure 3.15 - Installation of 4 in PVC in center R-Tank for instrumentation**



**Figure 3.16 - Tee fittings which allow conduit to exit IT**



**Figure 3.17 - Conduit from IT for instrumentation wires**

The final pieces of the infiltration trench construction involved the pervious pavers at the surface and the access door. While not necessary in a traditional setting, a Bilco door was installed on top of the crates over the five PVC pipes to allow for monitoring and sampling. The door can be opened to check for potential maintenance needs, obtain grab samples for water quality testing, and access instrumentation. *Figures 3.18 and 3.19* display the infiltration trench before and after the topsoil and Bilco door were placed. The infiltration trench is not connected to the traditional stormwater and sewer pipes,

rather the pervious pavers are intended to serve as the overflow device. The pervious pavers, from Xeripave, surround the access door and cover a majority of the infiltration trench R-Tanks and some area of the stone fill.



**Figure 3.18 - Infiltration trench before topsoil**



**Figure 3.19 - Infiltration trench near completion**

As the infiltration trench was being completed, the excavation of the swale and rain gardens was also completed. Once the SCMs were excavated to their desired depth, the weir plates were mounted to 4x4s, installed, and leveled at each of the four locations in the swale and rain gardens. While the 4x4 posts were installed over 1 m (3 ft) into the soil, a small amount of concrete was placed at the surface around the posts to maintain stability and keep them as level as possible due to their crucial role in water quantity calculations. The concrete, shown at the weir in the middle of the swale in *Figure 3.20*, also helps maintain the structure of the berm as flow builds up behind the weir plates.

With the weir plates installed, the backfill of the media could begin. The engineered media, comprised of 85% sand, 10% fines and 5% organics, was created and transported to the swale and rain gardens by the contractor. At each weir plate, the media was filled on the upstream side to the point of the v-notch, with care not to compact the media. On

the downstream side of each weir, there was a 15 cm to 23 cm (6 in to 9 in) drop for flow measurement purposes. Following the media, downstream of each weir plate a splash pad was also placed to prevent erosion. An example is shown in *Figure 3.21* at the second rain garden. These splash pads were designed to be 0.30 m by 0.30 m (1 ft by 1 ft) but the contractor suggested re-using extra concrete pavers from another project on campus. While these were larger than design at approximately 46 cm by 46 cm (18 in by 18 in), they provide the stability desired at the downstream side of each weir plate.



**Figure 3.20 - Weir plate installed with concrete**



**Figure 3.21 – Example of splash pads used to prevent erosion**

With the backfill complete, construction of the SCMs was also essentially completed. Since a majority of the media was distributed by mid-October, 2011, the first round of planting took place. The campus horticulturist chose the plants for the site, which are intended to provide stabilization of the soil. The plants, which are listed in *Appendix B*, were chosen for the soil type and wet-dry conditions at the site. Construction timing was not ideal from a planting perspective, as it would have been better to stabilize the system with significant plant root growth before the winter months. Despite planting later than the desired planting season, the plants, which were mainly in the rain gardens and only along the berm of the swale, were able to survive the mild winter. *Figures 3.22 and 3.23*

display the treatment train after the October 2011 planting. Additional plants, mainly for the bed of the swale, were planted in June 2012.



**Figure 3.22 - Rain gardens at October, 2011 planting**



**Figure 3.23 - Swale planting in October, 2011**

The final portion of construction by the contractor involved the first component of the system, the weir box. A few weeks after the backfill of the SCMs was finished, the concrete weir box was delivered and able to be installed. This weir box, designed specifically for this site, was intended to serve as the stormwater collection and distribution point as well as an initial monitoring location. While it does serve these purposes as the beginning of the treatment train, it also acts as a sedimentation basin as many of the stones and larger suspended solids are able to settle out inside the weir box. Removing these particles can potentially prevent clogging of the SCMs and ultimately help reduce maintenance of these systems. Since this design was unique to the project, the precast concrete structure did require some work prior to being installed.

The weir box, an original design, needed adjustments before being set into place in the treatment train. The weir plate needed to be attached to the box; in order to place it at the top of the downstream wall, a rectangular cut was made in the concrete. This

construction allowed the point of the v-notch to be one foot below the top of the box. The plate, positioned at the top of the box, as seen in *Figure 3.24*, was bolted and caulked in place. The baffle plates were also installed by the contractor at their locations previously described in the design. L-brackets were screwed in at each location, and the plates were then bolted to the brackets. The baffle plates slow the flow of stormwater and provide a steady flow for measurement over the v-notch weir. Once the weir plate and baffle plates were secured, the box was placed at the beginning of the treatment train. The lid, a thick concrete slab with a Bilco door for access, was laid on top of the open box.

The access door of the weir box is crucial for research purposes of installing and maintaining monitoring equipment and for water quality grab samples. The door also allows access for future maintenance and removal of sediment. Instrumentation is kept in the previously describe perforated PVC pipes, which were also installed by the contractor. The two larger 10.16 cm (4 in) perforated pipes were glued to the bottom of the box to prevent them from moving. The smaller, 3.18 cm (1.25 in) diameter conduit, attached to the perforated pipes with a reducing tee, was installed as designed and ended at the garage wall. The completed weir box is shown in *Figures 3.24* and *3.25*.



**Figure 3.24 - Weir box completed – outflow end with weir plate and splash pad**



**Figure 3.25 - Inside weir box – perforated pipes and second baffle plate**

In order to stabilize the swale, the planting plan, which included about 1000 plants, was adjusted in June 2012. A geotextile erosion mat was laid on top of the bare engineered media in the swale, followed by a layer of topsoil, as seen in *Figure 3.65*. Approximately 500 gallons or 1.90 m<sup>3</sup> (2.48 yd<sup>3</sup>) of topsoil were used. These elements were not in the original plan, but were required to mitigate swale erosion issues. About 10 pounds of grass seed was also spread both underneath the geotextile and on the topsoil. While this grass was also not originally desired, it was necessary to help stabilize the swale and keep the media and topsoil in place. Plants, once again chosen by Hugh Weldon, Villanova's horticulturist, were then planted in the swale and on the banks on June 7, 2012. Holes were cut in the geotextile so roots are embedded in the original media. *Figure 3.27* displays a portion of the swale after the June 7 planting. The remaining plants were planted on June 27, 2012, mostly on the berm of the swale.



**Figure 3.26 - Erosion control mat with topsoil along the swale**



**Figure 3.27 - Beginning of the swale following June 7, 2012 planting**

In addition to the changes in swale planting plans, extra geotextile from the infiltration trench (more of a blanket material) was used to try and prevent the topsoil and grass seed from washing away. This geotextile was bunched and staked in at the beginning of the system (following the weir box) and also applied at the second weir plate at the middle of the swale. This provided a means of energy dissipation and helped prevent further erosion.

The plants required watering throughout the first few months following their planting. A large barrel was placed in the golf cart, filled, and then a watering can was used to distribute the water to the plants a few times a week until the plants stabilized. Throughout late summer and early fall of 2012, weeds, such as *digitaria sanguinalis* (crabgrass) and *cyperus rotundus* (nut sedge), required removal from the swale and rain gardens. Weeds have continued to be removed as necessary and plants watered as needed. By the end of the growing season in the Fall of 2012, the plants throughout the system were thriving in their environment and both serve their purpose for the SCMs and

provide an aesthetically pleasing research site. Not only do the flourishing plants add aesthetics to the site, the plant growth provides stabilization for the system and infiltration and evapotranspiration. Images of the site following Hurricane Sandy on October 29, 2012 are in *Figures 3.28 and 3.29* and show plant growth and the site during storm conditions.



**Figure 3.28 - Weir box and beginning of the swale on October 29, 2012**



**Figure 3.29 - First rain garden on October 29, 2012**

### **3.2.2. Construction Conclusions**

Upon the completion of the construction process, a few conclusions and recommendations can be made. There were several successes and challenges during the construction process which are beneficial for future research and SCM implementation.

#### **3.2.2.1. Successes**

Overall, construction went smoothly and the contractors worked with the graduate students, advisors, and Villanova facilities to complete the treatment train. Communication was simple for the most part and all parties worked closely to follow the design. One graduate student regularly checked in on the progress and made corrections when necessary with the head contractor. The contractor initiated some beneficial

changes, which included the transition piece from the second rain garden to the infiltration trench and the reuse of the splash pads from another project on campus. Additionally, communication with the campus horticulturist, Hugh Weldon, was efficient and he chose plants to fit the unique conditions of the SCMs design and maintenance plan. The final part of the construction, completed by the same contractor but a different crew, involved re-routing the drainage pipes of the garage to direct stormwater runoff from the garage to the treatment train. This work was very quick and the contractor willingly adapted to some initial miscommunication and mistakes.

#### **3.2.2.2. Challenges**

Despite the contractors being willing and able to adjust to the specific design methods of the SCMs, there were a few challenges. One major initial problem was that the contractor spread grass seed along the berms which was not originally planned. However, the horticulturist had facilities blow away most of the seed from the berms and continued to use localized herbicide treatments to get rid of unwanted grass. Another issue at the site was not due to contractor errors, but from students and faculty walking through the site. Immediately following construction, many people walked through the swale and rain gardens, potentially compacting the media and reducing infiltration potential. In order to combat this problem, temporary construction fence was installed. Additionally, the increase in plants over the year and their increase in size somewhat deterred people from crossing the treatment train. However, after the fence was removed and even after the swale was filled in with plant growth, there are still issues with people walking through the site. This challenge may not have a permanent fix and hopefully as

plants continue to grow paths through the treatment train will become less desirable to those walking around campus.

### 3.3. Soil Analysis

The soil and media at the treatment train was analyzed in a variety of ways. Native soil samples were collected at the infiltration trench and in the upper and lower parts of the swale during excavation. These four samples were analyzed using a wash sieve analysis and hydrometer test. First, the ASTM D 2216 procedure to determine water content of the four samples (upper swale, lower swale, infiltration trench, and media) was completed. This water content was used to determine the initial mass of dry soil to ultimately determine the grain size distribution of each soil. Water contents for the wash sieve are displayed in *Table 3.4*.

**Table 3.4 – Water content of soils samples collected during construction**

Percent Water Content	
Upper Swale	3.66 %
Lower Swale	8.99 %
Infiltration Trench	3.41 %
Media	0.78 %

These samples were then analyzed with a wash sieve analysis since it could be assumed a majority of the samples were fines. The ASTM Method D422 was followed. Since a large portion of the soil passed through the number 200 sieve, the ASTM Method D422 hydrometer test was also completed. Once again, water content of the samples was determined to estimate the mass of dry soil used in the test. The estimates of the percent gravel, sand, and fines along with the U.S. Department of Agriculture (USDA) and Unified Soil Classification System (USCS) classifications are included in *Table 3.5*; the

grain size distributions of each sample are shown in the graph of *Figure 3.30*. From these distributions, it is evident for the upper swale and infiltration trench that there are large amounts of fines, as over 55% and 80%, respectively, passed through the number 200 sieve for these two samples. The media was more distributed and in the shape of a typical grain size analysis curve, which is expected since it was constructed for the site. The in-situ soils are all very similar in their characteristics, although the lower swale was more sandy and gravelly. From this testing and previous knowledge of soils on Villanova's campus, the in-situ USCS classification of the upper swale and IT is ML; the lower swale is SM. The hydraulic conductivity from these soils should be 0.036 cm/hr to 0.36 cm/hr. As discussed in Chapter 5, the soils may be performing better than this estimate as shown by the recession and infiltration rates at the infiltration trench.

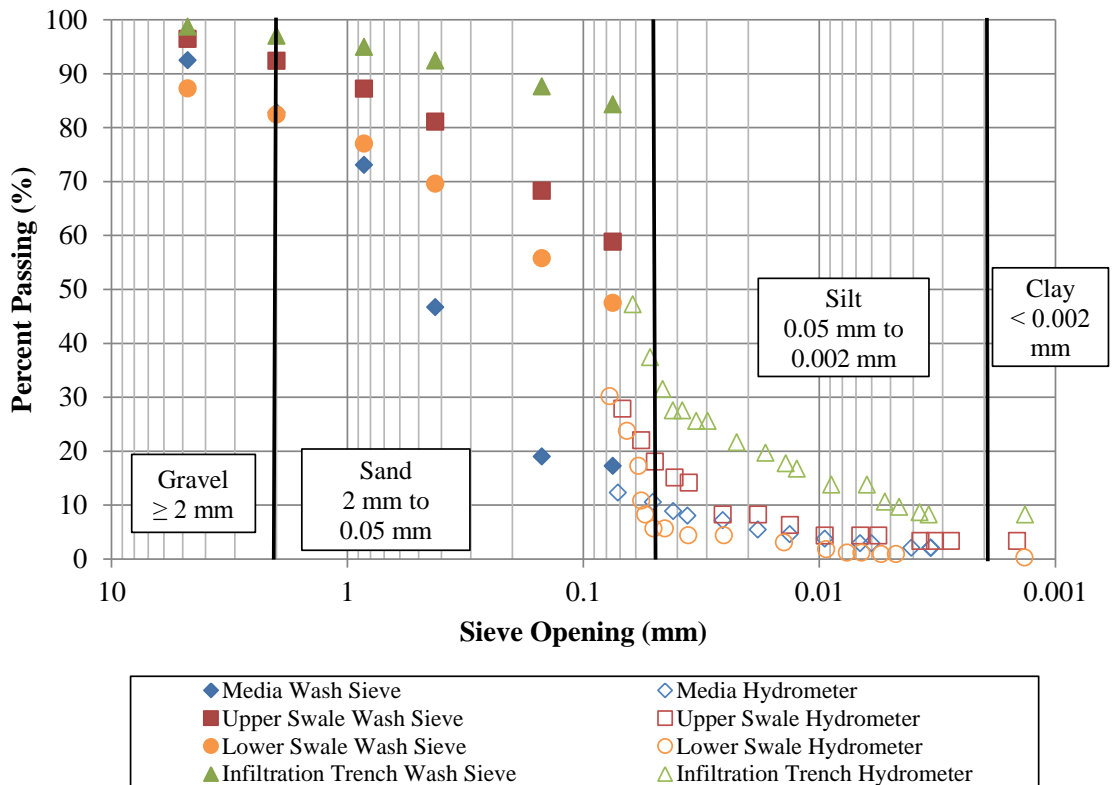


**Figure 3.30 - Wash sieve grain size analysis**

**Table 3.5 – Percent gravel, sand, silt, and clay for each soil sample and the classifications**

Soil	Gravel (%)	Sand (%)	Relative % Sand	Silt (%)	Relative % Silt	Clay (%)	Relative % Clay	USDA	Estimated Saturated Hydrologic Conductivity (cm/hr)	USCS
Media	17.2	72.8	87.9%	10.0	12.1%	0.0	0.0%	Gravelly Loamy Sand	5.0	SM
Upper Swale	7.6	74.4	80.5%	15.0	16.2%	3.0	3.2%	Sandy Loam	2.5	ML
Lower Swale	17.6	76.4	92.7%	5.0	6.1%	1.0	1.2%	Gravelly Sand	20.0	SM
IT	3.0	61.0	62.9%	28.0	28.9%	8.0	8.2%	Sandy Loam	2.5	ML

In addition to the wash sieve and hydrometer analysis, a nuclear density gauge test was completed to determine in situ weight and water content. This method followed ASTM standards D6938. A Troxler 2440 Moisture Density Gauge was used for this test procedure. Five locations were analyzed: the center of each rain garden, and the lower, middle, and upper swale. At the upper and middle parts of the swale (the beginning portion of the swale), hard soils were reached at 15.2 cm and 20.3 cm (6 in and 8 in), respectively. This is likely evidence of the in-situ soil beneath the media and topsoil. These depths are smaller than what was initially designed, but is likely due to the erosion of the swale media at the beginning of construction. At all other locations, the depth measurement was at 30.5 cm (12 in), indicating the media was still at least this deep. The in-situ dry unit weight, gravimetric water content, moist unit weight, and porosity are shown in *Table 3.6*.

**Table 3.6 - Summary of results from the nuclear density gauge test (in-situ values)**

Location	Dry unit weight (pcf)	Gravimetric water content (%)	Moist unit weight (pcf)	Porosity	Depth of measurement (in)
Upper swale	94.7	19.6	113.3	0.43	6
Middle swale	99.3	24.4	123.5	0.40	8
Lower swale	85.5	28.8	110.1	0.48	12
1st Rain Garden	81.8	21.4	99.3	0.51	12
2nd Rain Garden	80.4	20.0	96.5	0.51	12

## Chapter 4 Methods

### 4.1. Instrumentation and Monitoring Equipment

Treatment train monitoring consists of water quantity measurements throughout the system. The following sections describe the instrumentation installed at the site and some of the successes and challenges related to the installation and application to the data.

#### 4.1.1. Water Level and Flow

In order to measure flow through the treatment train, a system of weir plates were installed at several points: at the weir box (W1), in the middle of the swale (W2), at the end of the swale (W3), and at the end of each rain garden (W4 and W5) (*Figure 1.1*). These five weirs are used to calculate flow from a known head of water flowing over them. The weir plates, with a 90 degree v-notch, were machined to follow the USGS design and satisfy the equation  $Q(cfs) = 2.49h^{2.48}$ , where h is the head over the point of the v-notch in feet, which was measured by pressure transducers placed upstream of each v-notch weir (USBR 2001).

##### 4.1.1.1. CS450-L Pressure Transducer

The Campbell Scientific pressure transducers used (CS450-L) are shown in *Figure 4.1*. These sensors record pressure that is converted to a height of water, in feet, and have  $\pm 0.1\%$  accuracy. These pressure transducers were rated for 0 – 7.25 psig pressure, which accurately reads a maximum height of 5.09 m (16.7 ft), much higher than the maximum depth achievable at the site. The pressure transducer does not read the first 4.01 cm (1.58 in) of the probe if placed vertically, so the zero point of the device is not at its tip. This

offset is accounted for in the survey calculations. The output of the CS450-L is SDI-12 and the units are temperature compensated. The -L in the product name indicates that the length of the cable for each pressure transducer must be pre-selected; these lengths are later discussed in this section. The CS450s also provide temperature readings every minute, and this temperature data was also used for analysis. The temperature used in further analysis for each storm was averaged over the storm duration.



**Figure 4.1 - CS450-L**

At the treatment train, the accuracy of the pressure transducers is important due to the small amount of flow through the system. Often depths less than 2.54 cm (1 in) flow through the v-notch, so minimizing error is crucial in flow calculations. It was anticipated that there would be some drift in the pressure transducer reading, so optical level switch sensors were also installed to identify the point when water flows over the v-notch. These sensors, described later in section 4.1.1.2, were the OLS-10 purchased from Dwyer Instruments, Inc. The pressure transducer and optical level switch were installed in a 7.62 cm (3 in) perforated PVC pipe for protection and placed in a concrete base for stability. The pressure transducers were secured in the pipe with zip ties and the sensors were screwed into the side (the OLS-10 is a 0.5 inch male NPT fitting). *Figure 4.2* displays the pressure transducer casings in the laboratory and *Figure 4.3* shows them in the field at the treatment train.

The 0.91 m (3 ft) long pipes were set in a black, 5.08 cm (2 in) deep PVC cap and perforated to allow the pressure transducers to read water level flowing through the treatment train. The capped pipe was then placed into a plastic bin and Quikrete concrete was added to the bin up to the rim of the black cap, resulting in a 5.08 cm (2 in) deep concrete base for the casing. Once removed from the plastic bin, the pressure transducer casings were placed at the treatment train so that the top of the concrete was flush with the surface of the media. It was desirable to have the pressure transducer zero point below the v-notch in order to measure flow as it reaches the v-notch and spills over. The 5.08 cm (2 in) depth of the cap in the concrete casing is greater than the zero point [at 4.01 cm (1.58 in) from the bottom of the pressure transducer], thus this allows for the pressure transducer readings to begin before water flows over the weir.



**Figure 4.2 - Pressure transducer casing in the laboratory**



**Figure 4.3 – Pressure transducer casing in the field**

A survey was completed to determine the depth at which each pressure transducer should read when water flows over the v-notch (PT Zero to V in *Table 4.1*). The height at each concrete casing pad and the splash pad were directly recorded using survey equipment. On the downstream side of each weir, the point of the v-notch to the splash pad was measured with a tape measure to the nearest 1.59 mm (1/16 in). From these values and a series of calculations, the distance from the pressure transducer to the v-notch is known. *Figure 4.4* displays the measurements and defines each calculated parameter; *Table 4.1* summarizes the values from the survey in both metric and English units. To examine possible settling effects and check accuracy, several surveys were completed. All survey results are included in *Appendix C* but were not used in further analysis as the most recent survey, reported in *Table 4.1*, was determined to be most representative of field conditions. *Figure 4.4* demonstrates the measurement for the weir plates only in the swale and rain gardens. The weir box calculations are slightly different because the pressure transducer is below the surface of the splash pad (*Figure 4.5*), as indicated by the positive values for PT Concrete to V and Sensor to V (*Table 4.1*). The survey data was intended to solve for the depth from the pressure transducer to the v-notch to

ultimately identify the depth at which water should be flowing over the weir and a flow rate could be calculated.

Despite the apparent accuracy from repeatability in the survey, this method of calculating flow through the v-notch weir was not sufficient. Comparing the inflow to the weir measurements did not complete a mass balance and there were random increases and decreases in flow and volume throughout the system. The changes were not consistent from storm to storm or from weir plate to weir plate; the errors could not be modified to estimate flow since the values were not over- or underestimating the mass balance consistently. These errors are due to pressure transducer error or drifting, small flows, or back water effects. In addition, it is possible that the depth read by the pressure transducer was not equivalent to the depth at the weir plate since this is a more natural system and the soil may cause channelization or the surface to curve from the pressure transducer to the v-notch.

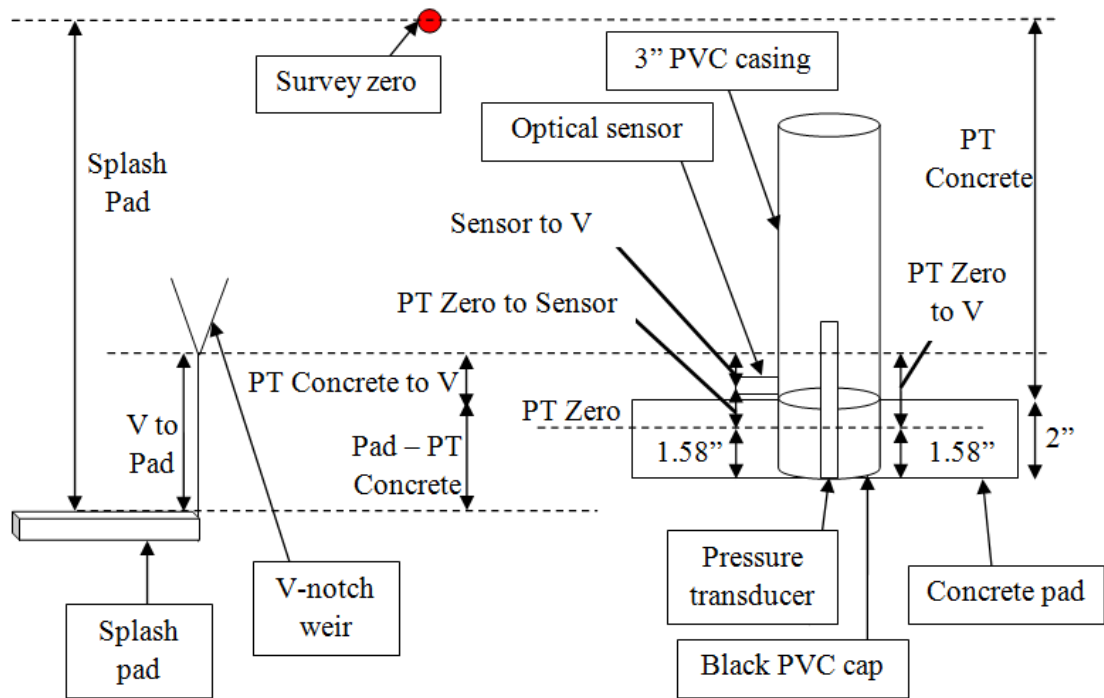
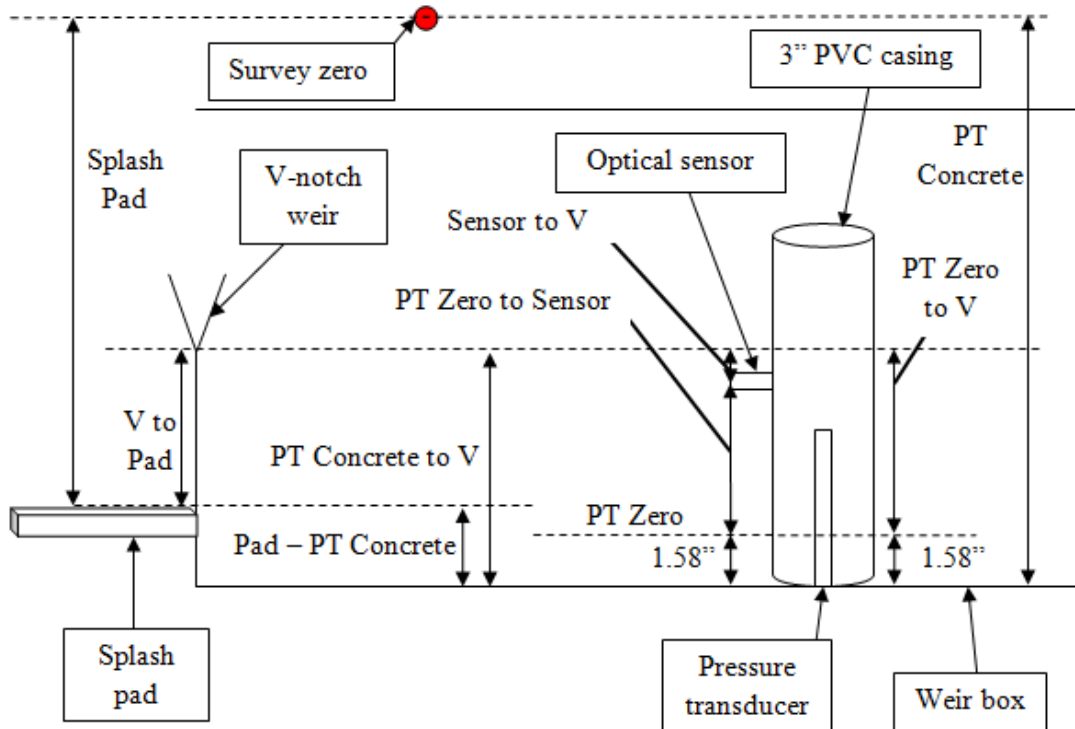


Figure 4.4 - Survey calculation diagram

Table 4.1 - Survey data for pressure transducers and sensors (top value in metric, bottom in English units)

Location	PT Concrete (cm) / (ft)	Splash Pad (cm) / (ft)	Pad - PT Concrete (cm) / (in)	V to Pad (cm) / (in)	PT Concrete to V (cm) / (in)	PT Zero to V (cm) / (ft)	PT Zero to Sensor (cm) / (in)	Sensor to V (cm) / (ft)
W1	156.972	109.118	66.694	13.653	61.506	<b>57.493</b>	57.175	0.318
	5.150	3.580	18.840	5.375	24.215	<b>1.886</b>	1.876	0.010
W2	165.811	165.811	0.000	6.350	-6.350	<b>-7.417</b>	4.559	-2.858
	5.440	5.440	0.000	2.500	-2.500	<b>-0.243</b>	0.150	-0.094
W3	223.114	231.343	11.470	13.970	-5.740	<b>-6.807</b>	4.559	-2.248
	7.320	7.590	3.240	5.500	-2.260	<b>-0.223</b>	0.150	-0.074
W4	242.316	249.326	9.770	15.875	-8.865	<b>-9.931</b>	4.559	-5.372
	7.950	8.180	2.760	6.250	-3.490	<b>-0.326</b>	0.150	-0.176
W5	254.508	276.758	31.010	29.845	-7.595	<b>-8.661</b>	4.559	-4.102
	8.350	9.080	8.760	11.750	-2.990	<b>-0.284</b>	0.150	-0.135



**Figure 4.5 - Weir box calculation diagram**

Each pressure transducer was routed to the data logger inside the parking garage through conduit as shown in *Figure 4.6*. The approximate locations of the six pressure transducers are represented by yellow dots, with the routing of their wires and conduit represented by the red lines (*Figure 4.6*). The location of the data logger, a Campbell Scientific CR1000, is noted by the green square. The pressure transducers are plugged into the CR1000 for continuous data collection averaging readings every minute. Each pressure transducer was given an ID for the database and an address for programming purposes. The pressure transducers were identified and addressed in order of their location in the treatment train. In the CR1000, the pressure transducers are plugged in as follows: the blue, white, and clear wires are grounds, the red is the 12V, and the black is the power ground. The white cord for each pressure transducer is the signal wire; they

are in the CR1000 COM ports as follows: TTW1-2 in C1, TTW3-4 in C3, and TTW5-6 in C5. C7 was left vacant for future use. *Table 4.2* shows the pressure transducer ID, SDI-12 address, cable length, and CR1000 COM port number. It was crucial to have enough cable to reach the data logger because adding more cable after receiving them from the factory is not possible, thus the length of cable was set when the pressure transducers were purchased.



**Figure 4.6 - Diagram of pressure transducer and sensor conduit to data logger** (Yellow dots represent pressure transducer locations and red lines indicate their wiring route)

**Table 4.2 - Pressure transducer information**

Pressure Transducer ID	SDI-12 Address	Wire Length (m) / (ft)		COM port
TTW1	1	9	30	C1
TTW2	2	24	80	C1
TTW3	3	30	100	C3
TTW4	4	38	125	C3
TTW5	5	40	130	C5
TTIT	6	46	150	C5

**4.1.1.2. Optical Level Switch**

The optical level switch, OLS-10, purchased from Dwyer Instruments, Inc., was intended to detect water at the exact level of the v-notch and send a “wet” signal to the data logger. An image of the sensor is shown in *Figure 4.7*. Once this sensor is dry, it sends a “dry” signal to the data logger to signify the pressure transducer reading is below the v-notch weir and flow should no longer be calculated. In the laboratory, the sensor was screwed into the side of a PVC pipe horizontally and the PVC with the sensor was placed in a flume. A tape measure was taped to the side of the flume for measuring consistency and as the flume water level increased and decreased the level was recorded as the sensor switched from “wet” to “dry.” The sensor sent a “wet” signal when water was slightly above the center point but turned “dry” at various points as water level decreased. The inconsistency in the measuring was considered an acceptable error since the largest difference was 0.87%. The sensors were then installed in the field in the PVC casings.

The sensors, similar to the pressure transducers, were identified by their order in the treatment train in both the programming code and database. In the CR1000, the sensors are plugged into differential channels one through five. The green wires from each high

port are connected to the 5V port with an additional piece of wire. The black wire is the ground and the red is the 12V power for each sensor. Their conduit follows the same pattern as the pressure transducers (*Figure 4.6*), and their database and programming IDs are simply TTS1, TTS2, TTS3, TTS4, and TTS5. Programming code for data collection along with a wiring diagram is included in *Appendix D-1 and D-2*. There is not a sensor in the infiltration trench since there is not a v-notch weir at this location. The cable length of each optical sensor was originally three feet in length and was extended by soldering 22-gage wire to a similar length of each corresponding pressure transducer.

It was also difficult to install the optical light switches directly at the point of the v-notch; they were installed in the casings so that their center point was 7.62 cm (0.25 ft) from the bottom, or 4.57 cm (0.15 ft) from the pressure transducer zero point. The sensors were included in the survey data to identify the distance of the sensor to the v-notch to ultimately calculate what pressure transducer reading and “wet” signal indicate flow over the weir. In addition to the inaccuracy of the sensors in the laboratory, upon installation in the field, it was discovered that these sensors were not only triggered by water, but also by sunlight. In order to block the sunlight and keep the sensors reading “dry” until water completes the signal, small PVC caps were cut and installed inside each pressure transducer casing, as seen in *Figure 4.8*.



**Figure 4.7 - Optical level switch**



**Figure 4.8 - Cap installed to block sunlight**

In the weir box, the sensor was installed directly to the side of the concrete wall near the outflow or weir plate. The sensor was intended to be as close to the exact point of the v-notch as possible to provide a “wet” signal that did not require adjustments. As previously reported (*Table 4.1*), the sensor was installed 0.318 cm (0.01 in) below the v-notch, therefore, it reads a wet/dry signal that is not directly aligned with water flowing over the v-notch. This difference was estimated from the survey data, but it appeared that

the measurement was not exact and consistent enough to relate to the pressure transducer data to ultimately estimate the flow.

#### **4.1.2. Instrumentation Success and Challenges**

The intention of the pressure transducers and sensors throughout the treatment train was to quantify the stormwater volume and flow during rainfall events. Villanova's SCM Park includes numerous research sites with pressure transducers and v-notch weirs that provide sufficient flow data. Thus, this technique was used at the treatment train and provided a simple flow calculation. The sensors were intended to turn off and on to signal the exact points of water flowing over the v-notch weir to confirm calculations. At the treatment train, calculating the flow and ultimately the volume of stormwater through the system has not been accurate using the method initially installed. The pressure transducer accuracy over the operating range is too large [ $\pm 0.1\%$  of  $5.09 \text{ m} = 0.005 \text{ m}$  ( $5 \text{ mm}$ )] for the small depth measurement that is observed in the swale and rain gardens ( $< 0.40 \text{ m}$ ). The error is accentuated by being raised to 2.48 in the weir equation ( $Q = 2.49h^{2.48}$ ) resulting in inaccurate readings of water flowing over the weir, and ultimately over or under estimating the flow. In addition to the potential error within the monitoring equipment, the potential for settling, and the need to continue to re-survey is challenging for computational consistency.

Since measuring flow and volume through the treatment train is a major portion of the project goals, fixing the errors was a priority. New instrumentation has been considered for increased water level measurement accuracy. A Gems XT-1000, pictured in *Figure 4.9*, was tested in the laboratory and ordered for installment in the weir box. This measurement device, a magnetic level, has a much higher accuracy than the pressure

transducers (up to  $\pm 0.2$  mm). The level sensor output is 4 to 20 mA, is temperature compensated, and the probe length was measured for site specific implementation at the weir box. The version chosen was the screw-in unit to allow for minor height adjustments in during installation. The device was not installed at the time of this thesis, but a calibration method is included in *Appendix E* for reference.



**Figure 4.9 - Gems XT-1000**

## **4.2. Rainfall**

Rainfall data was collected and analyzed to determine how much runoff was captured by the treatment train. The following sections describe how rainfall was analyzed for intensity and duration and how infiltration trench data is manipulated to determine the treatment train performance.

### **4.2.1. Rainfall Measurements**

A tipping bucket rain gage (*Figure 4.10*) was previously installed on top of the parking garage for another research site and was used for treatment train data analysis. The rain

gage is an American Sigma Bucket Rain Gage Model 2149 and measures 0.0254 cm (0.01 in) of rainfall per bucket tip at 0.5% accuracy for 0.5 in/hr, it is connected to a CR1000 and records the total depth every minute. There are no structures or vegetation round the rain gage to interfere with rainfall measurements. The rain gage was calibrated to ensure accuracy prior to data collection at the treatment train. Maintenance of the rain gage should include periodically checking to make sure the tipping bucket functions correctly, it is level, and that there is no debris clogging the screen or funnel collection piece.



**Figure 4.10 - Tipping bucket rain gage on the parking garage adjacent to the treatment train**

#### ***4.2.1.1. Rainfall Duration***

A few parameters were determined from the rain gage data. One of the major components of the rainfall data was the duration (d). Rainfall duration was calculated as the total time of rainfall; the time from the first 0.254 mm (0.01 in) to the final 0.254 mm (0.01 in) was included.

#### 4.2.1.2. *Rainfall Intensity*

Combining the rainfall volume and duration resulted in the calculation of the storm intensity. Three types of rainfall intensity were analyzed as each storm presented a unique type of rainfall distribution. The first storm intensity method (*Equation 4.1*) included the total time ( $d$ ) (hrs) and the total rainfall ( $rain_{tot}$ ) (cm), resulting in a calculated total intensity ( $i_1$ ) in cm/hr:

$$i_1 = \frac{rain_{tot}}{d} \quad (\text{Equation 4.1})$$

The other two intensities focused on the first 0.635 cm (0.25 in) of rainfall as the early part of a storm has been observed to be at a relatively low intensity and may artificially lower the overall storm intensity. The second storm intensity method ( $i_2$ ) was calculated by dividing the total rainfall volume by the total time minus the time to the first 0.635 cm (0.25 in). The initial time was reduced to eliminate the time of the low intensity at the start of a storm (*Equation 4.2*)

$$i_2 = \frac{rain_{tot}}{(d - \text{time to first } 0.635 \text{ cm})} \quad (\text{Equation 4.2})$$

The third method of storm intensity ( $i_3$ ) examined was calculated by dividing the total rain less the first 0.635 cm (0.25 in) by the total time minus the time to the first 0.635 cm (0.25 in). This intensity method removed both the volume and time of the first 0.635 cm (0.25 in) again to not artificially lower the intensity in the early part of a storm (*Equation 4.3*).

$$i_3 = \frac{(rain_{tot} - 0.635 \text{ cm})}{(d - \text{time to first } 0.635 \text{ cm})} \quad (\text{Equation 4.3})$$

### 4.3. Water Quantity Measurements

Depth readings from the infiltration trench (IT) pressure transducer were considered accurate for analysis since the depth is much greater than in other parts of the system, thus minimizing the error. Thirty storms were considered for analysis, and one did not reach the infiltration trench. The storms were chosen randomly from the downloaded data but were selected due to the ability to analyze the infiltration trench data as it relates to the treatment train. In the future, it should be a priority to setup and maintain a database to automatically analyze the large amount of data available at the treatment train. With more storm data, a more thorough analysis can be made about SCMs in series.

As mentioned in Chapter 3, the IT, which is the final SCM of the system, is not connected to the traditional storm sewer drain. Instead, stormwater can only exit the trench by infiltrating out of the bottom and sides of the IT or as overflow through the top. The pervious pavers at the surface of the IT allow for excess ponding to build up and runoff as necessary into the nearby storm drain. *Figure 4.11* shows some ponding on the pavers and runoff on the pavers during a May 2012 storm, with little flow making it to the storm drain in the upper right corner of the image. Recession and infiltration rates in the IT were determined in increments of 0.305 m (1 ft), where 0-0.305 m (0-1 ft) is the bottom of the trench and 0.914-1.280 m (3-4.199 ft) is the top of the trench. The highest range for calculations (0.914 m – 1.280 m) is slightly larger since the crates are taller than exactly 4.20 feet (1.280 m).



**Figure 4.11 - Ponding and runoff on the pervious pavers at the IT (May 2012)**

#### **4.3.1. Infiltration Trench Recession Rate Calculations**

The infiltration trench pressure transducer for each storm was graphed as a scatter plot of depth (m) vs. time (hrs). For each storm, the slopes of the falling limbs of the graphs were calculated to determine recession rates. These rates were not only determined on a storm basis, but also in four depth increments since slope of the falling limb slightly changed as the head in the IT decreased (see *Figure 4.12* for reference). Points taken from each depth increment were solved for recession rate (R) by *Equation 4.4*:

$$-R = \frac{y_2 - y_1}{x_2 - x_1} \quad (\text{Equation 4.4})$$

where  $y_1$  and  $y_2$  are depth measurements (m) and  $x_1$  and  $x_2$  are the corresponding times in hours. Since there is a negative slope, the negative of R is considered as the recession rate of water infiltrating into the ground. The recession rates were converted to cm/hr for further analysis.

### 4.3.2. Infiltration Trench Infiltration Rate Calculations

The sides of the old infiltration trench (OIT) at Villanova were shown to have significant infiltration out of the sides of the OIT, not just the bottom (Emerson 2008). Therefore, the recession rate was converted to an infiltration rate in order to account for the entire surface area of stormwater leaving the infiltration trench. First, the recession rate was converted into a flow rate or volume of water leaving the bottom of the tank by multiplying the recession rate (R) (m/hr) by the bottom area (5.435 m<sup>2</sup>). This new volume of infiltration in m<sup>3</sup>/hr was divided by the total surface area of the five sides where stormwater can leave the IT (bottom and four sides). This total surface area (SA) (m<sup>2</sup>) is calculated from *Equation 4.5* where z is the maximum height in the incremental depth range for the particular infiltration rate in meters. The total width and length of the tanks are 4 m and 5.720 m, respectively. These values are reflected in calculating the surface area in the following equation. The height of the tanks is 1.280 m (4.20 ft) (*Table 3.2*). Infiltration rates (I), were solved for by applying *Equation 4.6*.

$$SA = (z * 4m) + (z * 5.720m) + (5.435m^2) \quad (\text{Equation 4.5})$$

$$I = \frac{(R(\frac{m}{hr}) * (5.435 m^2))}{SA} \quad (\text{Equation 4.6})$$

### 4.3.3. Statistical Analyses

For both the recession rates and infiltration rates, box and whisker plots and t-tests were completed. These were intended to show the trends between each depth range as well as from the top to bottom of the infiltration trench.

#### **4.3.3.1. Box and Whisker Plots**

Box and whisker plots of the recession and infiltration rates at each depth increment were created to compare the data using the following values: minimum, lower quartile (Q1), middle quartile (Q2), upper quartile (Q3), and the maximum. These plots allowed for a display in the differences of rates per depth increment to be observed.

#### **4.3.3.2. Student's T-test**

A student's t-test was completed on some of the data from the treatment train. First, the recession and infiltration rates at each depth increment were compared to analyze their potential statistical significance. Each range was compared with those above and below it, in addition to the highest and lowest being compared. For these analyses, the Microsoft Excel function Student's t-test was applied (T.Test). The arrays were chosen based on the ranges being compared, a two-tailed test was selected, and a two-sample, unequal variance test was chosen. This method was chosen since no hypothesis was made and it was unknown whether the standard deviations were considered similar. In addition, the sample sizes for each case (rates calculated per depth range) were not consistent, so the unequal sample population size required type 3 tests.

#### **4.3.3.3. Correlation Test**

A correlation test was applied to compare the recession and infiltration rates to the average temperature for each storm. The correlation value was determined using Microsoft Excel and comparing the recession and infiltration rates to the corresponding temperatures. Once the correlation was determined, a test was run to determine if the correlation was significant. The single correlations were each tested against zero for significance. Assuming two-sided significance level of  $p = 0.05$ , the  $t_{(n-2)}$  value (*Equation*

4.7) must be greater than critical t-value (Bobko 2001). The  $t_{n-2}$  value for each depth increment was determined by:

$$t_{n-2} \sim \frac{r\sqrt{n-2}}{\sqrt{1-r^2}} \quad (\text{Equation 4.7})$$

where  $r$  is the correlation coefficient for the depth increment and  $n$  is the sample size. This type of test was chosen to ultimately determine if the recession and infiltration rates for each depth increment could be determined statistically dependent on the temperature. If the  $t_{n-2}$  value is greater than the t-critical determined assuming  $\rho = 0$ , the correlation is determined significant; the recession or infiltration rate would be determined dependent on temperature.

#### 4.3.4. Treatment Train Inflow

Volume into the treatment train ( $V_{in}$ ) in cubic meter was based on the amount of rainfall less initial abstractions over the contributing area. The  $V_{in}$  was solved for based on the initial abstractions of the SCS Curve Number (CN) equation. The initial abstraction was solved from  $I_a = (0.2*S)$  where  $S = ((1000/CN)-10)$  and the CN is 98. The volume into the treatment train was then solved using *Equation 4.8*:

$$V_{in} = (P - I_a) * \frac{1}{12} * A \quad (\text{Equation 4.8})$$

where volume ( $ft^3$ ) is solved from  $P$  (precipitation (in)),  $I_a$  ( $0.2*S$ ), and  $A$ , the contributing area in  $ft^2$ , (measured as  $10,000 ft^2$ ). The cubic feet of volume of inflow was converted to cubic meters by multiplying by a factor of 0.0283.

#### 4.3.5. Infiltration Trench Inflow

While the inflow from the parking garage estimates the stormwater volume loaded to the entire treatment train, the inflow into the infiltration trench as a single entity is also an important value in examining the performance of the system. The volume into the infiltration trench (VIT) was calculated two different ways. These methods were based on the recession or infiltration rate, time of stormwater in the infiltration trench, and the area corresponding to the recession or infiltration rate. The volume into the IT from the recession rate ( $R_{avg}$ ) ( $VIT_R$ ) was determined by *Equation 4.9*:

$$VIT_R = T_{IT} * \frac{R_{avg}}{100} * A_{bot} \quad (\text{Equation 4.9})$$

where  $T_{IT}$  is the time of water present in the IT (hrs),  $R_{avg}$  is the average recession rate (cm/hr) during the storm, and  $A_{bot}$  is the bottom area of the tank (5.435 m<sup>2</sup>). The volume into the IT was also calculated from the infiltration rate ( $VIT_I$ ) (*Equation 4.10*):

$$VIT_I = T_{IT} * \frac{I_{avg}}{100} * SA_{avg} \quad (\text{Equation 4.10})$$

where  $T_{IT}$  is the time of water present in the IT (hrs),  $I_{avg}$  is the average infiltration rate (cm/hr) during the storm, and  $SA_{avg}$  is the surface area determined by ( $A_{bot} + (4 * PT_{avg}) + (5.72 * PT_{avg})$ ). This surface area is the bottom surface of the crates plus sides times the average height in the IT during the storm. The average height in the IT during each storm was determined by the maximum height divided by 2.

#### 4.3.6. Infiltration Trench Overflow

Periods of overflow of stormwater from the infiltration trench were observed; this volume was related to the inflow to calculate the performance of the treatment train. Overflow

was estimated when the pressure transducer depth remained constant at depths of 1.330 m (4.363 ft) or higher. This depth was the bottom of the trench to the top of the pavers; it was determined as the crate height (1.280 m; 4.199 ft) plus the paver height (50 mm; 0.164 ft). Since the pressure transducers are susceptible to drifting and error and the pressure transducer may shift from its vertical position, if the pressure transducer data remained steady at a depth over 1.280 m (4.199 feet) overflow was also considered. Overflow was estimated by *Equation 4.11*:

$$V_{over} = R * \frac{1 \text{ m}}{100 \text{ cm}} * d * A_{pavers} \quad (\text{Equation 4.11})$$

where  $V_{over}$  ( $\text{m}^3$ ) is calculated where R (maximum recession (cm/hr)), d is the storm duration (hrs), and  $A_{pavers}$  (area of the pavers) is the area of overflow. The maximum recession rate was chosen to calculate  $V_{over}$  since it was the highest rate of water measured leaving the tank; it is assumed overflow occurs when water entering the tank is faster than the exit rate. The recession provides the maximum rate and ultimately the maximum volume of infiltration trench overflow. The total area of the 30 pavers is  $4.8 \text{ m}^2$ . Knowing the volume into the treatment train and the volume of overflow at the infiltration trench, the volume of treatment train capture ( $V_{capt}$ ) ( $\text{m}^3$ ) can be determined (*Equation 4.12*):

$$V_{capt} = V_{in} - V_{over} \quad (\text{Equation 4.12})$$

#### **4.3.7. Calculation Examples**

The August 14, 2012 data is used as an example of how calculations were completed and rates and volumes were determined (*Figure 4.12*); this set of data has one rising and falling limb and provide simple calculations. To calculate the recession rate for each

depth increment, points were chosen to determine the slope of that portion of the receding limb of the graph. In the August 14, 2012 dataset (*Figure 4.12*), the total rainfall depth is 3.68 cm (1.45 in), the peak depth is 1.236 m (4.055 ft). For the highest range (between the orange and blue dashed lines), a point just after the peak and just before the next depth range (0.914 m) were used to determine the recession. This pattern was repeated for each depth range; depths and corresponding times were chosen just inside the upper and lower limits. The orange, blue, purple, and green dashed lines in the graph represent the breakdown of the ranges used for calculating recession and infiltration rates. The pressure transducer readings are taken every minute, so the minute data was converted to hours to calculate recession rates. In this example, the first point was at hour 2.217 (133 min) and 1.208 m (3.963 ft) and the second point was at 5.067 hrs (304 min), 0.937 m (3.073 ft). For example (*Equation 4.4*),  $-R = \frac{(1.208 \text{ m} - 0.937 \text{ m})}{(2.217 \text{ hrs} - 5.067 \text{ hrs})} = 9.518 \text{ cm/hr}$ . *Equation 4.4* was applied to all depth increments to solve for recession rates. *Table 4.3* displays the data points from the August 14, 2012 example and the resulting recession rates.

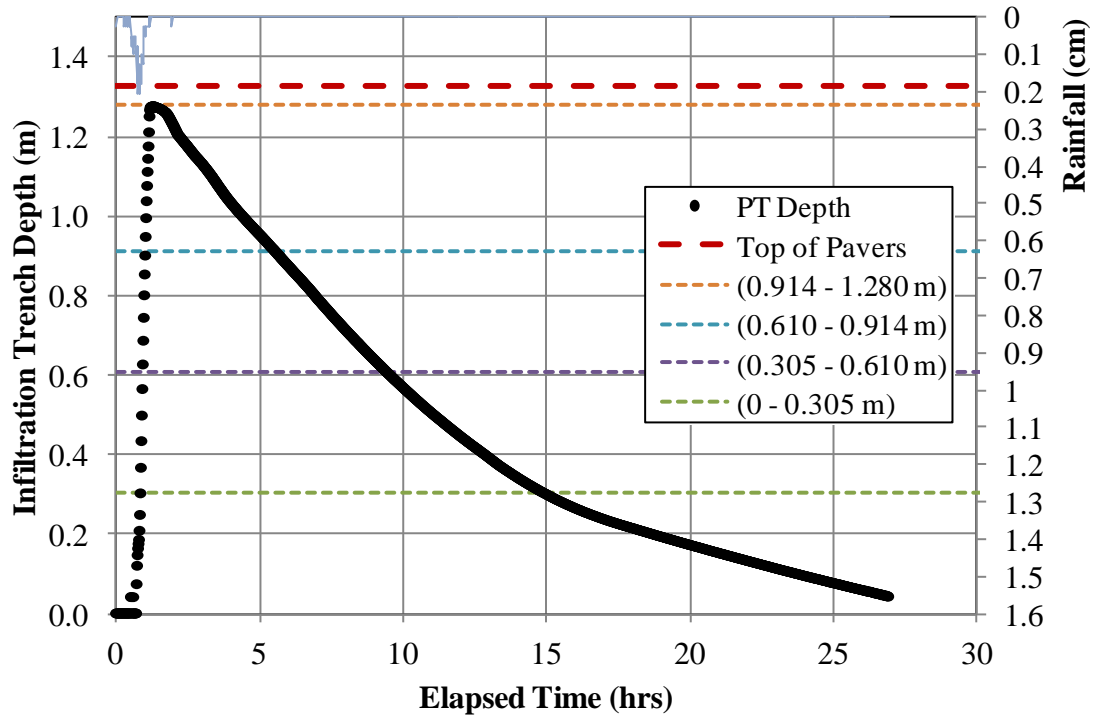


Figure 4.12 - August 14, 2012 IT pressure transducer depth and rainfall (orange, blue, purple, and green dashed lines represent the depth increments analyzed for recession and infiltration rates)

Table 4.3 - Recession rates for August 14, 2012 storm event

Depth Increment (m)	Point 1			Point 2			Recession Rate (cm/hr)
	(min)	(hrs)	(m)	(min)	(hrs)	(m)	
0.914-1.280	133	2.217	1.208	304	5.067	0.937	9.518
0.610-0.914	336	5.600	0.912	550	9.167	0.613	8.366
0.305-0.610	567	9.450	0.593	835	13.917	0.323	6.039
0-0.305	871	14.517	0.295	1568	26.133	0.018	2.388

In the example, the largest depth range (0.914 m - 1.280 m) had a recession rate of 9.518 cm/hr. This rate, first multiplied by the bottom area ( $5.435 \text{ m}^2$ ) results in a flow rate of  $0.505 \text{ m}^3/\text{hr}$ . The total surface area for this depth increment, from Equation 4.2, where  $z = 1.219 \text{ m}$ , is  $17.158 \text{ m}^2$ . Dividing the flow rate of  $0.505 \text{ m}^3/\text{hr}$  by the total surface area ( $17.158 \text{ m}^2$ ) results in an infiltration rate of  $0.0294 \text{ m/hr}$ , or  $2.943 \text{ cm/hr}$ . The remaining results for the infiltration rates of the August 14, 2012 storm are included in Table 4.4.

The infiltration rates (cm/hr) in the last column of *Table 4.4* for the August 14, 2012 storm event show how converting the recession rate to an infiltration rate levels normalizes the effects of the head in the infiltration trench and results in similar infiltration rates, although the lowest depth range has a slower rate. In this example, there was no overflow estimated, so the capture performance is 100%.

**Table 4.4 - Recession rates from August 14, 2012 converted to infiltration rates**

Depth Increment (m)	Point 1			Point 2			Recession Rate (cm/hr)	Rate (m <sup>3</sup> /hr)	A (m <sup>2</sup> )	Infil Rate (m/hr)	Infil Rate (cm/hr)
	(min)	(hrs)	(m)	(min)	(hrs)	(m)					
0.914-1.280	133	2.217	1.208	304	5.067	0.937	9.518	0.505	17.158	0.0295	2.945
0.610-0.914	336	5.600	0.912	550	9.167	0.613	8.366	0.444	14.197	0.0313	3.129
0.305-0.610	567	9.450	0.593	835	13.917	0.323	6.039	0.321	11.234	0.0285	2.854
0-0.305	871	14.517	0.295	1568	26.133	0.018	2.388	0.127	8.272	0.0153	1.533

Knowing the time at which depth recording began allowed for the amount of rain that fell before flow reached the IT to also be determined. The August 14, 2012 storm also demonstrates the typical trend with the rainfall data and the infiltration trench depths. For this storm, there was 0.72 hours (43 min) from the time the first 0.0254 cm (0.01 in) of rain fell to the time depth was visible in the IT. The amount of rainfall during this period was 1.04 cm (0.41 in).

The August 14, 2012 storm provides a simple example of the process followed to determine the IT recession and infiltration rates. As previously mentioned, if the depth in the IT peaks more than once, the recession and infiltration rates may be calculated multiple times for the same range. For example, there are three rates calculated for the highest range (0.914 – 1.280 m) from the 4.70 cm (1.85 in) September 2, 2012 storm (*Figure 4.13*). The September 2, 2012 storm also shows the continued performance during back to back storms. Rainfall continued into September 3, 2012 and the IT then

began to empty. As noted in the graph, the data stops on September 4, 2012 at 12:38 PM. However, on September 4, 2012 at 2:38 AM rain once again began to fall (*Figure 4.14*). This is difficult to see in the graph, but there were a few minutes of 0.0254 cm (0.01 in) where rain occurred. The IT did not increase in depth again until 9/4/2012 at 12:42 PM. *Figure 4.14* starts as soon as that first 0.0254 cm (0.01 in) of rain fell on September 4<sup>th</sup>, which overlaps the graph from *Figure 4.13*. Despite another 1.32 cm (0.52 in) of rain falling, the site manages the stormwater and the IT does not overflow during the second rain event.

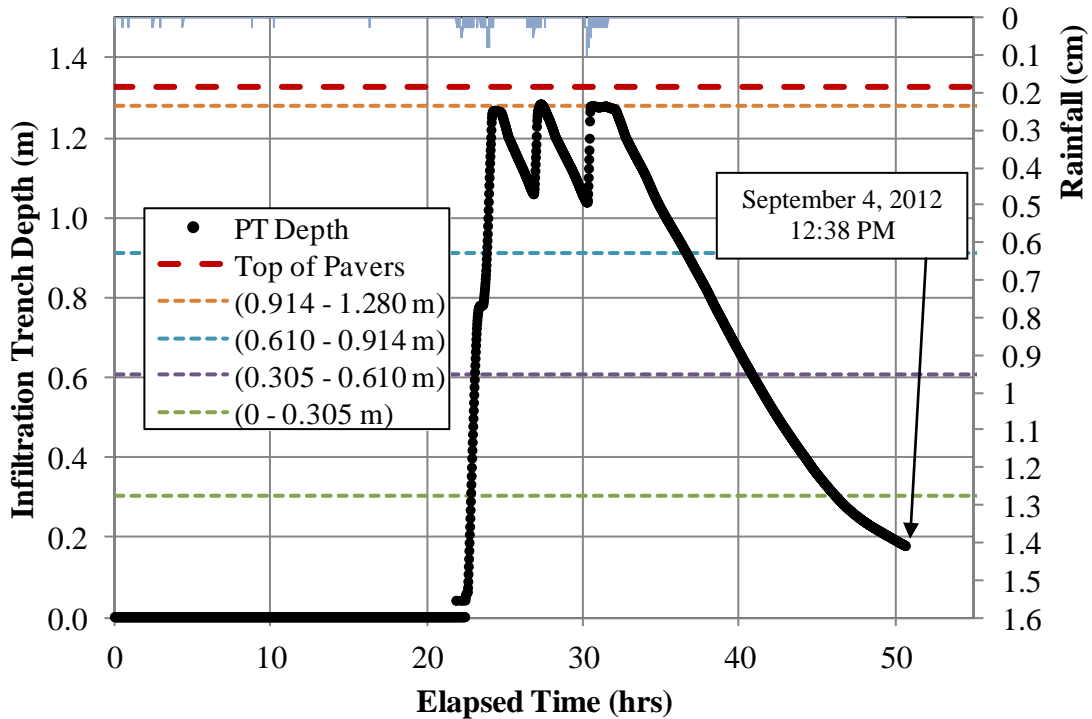


Figure 4.13 - September 2, 2012 infiltration trench storm data

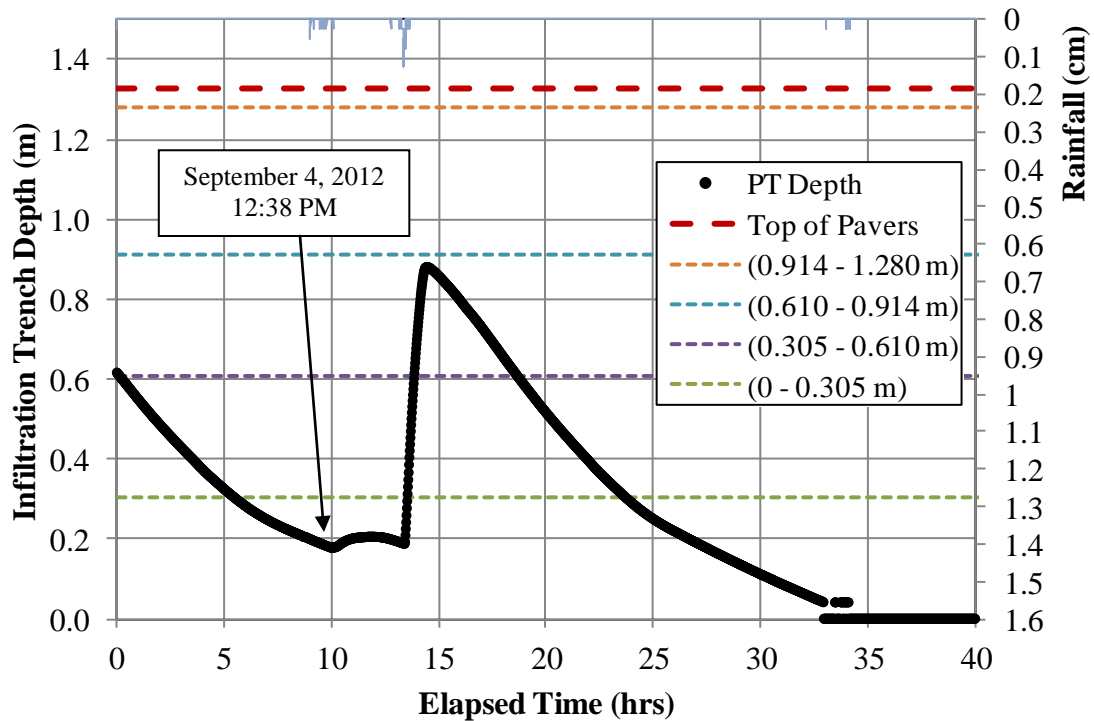


Figure 4.14 - September 4, 2012 infiltration trench storm data

The IT pressure transducer data was manipulated for analysis. Recession and infiltration rates were calculated from the direct raw data, but graphically the data was shifted to account for the first 4.01 cm (1.58 in) the pressure transducer does not read. This value makes a difference when ultimately looking at the depth in the IT related to overflow. Therefore, in *Appendix F-2* with the graph of each storm (later referred to in Chapter 5), 4.01 cm (1.58 in) was added to each raw data point. In addition to the zero point of the pressure transducer, an additional 0.061 cm (0.024 in) of drift was common in the readings. Therefore, raw data was set as a zero until the depth read at least 4.07 cm (1.604 in; 0.134 ft). This also allowed for a clear break in the data to identify when depth in the IT began (*Figure 4.14*).

#### 4.3.8. Old Infiltration Trench

Another, old infiltration trench (OIT) site on Villanova's campus will be compared to the treatment train infiltration trench. The OIT is highlighted in red and located on the left side of the parking garage in *Figure 4.15* the treatment train is highlighted by the yellow circle. The OIT was constructed in 2004 and the contributing area is half of the parking garage, about 1,900 m<sup>2</sup> (20,000 ft<sup>2</sup>). This site was intentionally undersized with a loading to SCM ratio of 150 to 1; the treatment train ratio is approximately 7 to 1. The large ratio of the OIT was intended to demonstrate longevity effects and age the system much faster than if it were designed to PA BMP Manual (2006) standards. The OIT data provided results that are comparable to the IT.



**Figure 4.15 - Aerial image of the treatment train (yellow) and old infiltration trench (red)** (Adapted from Google Maps)

#### 4.4. Water Quality Measurements

Measuring water quality at points along the treatment train is intended to demonstrate the system's ability to filter pollutants and ultimately improve the quality stormwater runoff. Ideally, water quality measurements would be taken immediately following the completion of construction of the SCMs. Unfortunately, a plan for water quality

measurement was not complete and the first set of grab samples were not taken at the site until October, 2012 even though the site began receiving stormwater in March, 2012. The site required extra work to prevent erosion issues and the water quantity instrumentation also required more work than expected. In October, samples were collected at the weir box and at the second rain garden at the beginning and end of Hurricane Sandy on October 28 and 30, 2012. These samples were tested for total suspended solids, total dissolved solids, pH, conductivity, chlorides, nitrogen, and phosphorus species. After this storm, it was determined that when permitted with coordination of other sites requiring testing, samples would be taken at the treatment train. Typically this implies the second storm of the month will be collected at the site. Testing focuses on the previously mentioned water quality indicators until further analysis is complete.

#### **4.4.1. Water Quality Collection Procedures**

Water quality samples at the treatment train are collected as grab samples. A clean bottle from the laboratory is used to obtain samples and return them to the lab. While various methods may be considered in the future, such as first flush samplers and autosamplers, at this time, mainly due to cost, samples will be collected by hand during storm events. Grab samples are to be taken after approximately 0.254 – 0.762 cm (0.1 – 0.3 in) of rain has fallen and again when the rainfall has ceased. The timing of collection can be difficult since the first set should be taken as soon as stormwater has reached all locations, and the final set should be collected after the rain has stopped but before the system is dry. Samples are planned to be taken at six locations and include the weir box, middle of the swale, end of the swale, the end of each rain garden, and the infiltration

trench. Since the system is designed for a 2.54 cm (1 in) storm, it should be expected that samples will only be available at the weir box and possibly in the middle of swale for the initial collection.

One of the difficulties of collecting samples as grab samples is timing the collection in correspondence with the rainfall event. Some of the sample locations or SCMs may not have water available for collection due to not only this timing, but the size of the storm. Therefore, the second set of samples should be collected immediately following the end of a storm to improve the likelihood of stormwater being at each sampling location. If a storm was too small to reach each SCM or if water infiltrated or moved downstream too quickly to provide a sample at the end of the storm, the reason for missing samples should be noted in the event sheets by the graduate student who completed the collection. When collecting grab samples, site disturbance should be minimal to prevent unnecessary soil particles from entering the bottle.

#### **4.4.2. Water Quality Testing Procedures**

Following sample collection, water quality tests for nutrients, chlorides, pH, conductivity, and solids. Testing procedures are to be completed following standard methods by graduate students and the laboratory manager. Water quality testing procedures can be obtained from the quality assurance project plans (QAPP) of the Villanova Stormwater Control Measure Research and Demonstration Park. However, as testing at the treatment train becomes standard, a QAPP specific for the site will need developed.

## **Chapter 5 Water Quantity Analysis**

### **5.1. Water Quantity Research Goals**

The research goals for the treatment train as an entire project include evaluating both water quantity and quality impacts along with maintenance and longevity effects of placing SCMs in series. Specifically for water quantity impacts, the research plan is to assess the volume removal and peak flow reduction abilities of the entire treatment train as system and each individual entity. Project construction was completed in March 2012 and water quantity measurements began in July 2012; as such, data analysis for this thesis spans from July 2012 to March 2013.

The treatment train was observed to function well, however thoroughly quantifying the hydrology was difficult due to monitoring challenges with the instrumentation. Research for this thesis focused on defining inflow to and outflow from the treatment train and examining the capture performance as it relates not only to rainfall volume, but also rainfall intensity and duration. In addition to analyzing the quantity impacts as related to capture performance, the system's potential maintenance and longevity effects were studied. Although the flow data was not accurate through the treatment train (i.e. swale and rain gardens), the depth data from the pressure transducer in the infiltration trench was acceptable and infiltration trench performance was analyzed.

### **5.2. Infiltration Trench Data**

The infiltration trench (IT) at the treatment train was monitored with a pressure transducer that measured depth (in feet) over time that was used when analyzing rainfall events. During storm events, it is apparent when water begins to flow into and pond in

the trench and when inflow recedes and infiltration is the sole mean of outflow. The graphs of each storm demonstrate these trends, in addition to how much rainfall was recorded during the event (*Appendix F-1*); as mentioned in Chapter 4, the raw data was slightly shifted to account for the zero point of the pressure transducer. The maximum depth in the IT was at the top of the crates (1.280 m) or above the pavers (1.330 m) to induce overflow, which are indicated along with precipitation depths and the lag time before water accumulated in the IT (*Appendix F-2*).

In order to examine the IT and to ultimately compare its performance to literature and other sites, recession and infiltration rates were computed. The recession rates for each storm evaluated were calculated directly from the pressure transducer readings as the slope on the falling limb of the graph of depth vs. time. This recession rate did not directly account for flow leaving the entire area of the IT; it was simply a measure of the water level change over time. The infiltration rate (*Equation 4.6*), converted from the recession rate (*Equation 4.4*), accounts for the entire surface area where stormwater could exit the IT.

### **5.2.1. Infiltration Trench Recession Rates**

Recession rates at the infiltration trench were calculated using the individual storm graphs, with pressure transducer (PT) depths and the depth to the top of the pavers (*Appendix F-1*), and presented in the data calculations table (*Appendix F-3*). Since the level of the infiltration trench was broken into four depth increments, there are multiple recession rates for most storms. During some storm events with varied rainfall distribution over time (e.g. a double-peaking storm), the depth in the infiltration trench

increased and decreased more than once. From the multiple peaks in the IT depth, one depth increment may have more than one recession rate.

The example in Section 4.3.7 demonstrates the changing recession rates depending on the level of water in the IT. There is substantial variability in the data, although clear trends emerge, as seen in *Figure 5.1* that includes the recession rates for each storm and the average temperature within the IT during each storm. *Figure 5.2* is a box and whisker plot of the recession rates (data tables in *Appendix F-3*).

One observed trend is the recession rates change with temperature – higher temperatures produce higher recession rates, except at the lowest depth range. Previous studies have shown that the recession/infiltration rates change depending on temperature, which affects the viscosity of the water (Emerson 2008; further discussed in section 5.2.4). An interesting note is that the recession rate trends are different when the temperature is above or below approximately 15°C. From this data, it appears that during colder temperatures, the data is tighter and less variable. There is a smaller difference between the rates of the depth increments. These changes could be due to the system clogging slightly over its first year of operation, but it is more likely that the temperature has a larger impact on the recession rate during warmer seasons. This trend is not as apparent for the lowest depth increment. It appears to be independent of temperature as fluctuations over the first year of data are minimal. This is discussed later, but the recession at the bottom of the tank may be more dependent on how much area is available for infiltration rather than the temperature. Further analysis over the next year (2013-2014) should provide more insight into the significance of temperature effects on the variation of recession rates.

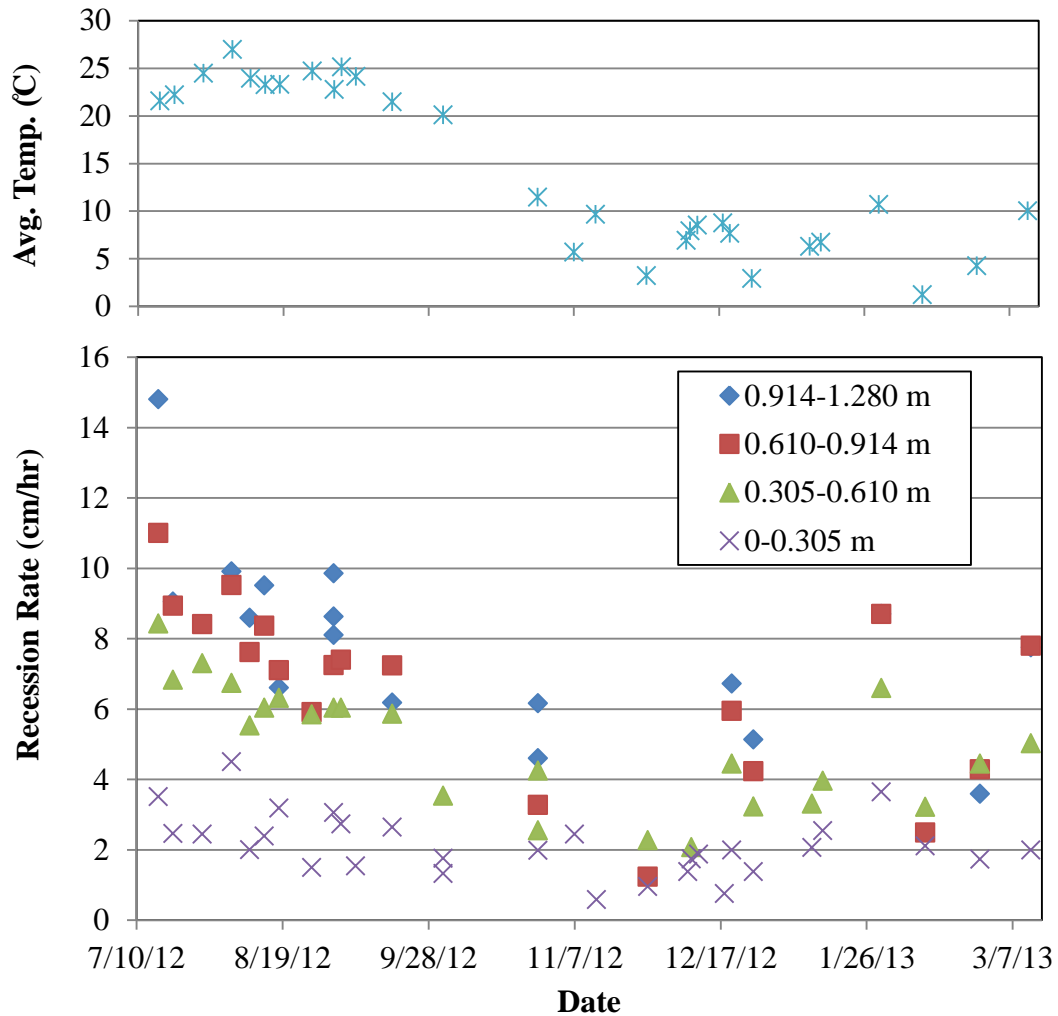


**Figure 5.1 - Recession rates (cm/hr) per depth increment for each storm event**

Another observed trend (*Figure 5.1*) is that the recession rate is dependent on the ponded level in the infiltration trench. The box and whisker plot (*Figure 5.2*), summary table (*Table 5.1*), and a Student's t-test (*Table 5.2*) comparing the data from the depth ranges proves some of these differences to be statistically variable. In the box and whisker plot, the blue boxes represent  $Q_1$  to the median ( $25^{\text{th}}$  percentile of the data) and green boxes include the median to  $Q_3$  ( $75^{\text{th}}$  percentile of the data). The error bars are to the minimum and maximum recession rates for each depth range. From the box and whisker plot, the median of each depth increment (where blue and green box meet), show the decreasing

trend in recession rates based on the head of water in the infiltration trench. In addition, the error bars show the range of rates calculated over the observation period, which can be partially attributed to seasonal temperature variation. Examining the mean and standard deviation (*Table 5.1*) shows the same trend that the recession rate decreases with ponded water level.

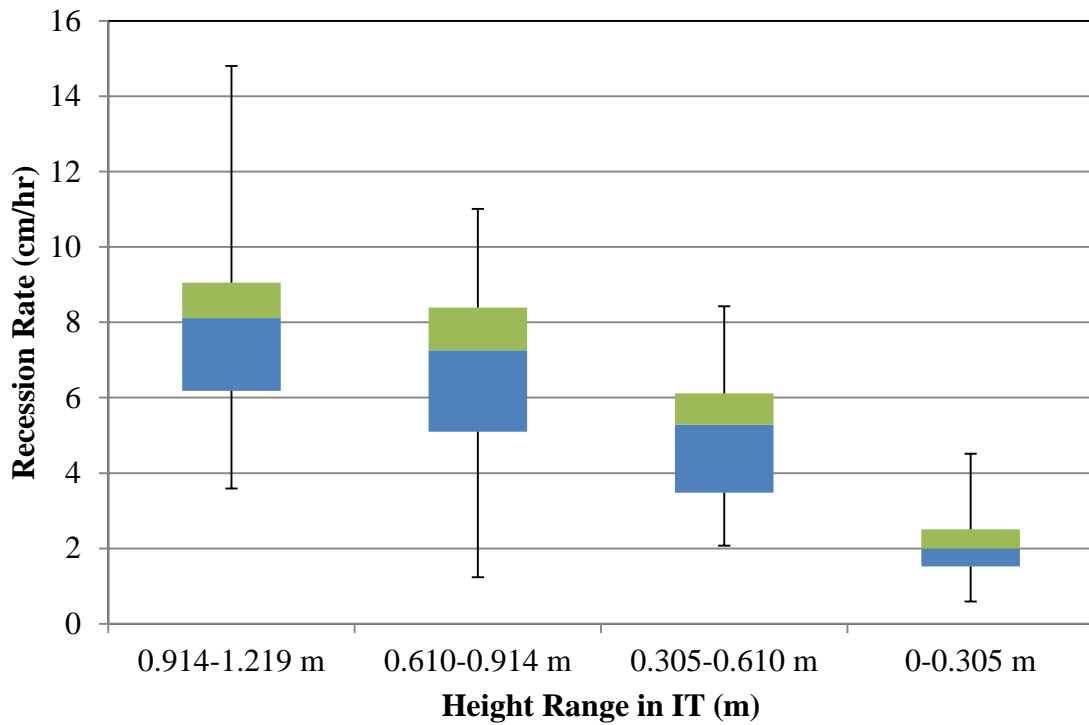


**Figure 5.2 - Box and whisker plot of recession rates**

**Table 5.1 - Mean, median, and first and third quartiles of recession rate box and whisker plot**  
(all data in cm/hr)

Range (m)	Mean	Std Dev.	Median	Q1	Q3
0.914-1.280	7.88	2.59	8.11	6.18	9.06
0.610-0.914	6.67	2.55	7.25	5.10	8.39
0.305-0.610	5.00	1.72	5.28	3.48	6.11
0-0.305	2.10	0.87	2.00	1.52	2.50

A Student's t-test provided a statistical analysis to determine whether the recession rates for each depth range were significantly different from each other to a 95% confidence level. The p-values for a two-tailed, two sample unequal variance test (*Table 5.2*) varied depending on the depth ranges compared. The highest ranges (0.914 – 1.280 m) vs. (0.610 – 0.914 m) proved to be statistically similar with an 83.2% confidence. The remaining compared ranges, which were the middle two, bottom two, and highest vs. lowest, were all statistically different from each other with at least 95% confidence. Therefore, while the head changes in the top 0.670 m (2.199 ft) of the IT, there are not significantly different recession rates; the recession rates as head changes toward the bottom 0.610 m (2 ft) of the IT are significantly different. When the water level in the IT is higher, there is more surface area for the stormwater to infiltrate. As the level decreases, the rates may change more significantly since the bottom of the trench becomes the main area of infiltration and the amount out of the sides of the IT decreases. Once the head decreases, flow out of the sides also decreases and recession out of the bottom may slow due to the smaller head and pressure energy. Since the recession rate does not incorporate the area of the IT, the rates were normalized as an infiltration rate (Section 5.2.2).

**Table 5.2 - T-test p-values for the recession rate depth range comparisons**

<b>Data Ranges Compared</b>	<b>P-Value</b>	<b>Stastically Different?</b>
0.914-1.280 vs 0.610-0.914	0.168	No
0.610-0.914 vs 0.305-0.610	0.020	Yes
0.305-0.610 vs 0-0.305	1.92E-08	Yes
0-0.305 vs 0.914-1.219	5.45E-08	Yes

### 5.2.2. Infiltration Trench Infiltration Rates

The infiltration rates are calculated to account for infiltration occurring over the entire surface area of the infiltration trench. While infiltration out of the bottom of the IT is important, the recession rates previously discussed demonstrate the change in rate as head in IT changes; this change in recession is likely due to the effects of stormwater leaving the trench from the sides. As determined in a previous study a nearby infiltration trench, there is a great amount of loss to consider out of the IT's sides and not just the bottom (Emerson 2008).

The recession rates had a decreasing trend with head increment depth decrease. When accounting for the stormwater's ability to leave the IT through all sides, infiltration rates became more consistent regardless of depth. However, these infiltration rates are slightly difficult to calculate since the calculated surface area assumes that the highest value of the depth increment is the height. For example, when the highest increment infiltration rate was calculated,  $z$  was assumed to be 1.280 m, which is only true for a portion of the time. The depth decreases to 0.914 m before a new increment is considered. Another approach would be to use an average depth of each increment to estimate the infiltration rates; this could be explored in the future.

The graphs *Figures 5.3 and 5.4* display the entire dataset for the storms analyzed (the tabulated results from every storm are included in *Appendix F-3*). *Figure 5.3* includes the infiltration rates for each storm event broken down into the depth increments and also includes the average temperature. The infiltration rates appear to show a similar trend as the recession rates; infiltration changes with the depth increment and the temperature. There are higher infiltration rates during higher temperatures ( $>15^{\circ}\text{C}$ ) and lower rates with

less variability at lower temperatures. However, there appears to be less of a relationship between the depth and the infiltration trench; the highest depth increment did not necessarily yield the highest infiltration rate. Since the infiltration rate normalizes the recession rates, the infiltration rates may be expected to be similar since the rate leaving the tank is related to the area. Upon further analysis, this may be true for the higher depth increments, but at lower depth increments it appears a significant difference remains (*Table 5.3*). In the graph of *Figure 5.3* it is more difficult to identify relationships since the data is appears less variable. However, there is still enough difference in the infiltration rates of the different depth increments and at varying temperatures that correlations are significant (*Section 5.2.3*).

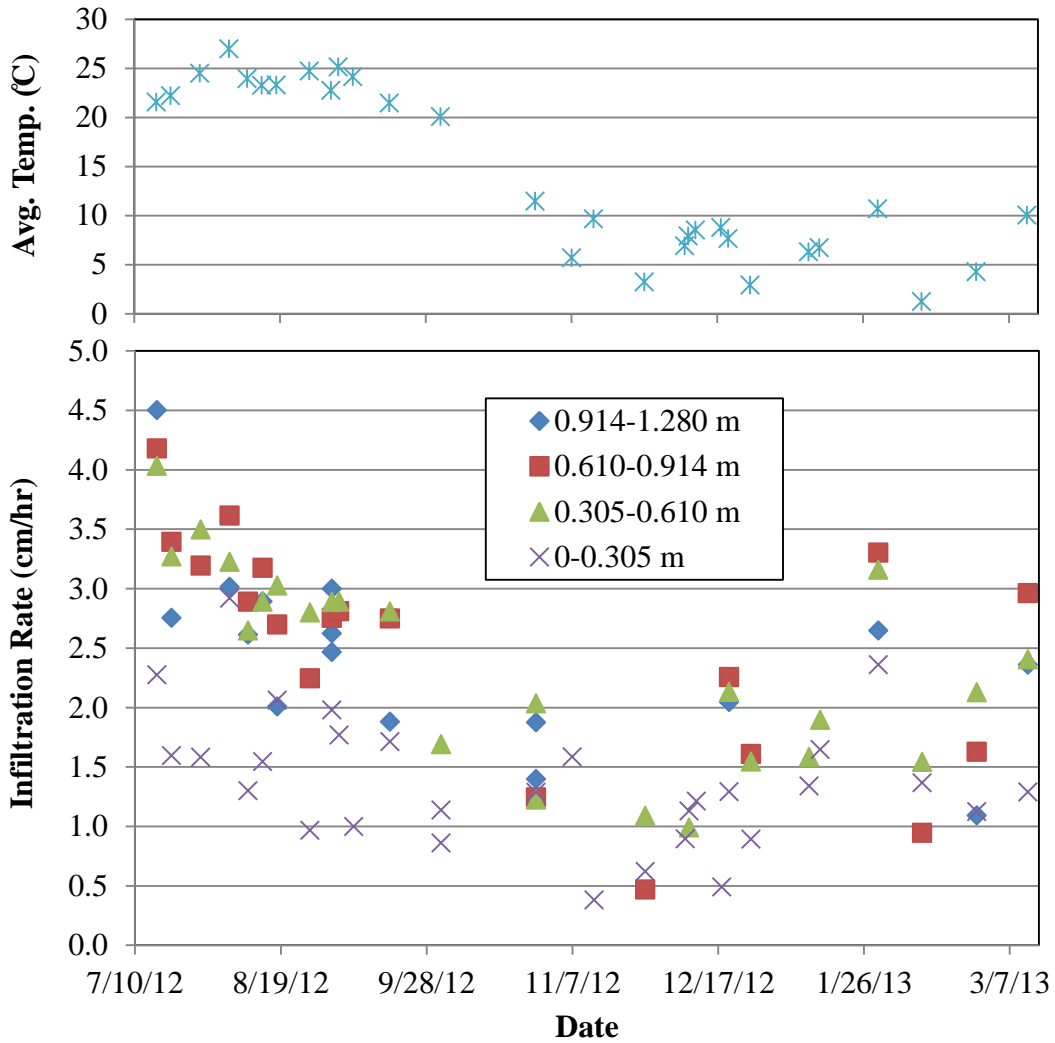


**Figure 5.3 - Infiltration rates (cm/hr) per depth increment**

The box and whisker plot in *Figure 5.4* shows some of the trends in the infiltration rate data. As with the recession rates, the blue boxes represent  $Q_1$  to the median and green boxes include median to  $Q_3$ . The error bars graphically display the maximum and minimum values for each IT depth range. The varying infiltration rates are likely linked to the changes in temperature; during warmer temperatures rates are typically higher (discussed further in Section 5.2.3). As also shown in the summary table (*Table 5.3*), the mean, median, and first and third quartiles display no obvious trend with depth.

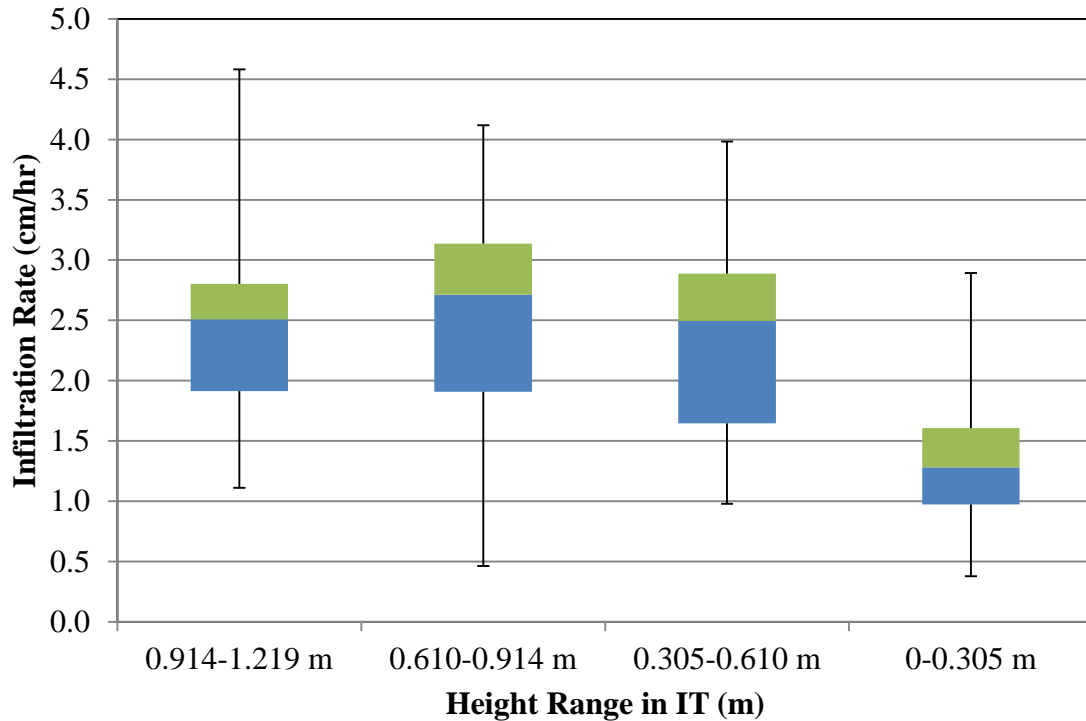


**Figure 5.4 - Box and whisker plot of infiltration rates**

**Table 5.3 - Mean, median, and first and third quartiles of infiltration rate box and whisker plot**  
(all data in cm/hr)

Range (m)	Mean	Std Dev.	Median	Q1	Q3
0.914-1.280	2.44	0.79	2.51	1.91	2.80
0.610-0.914	2.50	0.97	2.71	1.91	3.14
0.305-0.610	2.36	0.82	2.50	1.64	2.89
0-0.305	1.34	0.56	1.28	0.97	1.61

Applying a 95% confidence a two-tailed, two sample unequal variance tests showed that there were insignificant differences for the highest ranges ((0.914 – 1.280 m) vs. (0.610 – 0.914 m) and (0.610 – 0.914 m) vs. (0.305 – 0.610 m)) (Table 5.4). However, the bottom ranges and the top vs. the bottom ranges were significantly different. This may be due to pressure effects. As previously mentioned with the recession rates, a decrease in the water level not only decreases the surface area, but decreases the head of water and

resulting pressure in the IT. With less pressure, water will leave the tank at a lower rate both out of the sides and out of the bottom.

**Table 5.4 - T-test p-values for the infiltration rate depth range comparisons**

<b>Data Ranges Compared</b>	<b>P-Value</b>	<b>Stastically Different?</b>
0.914-1.280 vs 0.610-0.914	0.645	No
0.610-0.914 vs 0.305-0.610	0.617	No
0.305-0.610 vs 0-0.305	9.10E-06	Yes
0-0.305 vs 0.914-1.219	8.76E-05	Yes

### **5.2.3. Recession and Infiltration Rates and Temperature**

The recession and infiltration rates, as mentioned, are dependent on the temperature of the stormwater, as observed in Emerson (2008). The graphs in *Figures 5.5* and *5.6* show the recession and infiltration rates, respectively, with the corresponding average temperature during data collection. The depth ranges were kept separate to show the difference in rates depending on the water level in the IT in combination with the temperature changes.

The graphs show there is a slight trend in the rates and temperature. However, it is interesting that there is not data with corresponding temperatures between approximately 12 – 20 °C; this is a chance occurrence as data was collected consistently during the year. The graphs do not include the linear trendlines that correspond to the data, but *Table 5.5* displays the slope and  $R^2$  values. In addition, a correlation test was completed to see if the relationship between recession and infiltration rates and the temperatures were statistically significant. The t-critical values (Bobko 2001) and the determined  $t_{(n-2)}$  values based on the correlation coefficient (*Equation 4.7*) are included in *Table 5.5*. The

results are shown in the final column of *Table 5.5*; a statistically significant result indicates the correlation to be significant, although with rather shallow slopes. All of the depth ranges (recession and infiltration) were determined statistically significant, so it can be concluded that the recession and infiltration rates depend on the temperature during the storm. Also noted in the table is when the t-value was larger than other p-value critical t values. All of the correlations are greater than the  $p = 0.02$  critical values.

As previously mentioned (Section 5.2.1 and 5.2.2), not only are the rates dependent on temperature, there seem to be different trends during warmer and colder temperatures. For the recession rates (*Figure 5.5*), this graph shows there may be more variability at warmer temperatures; the data seems more variable and inconsistent than when temperatures were lower (less than 15°C). The infiltration rates (*Figure 5.6*) appear much more variable at any temperature. There is no apparent consistent trend in regards to variability in the rates at the different depth increments at higher and lower temperatures. As previously mentioned, since the infiltration rate attempts to normalize the recession rate, the water level in the trench may have a less significant influence on the rate of water exiting the IT.

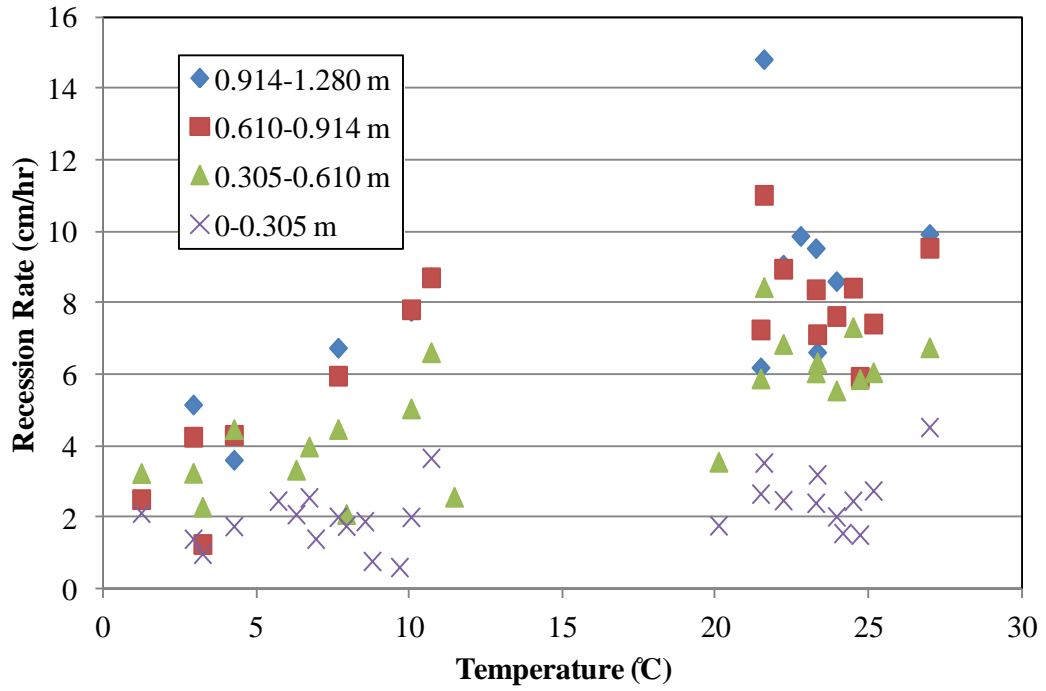


Figure 5.5 - Recession rates as a function of the average storm temperature

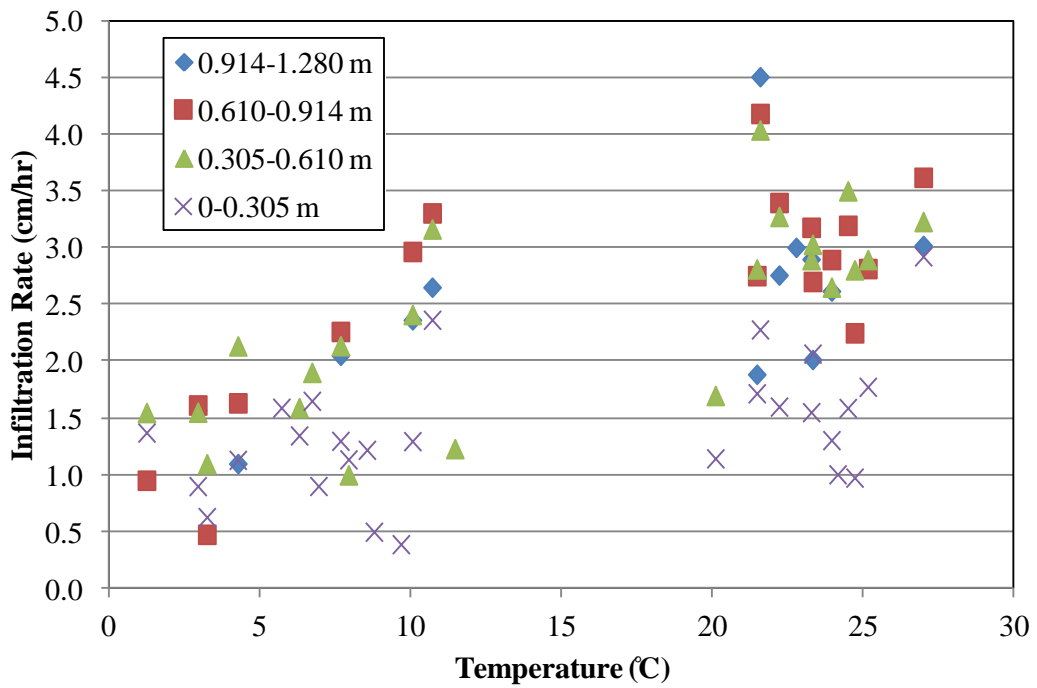


Figure 5.6 - Infiltration rates as a function of the average storm temperature

**Table 5.5 - Slope (m), R-squared, correlation coefficients, and t-test results for comparing recession and infiltration rates to temperature**

Recession and Infiltration vs. Temperature								
Range (m)	m		R <sup>2</sup>	Correlation	n	t-critical (p = 0.05)	t <sub>(n-2)</sub>	Significant?
	R	I						
0.914-1.280	0.20	0.06	0.36	0.62	17	2.13	3.06	Yes**
0.610-0.914	0.20	0.08	0.55	0.74	19	2.11	4.50	Yes**
0.305-0.610	0.15	0.07	0.57	0.76	24	2.07	5.45	Yes**
0-0.305	0.05	0.03	0.21	0.45	30	2.05	2.65	Yes*

\* Statistically significant to p = 0.02

\*\* Statistically significant to p = 0.01

#### 5.2.4. Volumes in Treatment Train and Infiltration Trench

The design of the treatment train included the capture of 2.54 cm (1 in), where the infiltration trench was designed to capture approximately 1/3 of that volume (0.76 cm; 0.3 in). The resulting expected volume of the entire treatment train from this design storm is 22.45 m<sup>3</sup> (825 ft<sup>3</sup>) and the expected volume in the IT is 6.95 m<sup>3</sup> (245 ft<sup>3</sup>). However, much greater volumes than this design volume were determined to be collected in the IT. Volumes into the treatment train were determined from the contributing area and the amount of rainfall (*Equation 4.8*). The volumes actually reaching the IT (*Equations 4.9 and 4.10*) were compared to the volume into the treatment train and to the designed capture volume. The graph *Figure 5.7* shows the trends of the volume reaching the IT as a ratio of the total volume entering the treatment train. In general, the volume in the IT based on recession rates (VIT<sub>R</sub>) were higher than those based on the infiltration rates (VIT<sub>I</sub>). The raw data calculations for each storm based on recession and infiltration rates are included in *Appendix H*. The recession data is highlighted in green and the infiltration data in blue in the graph (*Figure 5.7*).

When looking at the amount of stormwater volume entering the IT in compared to the volume entering the treatment train off of the garage ( $V_{in}$ ), the average ratio based on the recession and infiltration rates are 0.32 and 0.27, respectively. This implies that, on average, approximately 30% of the total volume entering the treatment train reaches the infiltration trench. This follows closely the design of 0.76 cm (0.3 in) (or 33%) of a 2.54 cm (1 in) storm event. Therefore, a significant amount (around two thirds) of the total rainfall volume collected off of the garage is captured in the swale and rain gardens. However, while the average ratio of volume entering the IT to volume into the treatment train is close to the design ratio, there is a large variability (*Figure 5.7*). The maximum ratio is close to 0.80 and the lowest is close to zero. This implies a large range of capture in the swale and rain gardens; the treatment train as individual entities do not consistently under- or over-perform. At times the swale and rain gardens capture more rainfall than expected, but at other times more a larger portion of the storm volume reaches the infiltration trench. This trend is particularly noticed during winter months, when infiltration in the early parts of the treatment train (swale and rain gardens) is inhibited by the cooler temperatures.

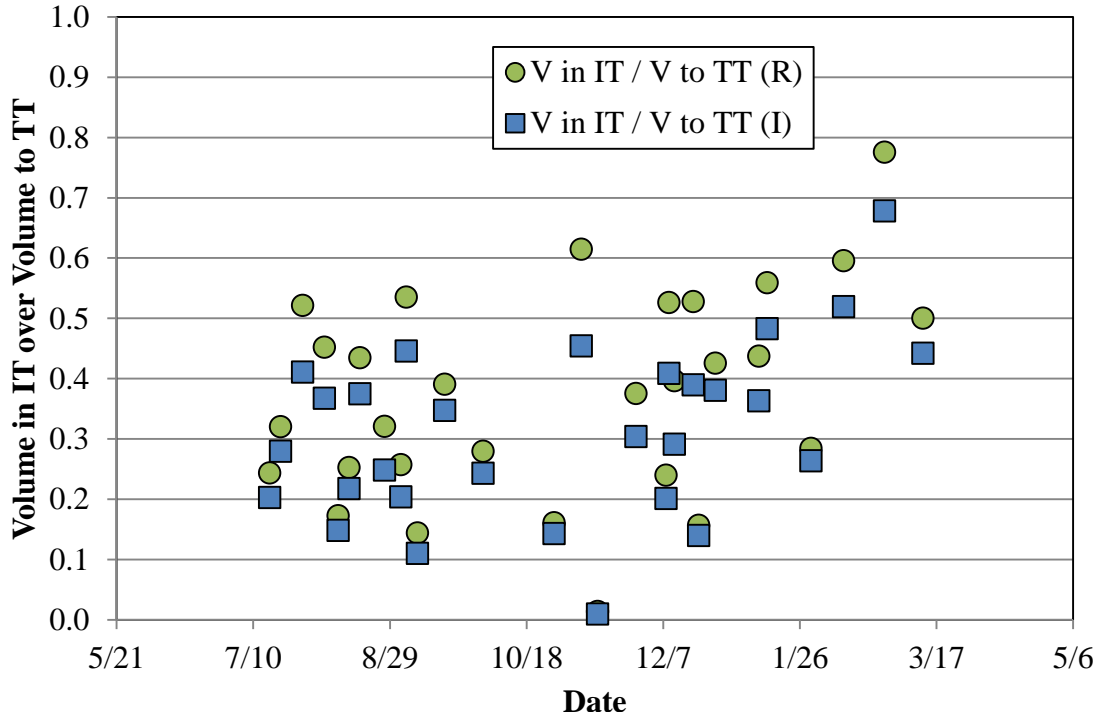


**Figure 5.7 - Volumes into the IT compared to the volume entering the treatment train**

In *Figure 5.8*, the same ratios as in *Figure 5.7* are presented by the volume of rainfall associated with the storm event. In this graph, the red x represents the design volume. As previously mentioned, by design, 33% of the stormwater volume from a 2.54 cm (1 in) storm was intended to be captured in the infiltration trench. For storms smaller than this design ratio, it should be expected that a smaller fraction of the total volume into the treatment train should reach the IT. However, as seen in *Figure 5.8*, there are a number of storms smaller than 2.54 cm (1 in) that have ratios larger than 0.3. In contrast, most of the storms larger than the design storm have ratios less than 0.3. Larger storms often cause a backwater effects in the treatment train; once the infiltration trench is filled, the rain gardens and swale begin to fill. During this retention time, more infiltration is possible, which ultimately prevents the stormwater from reaching the infiltration trench. During the smaller storms, the stormwater does not back up as much, allowing flow to

reach the IT faster than designed. These trends can be attributed to the v-notch weirs installed at the site for monitoring, which would not be necessary in a regular application. The v-notch weirs prevent ponding more than a few inches in the swale and rain gardens before overflow downstream. If overflow was prevented until the swale and rain gardens had a deeper ponding depth, more capture and ultimately treatment would likely occur from infiltration during retention.

The ratio of volume into the infiltration to the volume to the treatment train varied for each storm. The standard deviations when recession and infiltration rates were used were 0.17 and 0.14, respectively, and a majority of the ratios fall within the range of the standard deviation. However, there were a few outliers. The smallest ratio, which occurred on November 13, 2012, was 0.01 when both recession and infiltration rates were used to estimate the volume into the IT. This storm was a smaller storm (0.64 cm (0.26 in) of rain) and only 0.07 m<sup>3</sup> (R) and 0.05 m<sup>3</sup> (I) was estimated to enter the IT. A majority of the volume was captured in the swale and rain gardens during this storm, which should be expected since by design, no stormwater should reach the trench for a storm under 0.70 cm (0.3 in). In contrast, the highest ratios (0.78 (R); 0.68 (I)) occurred during a 1.47 cm (0.58 in) rain event on February 26, 2013. While the IT did not overflow during this storm, a majority of the volume reached the IT and it was estimated that water remained in the trench for over 50 hours. One reason a large volume of this storm may have entered the trench could be the temperature (4.25°C). Since the viscosity of the water is lower during cold temperatures, less infiltration would have occurred upstream, causing more volume to pass through the swale and rain gardens and end up in

the IT. The total intensity ( $i_1$ ) for this storm was below average at 0.186 cm/hr (0.073 in/hr), so this is unlikely the cause of the stormwater reaching the IT.

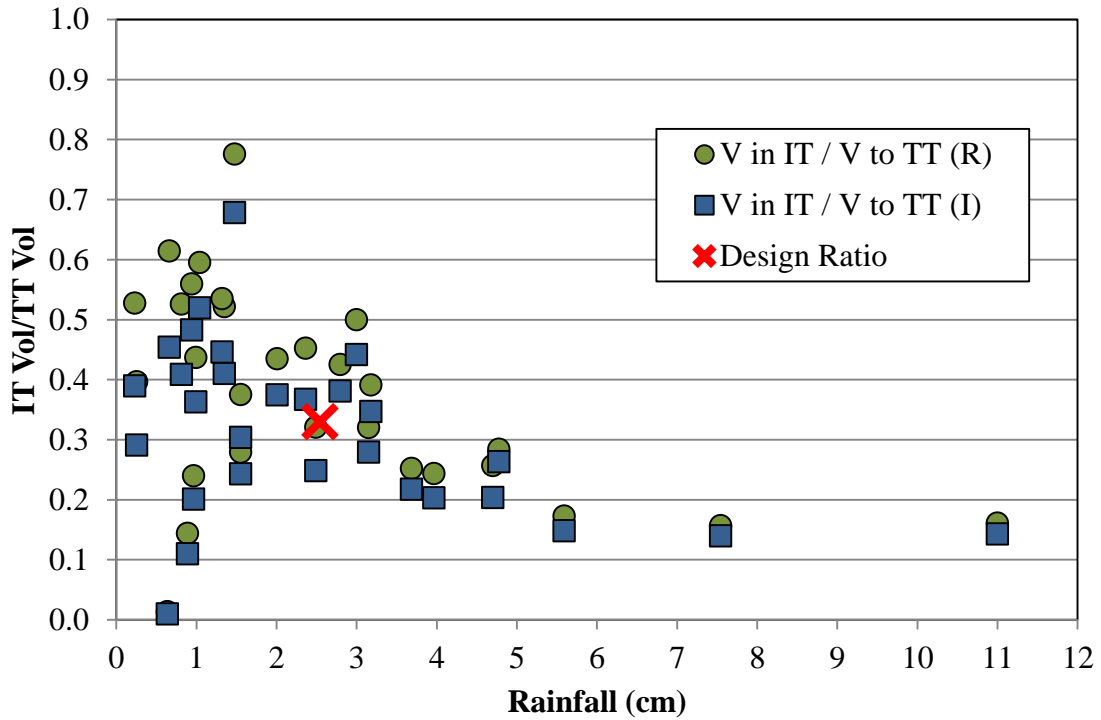


**Figure 5.8 - Infiltration volume to treatment train volume ratio vs. rainfall volume**

In addition to analyzing the amount of stormwater in the infiltration trench and the amount of rainfall into the treatment train, it is also interesting to include the ratio of overflow volume to the infiltration trench volume. For most of the storms, the amount of overflow volume compared to the volume entering the IT is small (less than 10%). As seen in *Figure 5.9*, this ratio was again considered from using both recession (R) and infiltration (I) rates as a means of estimating volume in the IT. The largest difference between the ratios using R and I was 2.3% on 12/20/2012; the methods produced similar ratios of overflow volume to volume entering the IT. Since the volume into the IT was smaller when the infiltration rate was used, the percentage of overflow as a fraction of the volume to the IT is always smaller than the method using the recession rate. Despite the

slight differences in values from the different methods of calculation, the percentage of volume of overflow was small compared to the amount of volume entering the IT. This demonstrates the ability of the IT as a component of the treatment train to capture large volumes of rainfall.

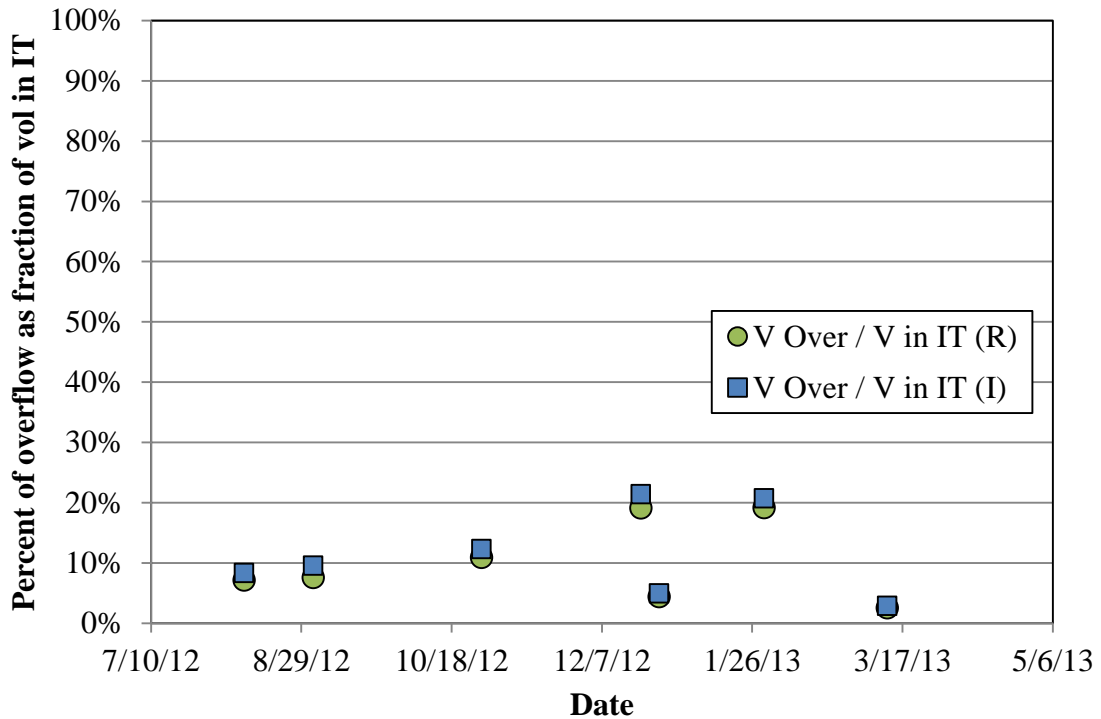


Figure 5.9 – Volume of overflow as a fraction of the volume entering the IT

### 5.2.5. Infiltration Trench Comparison

While there is little data available on the study of infiltration trenches in a series of SCMs, there are other stand-alone infiltration trench sites that have been observed for their recession and infiltration rates available for comparison. The following sections aim to compare the performance of the treatment train’s infiltration trench to Villanova’s old infiltration trench and to other sites discussed in literature.

### 5.2.5.1. Comparing Villanova's IT and OIT

As mentioned, the old infiltration trench (OIT), which is located on the opposite side of the parking garage from the treatment train, provides a comparison for predicting the performance of the treatment train IT. The OIT showed variation in recession rates depending on the head of water in the trench, and also a trend following the change in seasonal temperature (Figure 5.10). From the graph, there are much higher recession rates than observed in the treatment train IT, especially during the first year following construction. It is also important to recognize the values in Figure 5.10 are in inches per hour and not centimeters per hour. From the graph, it is obvious that there was seasonal variation.

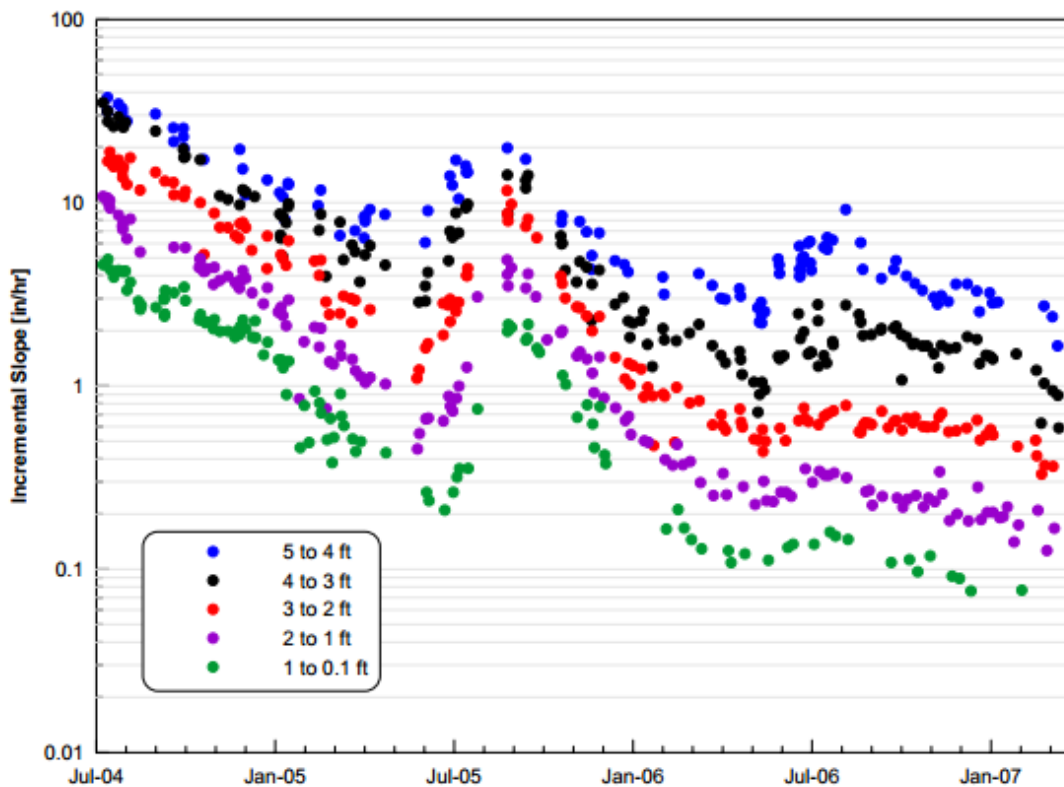


Figure 5.10 – OIT recession rates (in/hr) for the first three years of data collection (Emerson 2008)

From the graph of OIT recession rates per head increment, estimated high, low, and overall averages were determined in order to compare values to the treatment train IT (*Table 5.6*). The OIT recession rates are much higher than the treatment train's IT initial rates, regardless of the depth range (*Table 5.6*). A number of factors may contribute to the higher rates at the OIT. First, one layer of geotextile was used rather than two at the IT; second, a higher depth may result in increased pressure to force faster infiltration. Varying in-situ soil types may cause increased hydraulic conductivity, but a significant change between the two sites is unlikely due to their proximity. An infiltrometer test at the OIT estimated 20.5 cm/hr (8.1 in/hr) in the in-situ soil (Emerson 2008); as mentioned in Chapter 3, the soils were classified similarly and although an infiltrometer test was not completed at the treatment train, in-situ hydraulic conductivities are likely very similar. The treatment train was also subjected to erosion and during the first few weeks of storm events, large amounts of sand and soil was displaced downstream. Therefore, there could be clogging in the IT. Recession rates at the IT are still high enough to be considered effective by EPA standards (at least 1.27 cm/hr (0.5 in/hr)), so there is no immediate concern of decreasing performance.

**Table 5.6 - Estimated recession rates for the first and second year of monitoring for OIT** (Note: this data is converted to cm/hr from the graph in in/hr)

IT Depth (m)		Old IT Recession Rates (cm/hr)			TT IT Avg (cm/hr)
		High	Low	Avg	
1.524 - 1.219	1 <sup>st</sup> Yr	88.9	22.9	55.9	-
	2 <sup>nd</sup> Yr	45.7	6.4	26.0	-
	Diff	43.2	16.5	29.8	-
1.219 - 0.914	1 <sup>st</sup> Yr	63.5	12.7	38.1	7.9
	2 <sup>nd</sup> Yr	35.6	2.5	19.1	-
	Diff	27.9	10.2	19.1	-
0.914 - 0.610	1 <sup>st</sup> Yr	38.1	7.6	22.9	6.7
	2 <sup>nd</sup> Yr	25.4	1.3	13.3	-
	Diff	12.7	6.4	9.5	-
0.610 - 0.305	1 <sup>st</sup> Yr	25.4	3.8	14.6	5.0
	2 <sup>nd</sup> Yr	10.2	0.8	5.5	-
	Diff	15.2	3.0	9.1	-
0.305 - 0	1 <sup>st</sup> Yr	10.2	1.0	5.6	2.2
	2 <sup>nd</sup> Yr	5.1	0.3	2.7	-
	Diff	5.1	0.8	2.9	-

The OIT has no pretreatment and is undersized. Looking at the first two years of recession rates from the OIT, it is obvious that there are some large decreases in performance. While the performance reduction is larger at the top of the IT and smaller at the bottom, these decreases signify the clogging of the bottom of the OIT. It is now estimated that the bottom of the trench is clogged and infiltration is merely out of the sides of the OIT. To analyze the potential of pretreatment the IT at the treatment train was installed and the change in performance over time between the TT IT and the OIT will be monitored.

#### ***5.2.5.2. Comparing Villanova Site and Literature***

The treatment train infiltration trench recession and infiltration rates are dependent on temperature. While there is limited research on the continuous monitoring of stormwater control measures, a few studies have shown the benefits of long-term monitoring in relation to observing seasonal variations. From the seasonal variations, the temperature effects on infiltration can be identified. One example is the article titled “Hydrologic Modeling of a Bioinfiltration Best Management Practice” (Heasom, et. al 2006). This paper focused on a rain garden at Villanova University, but was a study that showed temperature dependency related to the fluid properties of water. The recession rates of the bioinfiltration rain garden were found to vary from 0.38 to 1.27 cm/hr (0.15 to 0.50 in/hr); the results demonstrated the need to consider seasonal variation in infiltration SCM monitoring as it relates to the viscosity of the water (Heasom, et. al 2006).

The rate of infiltration or recession from the infiltration trench should be compared to design requirements in stormwater manuals as well as other research sites to determine performance and potential longevity effects. The PA BMP Manual (2006) states a rate of 0.64 cm/hr (0.25 in/hr) is required for infiltrating SCMs in a sandy loam; for a loam, the design rate should be a minimum 0.43 cm/hr (0.17 in/hr). The Maryland Manual, however, suggests a rate of at least 1.33 cm/hr (0.52 in/hr) (MDE 2009). The Minnesota Manual suggests a minimum 0.51 cm/hr (0.20 in/hr) (MSSC 2008). None of the manuals discuss temperature effects. Thus far, the treatment train infiltration trench rates exceed the minimum requirements recommended in these manuals. However, with potential clogging and temperature effects, these rates should continue to be monitored and compared to suggested rates.

While there are only a few studies which focus on the effect of temperature specifically in the application of SCMs, there have been laboratory and field studies relating temperature to infiltration on soil. Duley and Domingo (1943) and Constantz and Murphy (1991) have reported on the effects of temperature changes on infiltration. Field studies, including one from Jaynes (1990), showed the variation in infiltration over the course of day that was related to the measured temperatures. As demonstrated by the changing infiltration and recession rates in the IT at the treatment train and from some prior research, the infiltration and recession rates can be expected to vary seasonally to the temperature effects on the viscosity of the water. There is limited data available on recession and infiltration rates in the application of SCMs, and this area should be a focus of research moving forward.

#### **5.2.6. Infiltration Trench Data Conclusions**

After collecting the infiltration trench data on the recession and infiltration rates, a few questions arose. Previous studies on the old infiltration trench at Villanova University demonstrated some of the longevity effects of the system. From the current available data at the treatment train, it is difficult to predict long term longevity effects.

Despite the need for a larger quantity of infiltration trench data to make better conclusions about its potential long-term performance, there are other aspects of the infiltration as it contributes to the treatment train that are of interest. The treatment train, designed to capture a 2.54 cm (1 in) rainfall event, should then be subject to overflow during any event greater. By applying the reliable infiltration data, this overflow concept became a focus of research. A few questions which revolved around how to quantify this overflow and what types of rainfall cause overflow were intended to be answered through

further analysis of the infiltration trench. Ultimately, the treatment train capture performance was estimated by examining the types of rainfall events at the site and the overflow events which occurred.

### **5.3. Infiltration Trench and the Treatment Train Performance**

The treatment train was designed to capture a 2.54 cm (1 in) storm. From observation during storm events, the system appears to be operating as designed, if not better. In order to analyze how much rainfall volume is being captured by the treatment train, the inflow volume and outflow volume were compared. Since instrumentation difficulties prevented quantity measurements from each SCM, the infiltration trench was monitored closely. In order to begin considering how much capture volume occurs at the site, it was important to analyze rainfall data and predict expected capture volumes.

#### **5.3.1. Rainfall Data**

Historical rainfall and rainfall data on site at the treatment train were needed to get an idea of what types of rainfall volume and intensity to expect.

##### **5.3.1.1. Rainfall Volume**

Rainfall data for the Philadelphia area, courtesy of the Philadelphia Water Department, has been collected at the Philadelphia Airport for over 50 years. As mentioned in Chapter 1, this data is useful for predicting the rainfall volume and storm frequencies at Villanova University. Since the treatment train has a rain gage at the site, the rainfall data collected during the period of analysis could be compared to the historical airport data. The event frequency data, displayed in *Figure 5.11* includes the event frequencies for storm events at the treatment train. There are significantly fewer data points (n = 30)

for the site data compared to a much larger  $n = 4107$  for the airport data. The event frequencies at the site are shifted to the right when compared to the airport frequency curve, but a similar curve is followed by both datasets. A rainfall depth at the treatment train site may have a lower frequency due to the small number of storm events included in analysis, but it could also be that the rainfall amounts actually differ locally. The site event frequency indicated over 60% of storms can be considered 2.54 cm (1 in) or less and should be completely captured by the treatment train.

In addition to comparing the historical rainfall data at the PHL site, the treatment train rainfall data was compared to the PHL data for the same collection period. This data, collected from NOAA and [www.accuweather.com](http://www.accuweather.com), provides an interesting perspective as rainfall from the same time period at the PHL rain gage is shifted to the left of the PHL historical data. There is a slightly large number of data points used compared to the site data since the site data only includes the storms that were analyzed for treatment train performance, but this shows that the rainfall certainly varies locally. The site data is likely a better prediction of the potential performance in terms of frequency of storms of the treatment train.

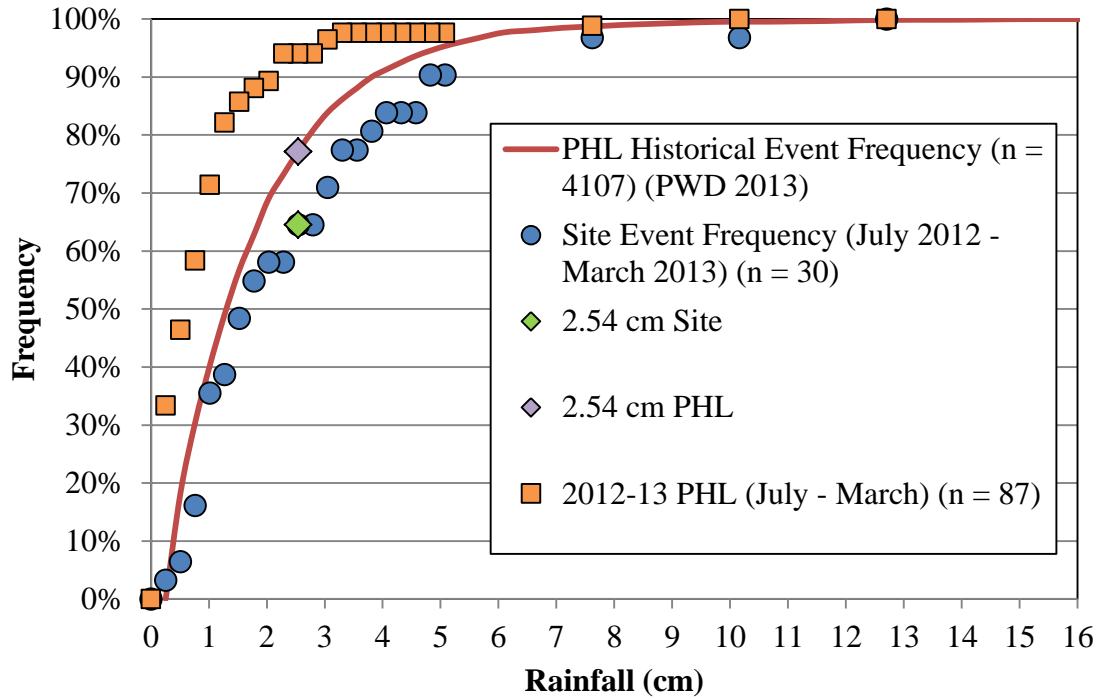


Figure 5.11 - Philadelphia historical event frequency vs. recent data frequency

### 5.3.1.2. Rainfall Duration

Rainfall volume is typically a major factor in SCM design, but rainfall duration may also influence performance. *Table 5.7* summarizes the durations (average, minimum, and maximum), which were determined on an event basis. The volume or rainfall (cm) is also included in *Table 5.7* for reference. A table of the individual storm data is in *Appendix I*. The average storm is around the design storm (2.54 cm (1 in)).

Table 5.7 - Storm durations and volumes summary

	Duration (hrs)	Rain (cm)
Average	15.01	2.52
Minimum	0.28	0.23
Maximum	66.96	11.00

### 5.3.1.3. *Rainfall Intensities*

Aside from analyzing the rainfall volume that contributes to the treatment train, rainfall intensity was a parameter of interest. The intensity incorporates the volume and the duration previously discussed. Rainfall intensity can be defined a number of ways and since each storm event is unique in regards to its intensity, the total intensity, or total rainfall over total time, was used as a representation of the event ( $i_1$ ). However, other forms of rainfall intensity were calculated in order to best describe the rainfall of each storm event ( $i_2$  and  $i_3$ ).

The different intensities were calculated to determine what intensity value may best represent the rainfall. When comparing the various intensities for the storm events, the total intensities appear to be a good overall representation. The total intensity is an approximate mean of the other forms of intensity, and it allows for an intensity to be calculated for every storm. Since some of the storms were too small for the second and third forms of intensity calculated, these forms are not feasible for further analysis. *Table 5.8* includes the total intensity and intensities based on the first 0.635 cm (0.25 in) and time to 0.635 cm (0.25 in) calculated for each storm. Total intensities in the events analyzed ranged from 0.027 cm/hr (December 12, 2012) to 2.244 cm/hr on July 28, 2012. The intensities helped to identify storm properties and the total intensity was further analyzed in combination with rainfall volume and duration. The other two intensities ( $i_2$  and  $i_3$ ) were not applied for further analysis since a t-test determined their values were not significantly different than the total intensity ( $i_1$ ) with a 95% confidence (*Table 5.9*). In addition to their statistical comparison, there was not always an alternate intensity calculated for some storms. Since most of the storms that did not have an  $i_2$  or  $i_3$  were

smaller but still resulted in stormwater reaching the infiltration trench, their total intensity was important to include.

**Table 5.8 - Storm intensities ( $i_1$ ,  $i_2$ ,  $i_3$ )**

<b>Storm</b>	<b>Total Intensity (<math>i_1</math>) (cm/hr)</b>	<b>(Total Rain) / (Total Time - Time to 0.635 cm) (<math>i_2</math>) (cm/hr)</b>	<b>(Total Rain - 0.635 cm) / (Total Time - Time to 0.635 cm) (<math>i_3</math>) (cm/hr)</b>
7/16/12	0.090	0.094	0.079
7/20/12	0.424	0.660	0.514
7/28/12	2.244	2.992	1.580
8/5/12	0.184	0.185	0.135
8/10/12	1.832	2.430	2.153
8/14/12	0.230	0.239	0.197
8/18/12	0.233	0.397	0.272
8/27/12	0.131	0.140	0.119
9/2/12	0.149	0.501	0.433
9/4/12	0.039	0.063	0.033
9/8/12	0.198	0.278	0.079
9/18/12	0.134	0.161	0.129
10/2/12	0.075	0.087	0.051
10/28/12	0.164	0.200	0.189
11/7/12	0.071	-	-
11/13/12	0.071	-	-
11/27/12	0.088	0.103	0.061
12/8/12	0.027	0.044	0.015
12/9/12	0.059	0.258	0.056
12/11/12	0.148	-	-
12/18/12	0.807	-	-
12/20/12	0.720	0.929	0.851
12/26/12	0.443	0.561	0.433
1/11/13	0.203	0.428	0.153
1/14/13	0.159	0.517	0.168
1/30/13	0.398	0.735	0.637
2/11/13	0.229	0.644	0.251
2/26/13	0.186	0.335	0.191
3/12/13	0.257	0.527	0.416

**Table 5.9 - Intensity t-test p-values**

<b>Intensities</b>	<b>P-Value</b>
$i_1$ vs. $i_2$	0.252
$i_1$ vs. $i_3$	0.866

### **5.3.2. Infiltration Trench Overflow**

After analyzing rainfall events for their volumes, durations, and intensities, defining infiltration overflow was necessary to determine the treatment train's capture performance. Overflow of the infiltration trench was difficult to quantify, but knowing the maximum depth of the trench and analyzing the pressure transducer data during each storm event identified when overflow was occurring and the duration of that overflow. Overflow of the infiltration trench was determined by a consistent pressure transducer reading over 1.280 m (4.199 ft) over a period of time. During this time of overflow, infiltration in the trench still occurred, but it can be assumed that the rate of flow into the infiltration trench from the second rain garden was greater than the recession or infiltration rates. The storm that prompted exploration into the concept of overflow was Hurricane Sandy.

During Hurricane Sandy, 11.0 cm (4.33 in) of rainfall was recorded at the treatment train's rain gage. The graph in *Figure 5.12* shows the pressure transducer depth reading over the duration of rainfall. In this graph, it is first noted that the rainfall increments never exceeded 0.0254 cm (0.01 in) per minute of recording. This implied a relatively low intensity for a large volume storm, which ultimately led to an investigation of the capture performance of the treatment train based on IT overflow. At first glance, the graph does not appear to remain level above the 1.280 m (4.199 ft) line for a long period

of time. However, a closer look where rainfall appeared to be heaviest proved there was a percentage of time where overflow of the IT occurred (red circle in graph). The second circle (yellow) signifies a second period of overflow. This hour of time where the water level exceeded the paver depth is included in the overflow calculation, despite the fact that the water level does not remain constant during this time. Instead, the depth was constantly decreasing, indicating infiltration was occurring and the water did not stay ponded at the surface for long.

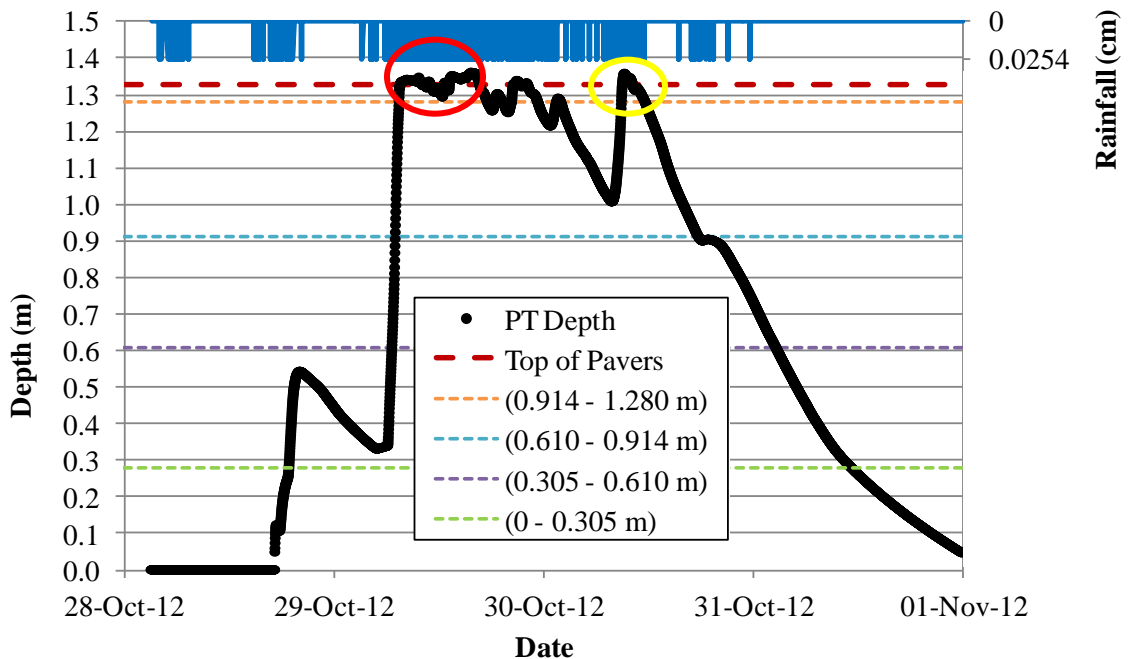


**Figure 5.12 - Hurricane Sandy infiltration trench pressure transducer and rainfall data** (red and yellow circles indicate periods of possible overflow, areas to zoom into)

Overflow at the IT during Hurricane Sandy was suspected during the day on October 29, 2012. Zooming into this part of the pressure transducer readings (*Figures 5.13a* and *5.13b*), it was evident that overflow could be estimated. During three different time periods, approximately six hours of overflow was estimated (green arrows of *Figures 5.13a* and *b*). As mentioned, overflow duration was estimated from the time when there

was a relatively constant pressure transducer depth recording of 1.280 m (4.199 ft). Using this overflow duration, the overflow volume was calculated; overflow implied incoming flow must be greater than infiltration out of the IT so overflow volume was calculated using recession rates. Recession rates in cm/hr were higher than both rainfall intensities and infiltration rates for each storm analyzed, so the recession rate multiplied by the duration of overflow and the area of the pavers which would allow overflow, served as the worst case or maximum overflow volume. This overflow volume could then be compared to the inflow volume of rainfall over the area of the parking garage.

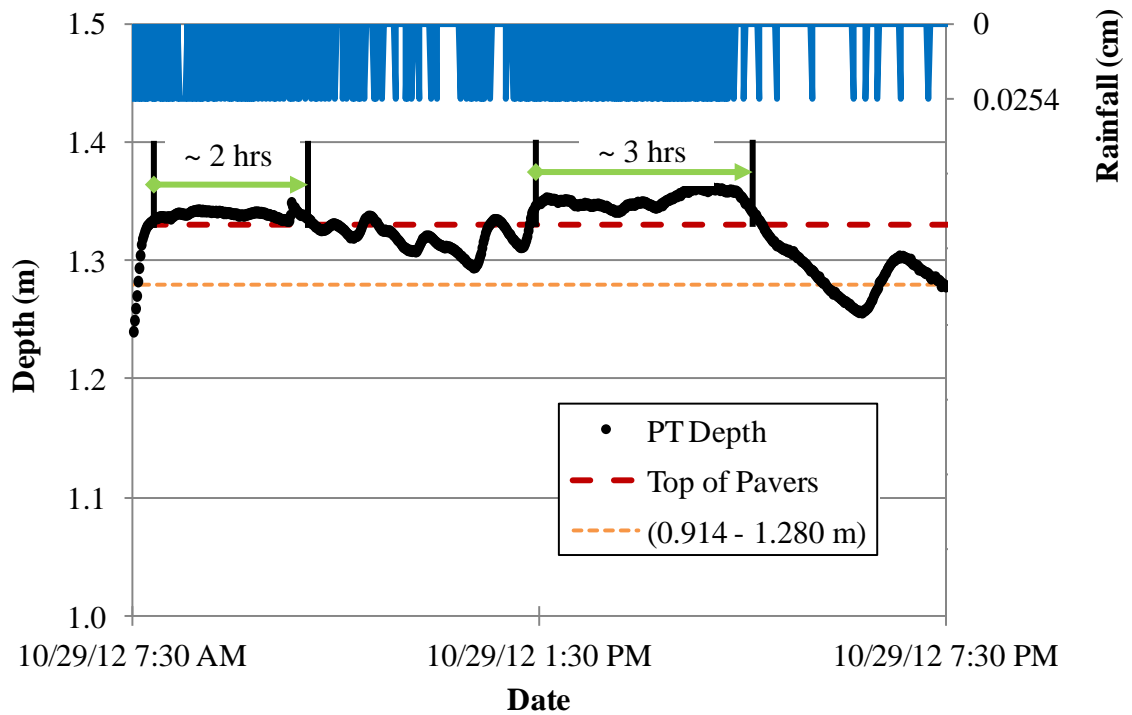
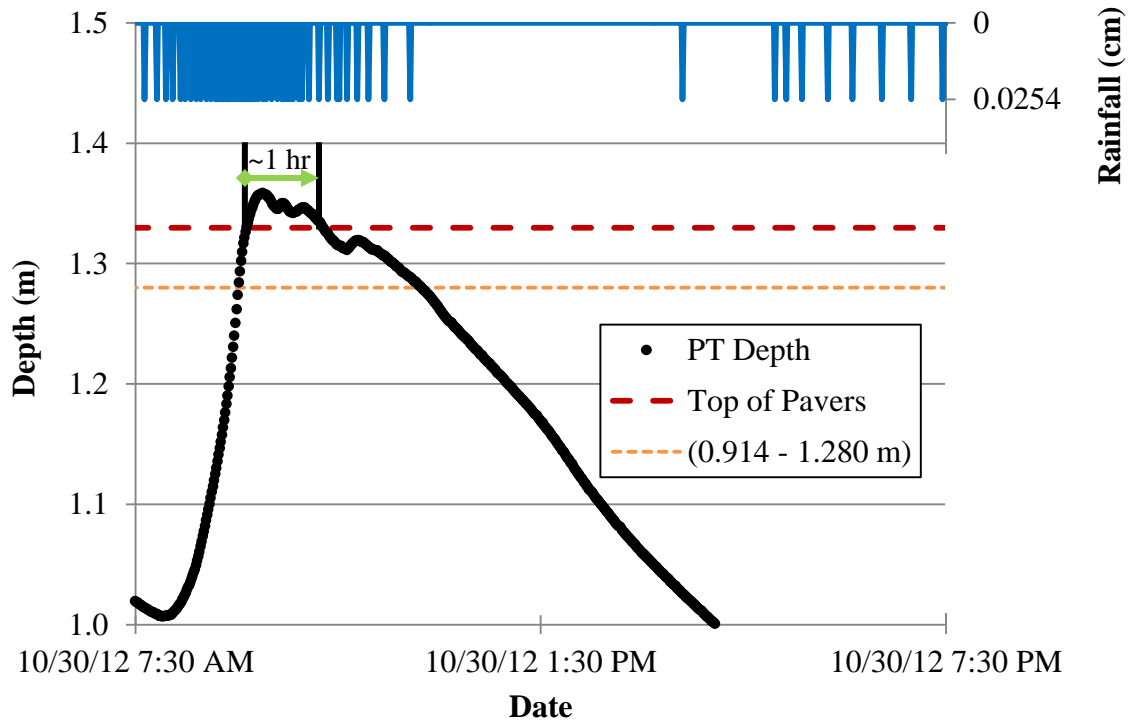


Figure 5.13a - Hurricane Sandy (October 29, 2012) overflow duration (10/29/12)



**Figure 5.13b – Hurricane Sandy (October 28, 2012) overflow duration (10/30/12)**

The performance of the treatment train, and more specifically the data from the infiltration trench during Hurricane Sandy in October, 2012, influenced the research on the capture performance of the treatment train. Inflow volumes and their relation to the amount of overflow at the infiltration trench result in the capture volume of the entire system. During Hurricane Sandy, the volume of inflow was calculated as  $V_{in} = ((4.33in - 0.04in)/12 * 10,000 ft^2) = 3,575 ft^3 (101.23 m^3)$  (Equation 4.8).

In Equation 4.11 for Hurricane Sandy, the  $V_{over}$  is  $6.17 cm/hr * (1m/100cm) * 6 hrs * 4.8 m^2 = 1.78 m^3$ . The capture volume for Hurricane Sandy was estimated to be  $101.23 m^3 - 1.78 m^3 = 99.45 m^3$  (Equation 4.12). The remaining storms in which overflow was observed were also analyzed using the Equations 4.8, 4.11, and 4.12 from Chapter 4. Appendix F includes a table of the calculated inflow, overflow, and capture volumes for

each storm. The overflow storms (*Table 5.10*) typically had higher intensities in addition to larger volumes of rainfall.

All of the overflow storms were over the 2.54 cm (1 in) design storm, but there were several storms that were greater than the design storm that did not overflow. From this summary table, it can also be noted that larger volume storms did not always produce the largest amount of overflow volume. In fact, the largest overflow volume (2.37 m<sup>3</sup> 1/30/2013) occurred during one of the high intensity storms (0.157 cm/hr) and was not one of the larger volumes of rainfall (4.78 cm). Determining the performance of the treatment train based on rain intensity and inflow (volume to the treatment train; *Equation 4.8*) and overflow volumes (*Equation 4.11*) is difficult to generalize. Analysis on a case-by-case basis is necessary to understand the causes of overflow for each storm. Most storms had large intensities, but some, such as Hurricane Sandy (10/28/2012), may have been subjected to a short period of high intensity to cause overflow rather than the entire storm being a high intensity. For this storm, as evident in the graph of *Figure 5.12*, rainfall was slow and steady over the duration with short periods of heavy rain. Other storm events had significantly more rain during the one minute measured increments. For example, during the storm on 1/30/2012, the maximum rainfall recorded in one minute was 0.178 cm (0.07 in). This short period of rainfall influenced the overflow as water was distributed to the treatment train faster than it could be removed through infiltration.

**Table 5.10 - Summary of events with overflow**

<b>Date</b>	<b>Duration (hrs)</b>	<b>Rain (cm)</b>	<b>Total Intensity (cm/hr)</b>	<b>TT Inflow Volume (m<sup>3</sup>)</b>	<b>Overflow Volume (m<sup>3</sup>)</b>	<b>Capture Volume (m<sup>3</sup>)</b>	<b>% Capture</b>
8/10/12	3.05	5.59	1.83	50.97	0.63	50.34	99%
9/2/12	31.58	4.70	0.15	42.71	0.83	41.88	98%
10/28/12	66.96	11.00	0.16	101.23	1.78	99.45	98%
12/20/12	10.48	7.54	0.72	69.14	2.07	67.07	97%
12/26/12	6.30	2.79	0.44	25.01	0.47	24.54	98%
1/30/13	11.98	4.78	0.40	43.42	2.37	41.05	95%
3/12/13	11.65	3.00	0.26	26.90	0.34	26.56	99%

### **5.3.3. Treatment Train Performance and Rainfall**

The treatment train performance can be evaluated through the rainfall characteristics, overflow volumes, and the design parameters. Since the rainfall intensities were determined in a number of ways and only the total intensity ( $i_1$ ) could be determined for every storm due to rainfall volume, the total intensity was applied for further analysis. The following graph (*Figure 5.14*) shows the total rainfall intensities vs. the rainfall volumes (cm). For reference, the additional graphs with  $i_2$  and  $i_3$  are included in *Appendix G*. In *Figure 5.14*, which includes the design storm rainfall volume (2.54 cm) and all storm intensities, it is apparent that regardless of intensity, storms less than the design volume (2.54 cm) are captured without overflow. Additionally, the treatment train does not overflow immediately following the design capture volume. Instead, there is general more than 4 cm captured, depending on intensity, before overflow. Larger volumes, but more importantly, higher intensity events, are more likely to cause overflow.

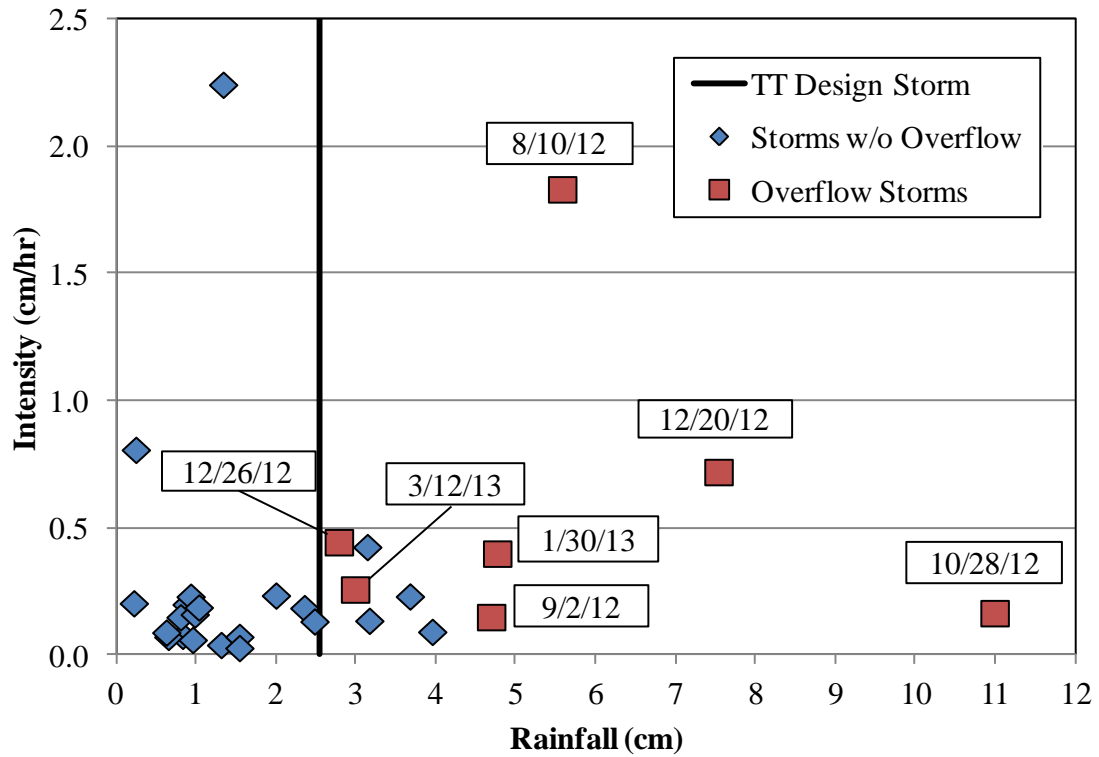


Figure 5.14 - Total intensity (cm/hr) vs. rainfall volume (cm)

Not only is the rainfall intensity an important factor important in analyzing the treatment train performance, but the duration also shows similarities in overflow events. From a graph of rainfall volume (cm) vs. storm duration (hrs) (*Figure 5.15*), most of the storms with overflow had shorter storm durations (less than 15 hours) in combination with larger volumes.

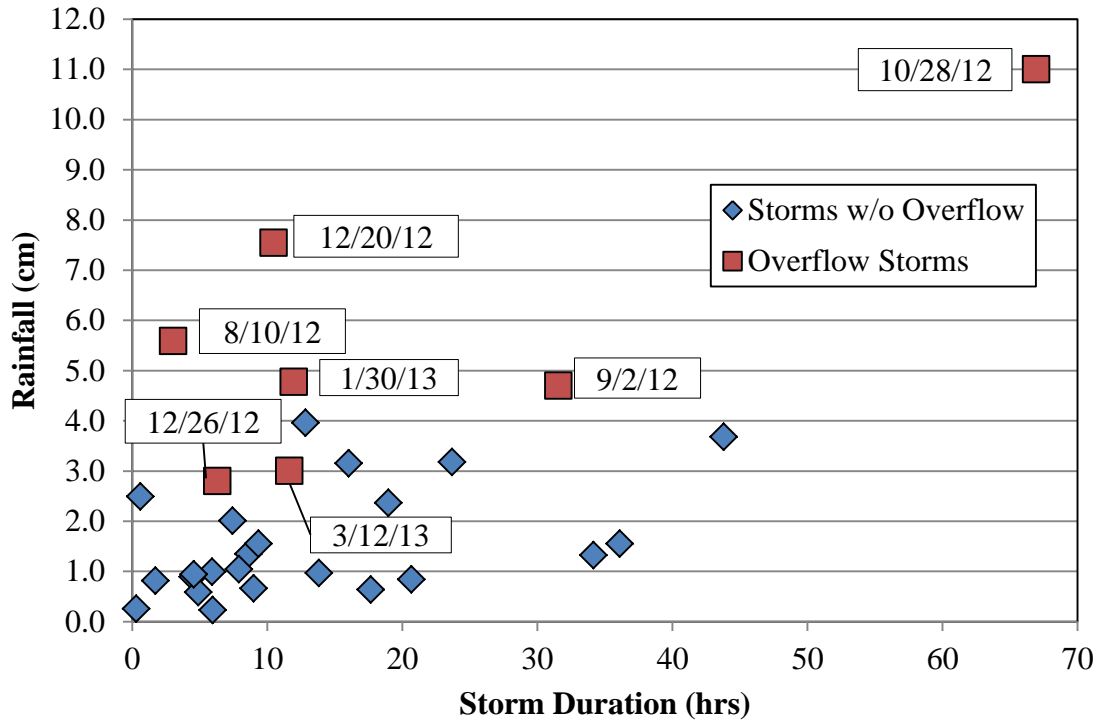


Figure 5.15 - Rainfall volume and storm duration

The seven overflow storms analyzed typically have higher intensities as a result of larger volumes of rainfall over a shorter duration. Since estimating overflow volume was a determining factor in the treatment train performance, another parameter to examine was the amount of time overflow as a percentage of the total duration of the storm. The overflow percentage, as it is referred to, is shown in a graph versus the storm duration (Figure 5.16). Storms without overflow were included in this graph to compare their durations to those with overflow. A number of storm events were longer in duration than some of the overflow events. This once again stresses the idea that overflow storms with higher intensities typically had shorter durations. In addition, a number overflow events had a large amount of time of overflow compared to the total storm duration. Three of the overflow events (8/10/12, 12/20/12, and 12/26/12) had percentages of 30% or higher.

These events were also the highest intensities of the overflow events. The remaining four overflow events were storms of at least 3 cm in volume but had the smallest intensities.

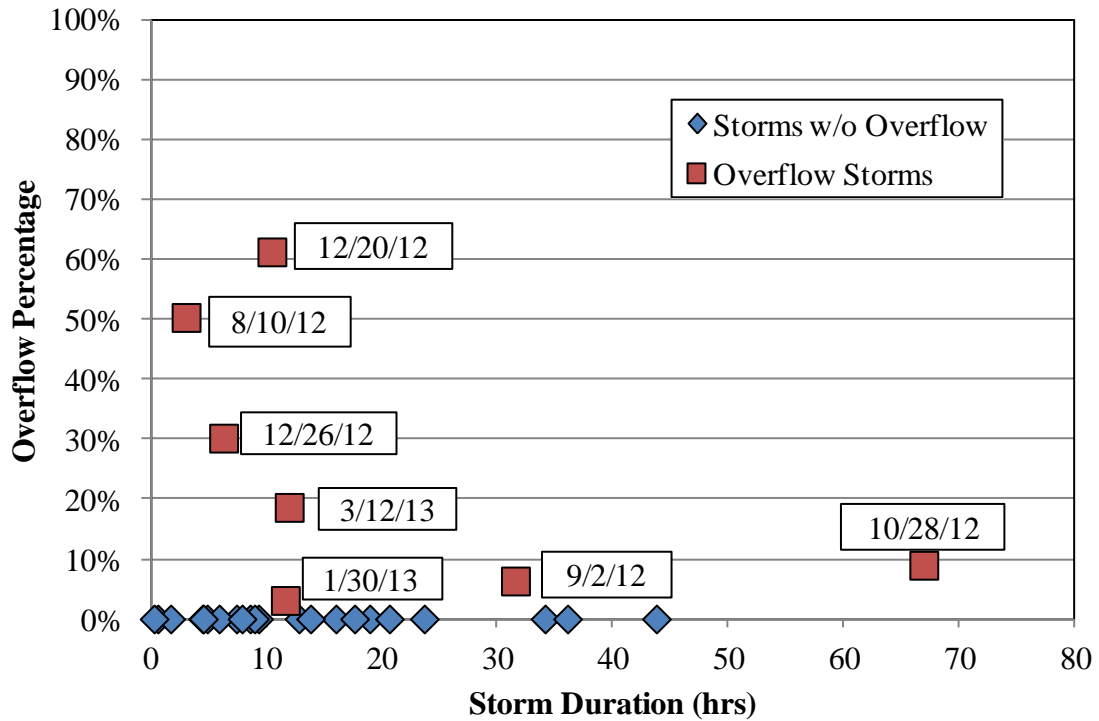
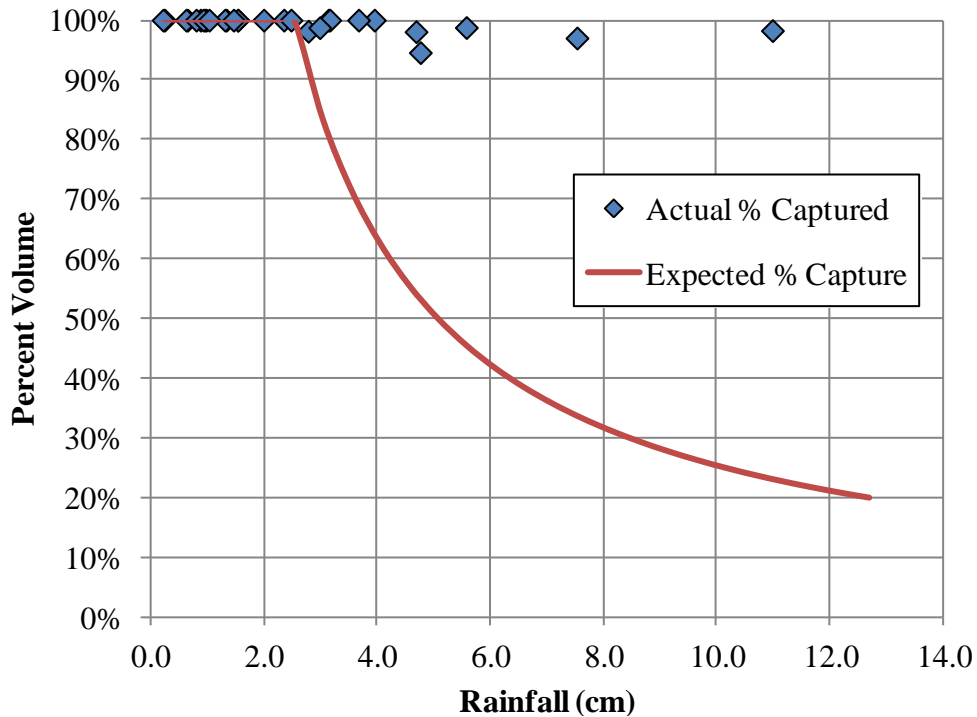


Figure 5.16 - Overflow percentage vs. storm duration

The treatment train was designed to capture a 2.54 cm (1 in) storm. However, after analyzing overflow events, more than this design volume appears to be captured. Graphically, this is shown by comparing the expected capture percentage and the actual capture percentage depending on the volume of rainfall (Figure 5.17). The capture percentage is the fraction of captured volume (volume in minus overflow volume) to the total volume in. For most of the storms, this value was 100%, and for overflow storms, the capture percentage was still no less than 95%. All storms were above the expected capture percentage, regardless of volume.



**Figure 5.17 - Expected capture performance vs. actual capture as a percentage of inflow and outflow volumes**

The treatment train has been capturing more stormwater runoff than originally designed. From *Figure 5.17*, the treatment train has demonstrated its ability to capture at least 95% of every storm analyzed up through mid-March, 2013. Even during higher intensity events which caused overflow, the amount of runoff captured was still large. In addition to the high percentage of volume captured, it is important to recognize the unique construction of the Villanova treatment train. At the infiltration trench, the pavers at the surface are not only the means of system overflow; they also allow water to infiltrate from the surface. It has been observed that due to the grading of the pavers and surrounding grass, stormwater often ponds prior to overflow at the upstream side of the trench. Therefore, while overflow volumes have been estimated and ultimately used to predict the treatment train's capture performance, overflow volumes may be even less.

Since the overflowing water ponds on top of the trench, it may not actually leave the site as overland flow, but instead pond until there is sufficient room to re-infiltrate into the IT. The photo in *Figure 5.18* was taken following the March 12, 2013 storm and shows ponded water which would be expected to re-infiltrate rather than runoff. This quantity of ponded water which may re-infiltrate is difficult to quantify, but it is a reasonable assumption following several observations at the site during storm events.



**Figure 5.18 - Ponding on the pervious pavers at the IT after a March 12, 2013 storm event**

#### **5.4. Summary and Recommendations**

The treatment train's performance exceeds its design. Based on the capture volume of the storms analyzed, regardless of storm size, most of the storm should be captured by the treatment train. It appears that more stormwater is reaching the infiltration trench than anticipated. The weir plates allow water to flow downstream until backwater effects occur; the stormwater may reach the infiltration trench for treatment sooner than expected. The infiltration trench often must fill in order for the rain gardens and swale to begin filling and retaining water for infiltration and treatment.

Continued research at the treatment train should focus on quantifying the effects of the system. Since it is apparent from this analysis of inflow versus overflow that the system captures large volumes of water, identifying the contributions of each individual SCM to the system will be beneficial. At this time, the infiltration trench appears to capture a much larger volume than originally designed for. Determining the volumes captured in the swale and rain gardens will provide more information on which parts of the system are performing better or worse than was expected.

In addition to quantifying the treatment train in terms of each individual SCM, it will also be of interest to further explore how different types of storms (volumes, durations, intensities) are captured by the treatment train. As mentioned, only the total intensity was used in this analysis. Other forms of intensity may provide further analysis. Since the system was designed for a 2.54 cm (1 in) storm, it would be interesting to examine what the characteristics of the rainfall are following the first 2.54 cm (1 in) storm. Perhaps the intensity of the rainfall after the design volume has fallen may be more influential on the capture performance than the total intensity over the entire storm duration. There are many directions for future research at the treatment train; both quantifying the effects of the SCMs and determining the water quality impacts should remain priorities.

## **Chapter 6 Summary and Future Research**

### **6.1. Project Summary**

The treatment train at Villanova University was constructed in October, 2011, with water first being routed to the system from the parking garage in March, 2012. Construction of the site provided useful information as these systems are not built by means of traditional construction procedures. There were difficulties preventing soil compaction and erosion problems, but these challenges provide useful observations for future projects. Monitoring began in July, 2012 with Campbell Scientific pressure transducers and v notch weirs being installed at six points in the system. While there were difficulties in water quantity measurements, observations during storm events prove the site functions well.

Data from the infiltration trench allowed for the determination of volumes of stormwater into the trench and estimates of overflow volumes. The trench was estimated to have overflowed during 7 of the 30 analyzed storms over the period of study. During these overflow events, only a small volume of the storms overflowed. Capture performance based on the total volume into the treatment train and the overflow volume was a minimum 95%; meaning that the volume of runoff from almost every storm was completely captured. Of the storms analyzed, a total of 668 m<sup>3</sup> entered the treatment train (75 cm of rain) and approximately 185 m<sup>3</sup> entered the infiltration trench. Only 8.5 m<sup>3</sup> of rainfall was determined to overflow from the system.

The recession and infiltration rates of the infiltration trench provide insight into the capture performance of the treatment train. While further research will allow for the

determination of the contribution of the swale and rain gardens to the performance, the recession and infiltration rates of the IT allowed for this initial assessment of the site. The rates, which show seasonal variation, provided data to ultimately estimate the volume that entered the IT during each storm and the volume of overflow. These rates will also allow for longevity and maintenance research in the future.

Rainfall characteristics prove to be an important factor in the treatment performance. High intensity storms, were more likely to cause overflow, regardless of total rainfall volume. Due to the infiltration throughout the system, it can handle larger storms than originally designed (2.54 cm (1 in)). Determining what individual entities of the treatment contribute to the greater capture volume is of interest for future research.

## **6.2. Future Research**

The treatment train at Villanova, the newest site of the SCM Research and Demonstration Park, has potential for numerous future research projects. For this thesis, limited data was available, but as the monitoring equipment is improved and water quality samples are prioritized, many projects focusing on the performance of the SCMs in series will be feasible.

### **6.2.1. Water Quantity Future Research**

The water quantity research at the treatment train thus far has been limited, mainly due to instrumentation and monitoring challenges. However, with these issues corrected, the site has great potential to measure the quantity effects of SCMs in series during rainfall events. Ideally, future research will be able to identify the volume of flow and rate of flow through the SCMs as a system, and also as individual entities. The weir plates and

depth readings should ultimately provide a means calculating the flow reduction of the stormwater from the parking garage. With this data, volume and peak flow reduction can be evaluated.

In addition to analyzing the water quantity throughout the system, it will also be interesting to identify more specifically the characteristics of the rainfall as it corresponds to the treatment train performance. Throughout this study, only a total intensity was considered, and as mentioned in Chapter 5, not only looking at this intensity, but perhaps the intensity after the first 2.54 cm (1 in) of rainfall may provide more information. In addition to intensity after the design storm, looking at the rainfall intensity as overflow in the IT occurs may provide interesting results. Many of the overflow events appear to have high intensity rainfall, not just a large volume, occur just before the depth in the IT reaches the top of the pavers. Quantifying the rainfall intensity prior to overflow could show more consistency in the type of rainfall causing overflow. Not only will it be interesting to explore the rainfall characteristics, but it will also be worthwhile to understand overflow better. As mentioned, the overflow volume for this study was based on the time the water level was above the crates and pavers and the maximum recession rate during that storm. Developing a more accurate means of determining overflow will allow for a more accurate estimation of the treatment train performance.

Continuing research on the treatment train will provide more information on how the treatment train performs as a system, but also the benefits of each individual SCM. With improved monitoring equipment, quantifying the stormwater runoff throughout the system will become more accurate. Estimating the performance of each SCM in the treatment train by the volume and flow aligns with the overall project goals regarding

water quantity. By determining the performance of the treatment train and its SCMs, future design recommendations will be feasible.

### **6.2.2. Water Quality Future Research**

Water quality should be a major focus point of research moving forward with the treatment train. As implied by the project research goals, water quality analysis should include comparing samples from the beginning to end of the series of SCMs. Grab samples will allow for such analysis of water quality. In addition to analyzing the water quality of the system, individual SCMs can be examined for their water quality reduction ability. Water quality samples other than grab samples may produce interesting results of the treatment train's quality performance. Installing lysimeters in the ground both underneath the SCMs and in the surrounding area of the treatment train would allow for the effect of infiltration on water quality to be analyzed. Currently, there is no means of measuring how the infiltrating SCMs at this site contribute to pollutant removal. Having the ability to collect these samples would certainly enhance the research potential of the treatment train from a water quality perspective.

### **6.2.3. Longevity and Maintenance**

One of the primary goals of the treatment train project is to evaluate the potential of pretreatment to increase SCM longevity and decrease maintenance needs. Collecting continuous data at the site will allow the SCM performance to be measured, similar to studies on the old infiltration trench. The recession rates at the infiltrating SCMs can be measured and compared over time to determine if any change in performance is evident; this work aligns with previous studies at Villanova, such as Emerson (2008).

In addition to determining whether the SCMs in series are beneficial for longevity and maintenance, the treatment train could demonstrate potential considerations for SCM design. The rainfall intensity, duration, and volume have been considered when determining the performance of the system, and if these rainfall characteristics are further analyzed, they may provide a different design parameter not typically considered. In this current study, rainfall intensity was generalized as the total intensity in further analysis, but this may not be the best representation of all storms. As previously mentioned, determining a more specific calculation for rainfall intensity may be helpful in determining design parameters. The treatment train at Villanova has a large potential for research and providing data for future stormwater control measure design and performance standards.

## References

- Akan O. (2002). "Modified rational method for sizing infiltration structures." *Canadian J. of Civil Eng.*, 29(4), 539-542.
- Bäckström, M. (2002). "Sediment transport in grassed swales during simulated runoff events." *Water Sci. Technol.*, 45(7), 41-49.
- Barraud S., Dechesne M., Bardin J. P., Varnier J. C. (2005). "Statistical analysis of pollution in stormwater infiltration basins." *Water Sci. and Technol.*, 51(2): 1-9.
- Barrett, M. E., Walsh, P. M., Malina, J. F., and Charbeneau, R. J. (1998). "Performance of vegetative controls for treating highway runoff." *J. Environ. Eng.*, 124(11), 1121-1128.
- Birch G. F., Fazeli M. S., Matthai C. (2005). "Efficiency of an infiltration basin in removing contaminants from urban stormwater." *Environmental Monitoring and Assessment*, 101(1-3), 23-38.
- Bobko, P. (2001). *Correlation and Regression Second Edition*. Thousand Oaks, CA: Sage Publications.
- Brown, R. A., Line, D. E., and Hunt, W. F. (2012). "LID treatment train: pervious concrete with subsurface storage in series with bioretention and care with seasonal high water tables." *J. Environ. Eng.*, 138(6), 689-697.
- Constantz, J., and Murphy, F. (1991). "Temperature dependence of ponded infiltration under isothermal conditions." *J. Hydr.*, 122(1): 119.

- Davis, A. P. (2005). "Green engineering principles promote low impact development." *Environ. Sci. Technol.*, 39(16), 338A-344A.
- Davis, A. P. (2008). "Field performance of bioretention: Hydrology impacts." *J. Hydrol. Eng.*, 13(2), 90-95.
- Davis, A. P., Shokouhian, M., Sharma, H., and Minami, C. (2006). "Water quality improvement through bioretention media: Nitrogen and phosphorus removal." *Water Environ. Res.*, 78(3), 284-293.
- Duchene, M., McBean E. A., Thomson, N. R. (1994). "Modeling of infiltration from trenches for stormwater control." *J. Water Resour. Plann. Manage.* 120(3), 276-293.
- Duley, F. L. and Domingo, C. E. (1943). "Effect of water temperature on rate of infiltration." *Proceedings of the Soil Science Society of America*, 8: 129-131.
- Emerson, C. (2008). "Evaluation of infiltration practices as a means to control stormwater runoff," thesis, presented to Villanova University, PA, in partial fulfillment of the requirements for the degree of Doctor of Philosophy.
- Emerson, C. H., Wadzuk B. M., Traver, R. G. (2010). "Hydraulic evolution and total suspended solids capture of an infiltration trench." *Hydrol. Process.* 24, 1008-1014.
- Hathaway, J. M. and Hunt, W. F. (2010). "Evaluation of stormwater wetlands in series in Piedmont, North Carolina." *J. Environ. Eng.*, 136(1), 140-146.

- Heasom, W., Traver R. G., and Welker, A. L. (2006). "Hydrologic modeling of a bioinfiltration best management practice." *J. of the American Water Resour. Assoc.*, 42 (5): 1329-1347.
- Jaynes, D. B. (1990). "Temperature variation effect on field-measured infiltration." *Soil Science Society of America Journal*, 54(2): 305.
- Kaighn, F.J., Jr., and Yu, S. L. (1996). "Testing of roadside vegetation for highway runoff pollutant removal." *Transportation Research Record 1523*, Transportation Research Board, Washington, DC, 116-123.
- Li, H. and Davis, A. P. (2009). "Water quality improvement through reductions of pollutant loads using bioretention." *J. Environ. Eng.*, 135(8), 567-576.
- Living Machine. (2012). "Living machine technology: How it works." *Living Machine*. <<http://livingmachines.com/About-Living-Machine/How-it-Works.aspx>>.
- Maryland Department of the Environment (MDE). (2009). Maryland Stormwater Design Manual.
- Minnesota Stormwater Steering Committee (MSSC). (2008). Minnesota Stormwater Manual. V. 2. Minnesota Pollution Control Agency, St. Paul, MN.
- National Research Council (NRC) (2009). *Urban stormwater management in the United States*. Washington, D.C.: The National Academies Press.
- PA Department of Environmental Protection (PADEP). (2006). Pennsylvania Best Management Practices Manual. Bureau of Watershed Management, Harrisburg, PA.

Philadelphia Water Department (PWD) (2013). "PIA\_1948-2011\_CDP\_Final\_24hr."

Roy-Poirier A., Champagne, P., Filion, Y. (2010). "Review of bioretention system research and design: Past, present, and future." *J. Environ. Eng.*, 136(9), 878-889.

Scholz M., Yazdi S. K. (2008). "Treatment of road runoff by a combined stormwater treatment, detention and infiltration system." *Water Air Soil Pollut.* 198, 55-64.

Shaver E. 1986. Urban runoff quality: impact and quality enhancement technology. *Proceedings of an Engineering Foundation Conference*. New England College, Henkier, New Hampshire.

Siriwardene N. R., Deletic A., Fletcher T. D. (2007). "Clogging of stormwater gravel infiltration systems and filters: Insights from a laboratory study." *Water Research.* 41, 1433-1440.

Strecker, E., Quigley, M., Urbonas, B., Jones, J., and Clary, J. (2001). "Determining urban storm water BMP effectiveness." *J. Water Resour. Plann. Manage.*, 127(3), 144-149.

U.S. Dept. of the Interior, Bureau of Reclamation (USBR). (2001). "Water Measurement Manual: a guide to effective water measurement practices for better water management." (3). Denver, CO.

Water Environment Federation (WEF) and American Society of Civil Engineers (ASCE). (2012). Design of Urban Stormwater Controls. "WEF Manual of Practice No. 23; ASCE/EWRI Manuals and Reports on Engineering Practice No. 87."

- Winston, R. J., Hunt, W. F., Kennedy, S. G., and Wright, J. D., and Lauffer, M. S. (2012). "Field evaluation of stormwater control measures for highway runoff treatment." *J. Env. Eng.*, 138(1), 101-111.
- Winston, R. J., Hunt, W. F., Osmond, D. L., Lord, W. G., and Woodward, M. D. (2011). "Field evaluation of four level spreader – Vegetative filter strips to improve urban water quality." *J. Irrig. Drain. Eng.*, 137(3), 170-182.
- Wright Water Engineers and Geosyntec Consultants (WWEGC). (2007). "Frequently Asked Questions Fact Sheet for the International Stormwater BMP Database: Why does the International Stormwater BMP Database Project omit percent removal as a measure of BMP performance?" [www.bmpdatabase.org](http://www.bmpdatabase.org)
- Yousef, Y. A., Wanielista, M. P., and Harper, H. H. (1985). "Removal of highway contaminants by roadside swales." *Transportation Research Record 1017*, Transportation Research Board, Washing, DC, 62-68.
- Yu, S. L., Kuo, J.-T., Fassman, E. A., and Pan, H. (2001). "Field test of grassed-swale performance in removing runoff pollution." *J. Water Resour. Plann. Manage.*, 127(3), 168-171.

## Appendices

### Appendix A: Construction Cost Breakdown

Table A.1 - Treatment train construction costs

<i>SCM Construction</i>			
	Labor/Equip	Material	Total
Day 1 - 9/30/2011	\$2,600	\$550	\$3,150
Day 2 - 10/3/2011	\$3,260	\$300	\$3,560
Day 3 - 10/4/2011	\$2,710	\$500	\$3,210
Day 4 - 10/6/2011	\$2,600	\$150	\$2,750
Day 5 - 10/7/2011	\$2,600	\$200	\$2,800
Day 6 - 10/10/2011	\$2,600	\$800	\$3,400
Day 7 - 10/11/2011	\$3,045	\$150	\$3,195
Day 8 - 10/17/2011	\$3,740	\$2,200	\$5,940
Day 9 - 10/18/2011	\$3,520	\$2,800	\$6,320
Day 10 - 11/1/2011	\$1,685	\$0	\$1,685
Day 11 - 11/2/2011	\$3,272	\$7,400	\$10,672
Day 12 - 11/4/2011	\$3,860	\$700	\$4,560
			<b>\$51,242</b>
<i>Parking Garage Piping</i>			
4/30/2012			<b>\$13,545</b>
<b>Construction Total</b>			<b>\$64,787</b>

## Appendix B: Plant List

**Table B.1 - List of plants at the treatment train**

Quantity	Genus	Variety
6	Aronia	Melanocarpa
30	Asclepias	Tuberosa
10	Aster	Novi-Belgii
50	Carex	Lurida
65	Carex	Pensylvanica
15	Carex	Stricta
6	Clethra	Alnifolia
50	Coreopsis	Lancelata
15	Echinacea	Purpurea
15	Eupatorium	Coelestium
15	Iris	Versicolor
25	Juncus	Effusus
50	Lobelia	Cardinalis
50	Lobelia	Siphilitica
15	Monarda	Punctata
50	Panicum	Amarum
15	Penstemon	Digitalis
15	Rudbeckia	Laciniata
50	Schizachyrium	Scoparium
50	Sorghastrum	Nutans
6	Spiraea	Latifolia
4	Verbena	Hastata

## Appendix C: Unused Survey Data

Table C.1 - July 10, 2012 survey data

10-Jul-12										
Location	PT Concrete (ft)	PT Concrete (in)	Splash Pad (ft)	Splash Pad (in)	Pad - PT Concrete (in)	V to Pad (in)	PT Concrete to V (in)	2 in from cap + 1.58 in zero	PT to Bottom V (in)	PT to Bottom V (ft)
W1	5.92	71.04	4.31	51.72	19.32	5.38	24.70	23.12	24.70	<b>2.06</b>
W2	5.75	69.00	6.20	74.40	5.40	2.50	2.90	2.48	2.48	<b>0.21</b>
W3	8.04	96.48	8.36	100.32	3.84	5.50	-1.66	-2.08	-2.08	<b>-0.17</b>
W4	8.68	104.16	8.94	107.28	3.12	6.38	-3.26	-3.68	-3.68	<b>-0.31</b>
W5	9.11	109.32	9.80	117.60	8.28	10.75	-2.47	-2.89	-2.89	<b>-0.24</b>

Table C.2 - July 11, 2012 survey data

11-Jul-12													
Location	PT Concrete (ft)	PT Concrete (in)	Splash Pad (ft)	Splash Pad (in)	Pad - PT Concrete (in)	V to Pad (in)	PT Concrete to V (in)	2 in from cap + 1.58 in zero	PT to Bottom V (in)	PT to Bottom V (ft)	PT to Sensor (ft)	Sensor to V (ft)	Sensor to V (in)
W1	6.28	75.36	4.68	56.16	19.20	5.38	24.58	23.00	23.00	<b>1.916</b>	1.91	1.90	22.75
W2	6.36	76.32	6.54	78.48	2.16	2.50	-0.34	-0.76	-0.76	<b>-0.063</b>	0.15	0.09	1.04
W3	8.41	100.92	8.71	104.52	3.60	5.50	-1.90	-2.32	-2.32	<b>-0.193</b>	0.15	-0.04	-0.52
W4	9.04	108.48	9.31	111.72	3.24	6.38	-3.13	-3.55	-3.55	<b>-0.296</b>	0.15	-0.15	-1.76
W5	9.47	113.64	10.18	122.16	8.52	10.75	-2.23	-2.65	-2.65	<b>-0.221</b>	0.15	-0.07	-0.86

Table C.3 - July 18, 2012 survey data

18-Jul-12													
Location	PT Concrete (ft)	PT Concrete (in)	Splash Pad (ft)	Splash Pad (in)	Pad - PT Concrete (in)	V to Pad (in)	PT Concrete to V (in)	2 in from cap + 1.58 in zero	PT to Bottom V (in)	PT to Bottom V (ft)	PT to Sensor (ft)	Sensor to V (ft)	Sensor to V (in)
W1	6.28	75.36	4.68	56.16	19.20	5.38	24.58	23.00	23.00	<b>1.916</b>	1.91	0.01	0.13
W2	5.7	68.4	5.7	68.4	0.00	2.50	-2.50	-2.92	-2.92	<b>-0.243</b>	0.15	-0.09	-1.13
W3	7.56	90.72	7.86	94.32	3.60	5.50	-1.90	-2.32	-2.32	<b>-0.193</b>	0.15	-0.04	-0.52
W4	8.19	98.28	8.43	101.16	2.88	6.25	-3.37	-3.79	-3.79	<b>-0.316</b>	0.15	-0.17	-2.00
W5	8.61	103.32	9.32	111.84	8.52	10.75	-2.23	-2.65	-2.65	<b>-0.221</b>	0.15	-0.07	-0.85

Table C.4 - August 17, 2012 survey data

17-Aug-12													
Location	PT Concrete (ft)	PT Concrete (in)	Splash Pad (ft)	Splash Pad (in)	Pad - PT Concrete (in)	V to Pad (in)	PT Concrete to V (in)	2 in from cap + 1.58 in error	PT to Bottom V (in)	PT to Bottom V (ft)	PT to Sensor (ft)	Sensor to V (ft)	Sensor to V (in)
W1	5.06	60.72	3.89	46.68	14.04	5.38	19.42	17.84	17.84	<b>1.486</b>	1.48	0.01	0.13
W2	5.76	69.12	5.76	69.12	0.00	2.50	-2.50	-2.92	-2.92	<b>-0.243</b>	0.15	-0.09	-1.13
W3	7.62	91.44	7.91	94.92	3.48	5.50	-2.02	-2.44	-2.44	<b>-0.203</b>	0.15	-0.05	-0.64
W4	8.27	99.24	8.5	102	2.76	6.25	-3.49	-3.91	-3.91	<b>-0.326</b>	0.15	-0.18	-2.12
W5	8.66	103.92	9.36	112.32	8.40	11.75	-3.35	-3.77	-3.77	<b>-0.314</b>	0.15	-0.16	-1.98

## Appendix D-1: CR1000 Programming Code for Data Recording

'CR1000

'This statement should keep the public variables (calibration coefs. in memory after power down.

PreserveVariables

'Declare Variables and Units

Public BattV

Public CS450Data(2)

Public CS450Da\_2(2)

Public CS450Da\_3(2)

Public CS450Da\_4(2)

Public CS450Da\_5(2)

Public CS450Da\_6(2)

Public TTS1, TTS2, TTS3, TTS4, TTS5,  
TTS6

Const W1\_M=1

Const W1\_B=0

Const W2\_M=1

Const W2\_B=0

Const W3\_M=1

Const W3\_B=0

Const W4\_M=1

Alias CS450Data(1)=TTW1

Alias CS450Data(2)=Temp\_1

Alias CS450Da\_2(1)=TTW2

Alias CS450Da\_2(2)=Temp\_2

Alias CS450Da\_3(1)=TTW3

Alias CS450Da\_3(2)=Temp\_3

Units BattV=Volts

Units TTW1=feet

Units Temp\_1=deg C

Units TTW2=feet

Units Temp\_2=deg C

Units TTW3=feet

Units Temp\_3=Deg C

Units TTW4=feet

Units Temp\_4=deg C

Public

S1\_Volt,S2\_Volt,S3\_Volt,S4\_Volt,S5\_Volt,S6\_Volt

Public

S1\_switchDepth,S2\_switchDepth,S3\_switchDepth,S4\_switchDepth,S5\_switchDepth,S6\_switchDepth

Dim

Last\_S1,Last\_S2,Last\_S3,Last\_S4,Last\_S5,Last\_S6

Const W4\_B=0

Const W5\_M=1

Const W5\_B=0

Const IT\_M=1

Const IT\_B=0

'Keeping these values constant unless calibration needed

Alias CS450Da\_4(1)=TTW4

Alias CS450Da\_4(2)=Temp\_4

Alias CS450Da\_5(1)=TTW5

Alias CS450Da\_5(2)=Temp\_5

Alias CS450Da\_6(1)=TTIT

Alias CS450Da\_6(2)=Temp\_6

Units TTW5=feet

Units Temp\_5=Deg C

Units TTIT=feet

Units Temp\_6=deg C

Units S1\_Volt=mV

Units S2\_Volt=mV

Units S3\_Volt=mV

Units S4\_Volt=mV

Units S5\_Volt=mV

Units S6\_Volt=mV  
Units S1\_switchDepth=feet  
Units S2\_switchDepth=feet  
Units S3\_switchDepth=feet

Units S4\_switchDepth=feet  
Units S5\_switchDepth=feet  
Units S6\_switchDepth=feet

'Define Data Tables

DataTable(TT\_DATA,1,-1)  
    DataInterval(0,1,Min,10)  
    Average(1,TTW1,FP2,False)  
    Average(1,Temp\_1,FP2,False)  
    Average(1,TTW2,FP2,False)  
    Average(1,Temp\_2,FP2,False)  
    Average(1,TTW3,FP2,False)  
    Average(1,Temp\_3,FP2,False)  
    Average(1,TTW4,FP2,False)  
    Average(1,Temp\_4,FP2,False)  
    Average(1,TTW5,FP2,False)  
    Average(1,Temp\_5,FP2,False)  
    Average(1,TTIT,FP2,False)  
    Average(1,Temp\_6,FP2,False)  
    Average (1,TTS1,FP2,False)  
    Average (1,TTS2,FP2,False)  
    Average (1,TTS3,FP2,False)

Average (1,TTS4,FP2,False)  
Average (1,TTS5,FP2,False)  
Average (1,TTS6,FP2,False)  
Average (1,S1\_Volt,FP2,False)  
Average (1,S2\_Volt,FP2,False)  
Average (1,S3\_Volt,FP2,False)  
Average (1,S4\_Volt,FP2,False)  
Average (1,S5\_Volt,FP2,False)  
Average (1,S6\_Volt,FP2,False)  
Sample (1,S1\_switchDepth,FP2)  
Sample (1,S2\_switchDepth,FP2)  
Sample (1,S3\_switchDepth,FP2)  
Sample (1,S4\_switchDepth,FP2)  
Sample (1,S5\_switchDepth,FP2)  
Sample (1,S6\_switchDepth,FP2)

EndTable

DisplayMenu("Treatment Train",-2)

SubMenu("Current Data")  
    DisplayValue("TTW1",TTW1)  
    DisplayValue("Temp\_1",Temp\_1)  
    DisplayValue("TTW2",TTW2)  
    DisplayValue("Temp\_2",Temp\_2)  
    DisplayValue("TTW3",TTW3)  
    DisplayValue("Temp\_3",Temp\_3)  
    DisplayValue("TTW4",TTW4)  
    DisplayValue("Temp\_4",Temp\_4)  
    DisplayValue("TTW5",TTW5)  
    DisplayValue("Temp\_5",Temp\_5)  
    DisplayValue("TTIT",TTIT)  
    DisplayValue("Temp\_6",Temp\_6)  
    DisplayValue("TTS1",TTS1)

DisplayValue("TTS2",TTS2)  
DisplayValue("TTS3",TTS3)  
DisplayValue("TTS4",TTS4)  
DisplayValue("TTS5",TTS5)  
DisplayValue("TTS6",TTS6)  
DisplayValue("S1\_Volt",S1\_Volt)  
DisplayValue("S2\_Volt",S2\_Volt)  
DisplayValue("S3\_Volt",S3\_Volt)  
DisplayValue("S4\_Volt",S4\_Volt)  
DisplayValue("S5\_Volt",S5\_Volt)  
DisplayValue("S6\_Volt",S6\_Volt)  
DisplayValue("BattV",BattV)

EndSubMenu

EndMenu

'Main Program

BeginProg  
    Scan(20,Sec,1,0)

'Default Datalogger Battery Voltage measurement BattV

Battery(BattV)  
 'CS450/CS455 Pressure Transducer measurements TTW1 and Temp\_1  
 '30 foot cable length  
 SDI12Recorder(TTW1,1,"1","M1!",W1\_M,W1\_B)  
 TTW1=TTW1\*2.30666  
 'CS450/CS455 Pressure Transducer measurements TTW2 and Temp\_2  
 '80 foot cable length  
 SDI12Recorder(TTW2,1,"2","M1!",W2\_M,W2\_B)  
 TTW2=TTW2\*2.30666  
 'CS450/CS455 Pressure Transducer measurements TTW3 and Temp\_3  
 '100 foot cable length  
 SDI12Recorder(TTW3,3,"3","M1!",W3\_M,W3\_B)  
 TTW3=TTW3\*2.30666  
 'CS450/CS455 Pressure Transducer measurements TTW4 and Temp\_4  
 '125 foot cable length  
 SDI12Recorder(TTW4,3,"4","M1!",W4\_M,W4\_B)  
 TTW4=TTW4\*2.30666  
 'CS450/CS455 Pressure Transducer measurements TTW5 and Temp\_5  
 '130 foot cable length  
 SDI12Recorder(TTW5,5,"5","M1!",W5\_M,W5\_B)  
 TTW5=TTW5\*2.30666  
 'CS450/CS455 Pressure Transducer measurements TTIT and Temp\_6  
 '150 foot cable length  
 SDI12Recorder(TTIT,5,"6","M1!",IT\_M,IT\_B)  
 TTIT=TTIT\*2.30666

'Weir Alarm sensors. When it's wet, it returns about 5000mV, otherwise, no voltage

VoltDiff(S1\_Volt,1,mV5000,1,True,0,\_60Hz,1,0)  
 If S1\_Volt > 4900 Then TTS1 = 1 Else TTS1 = 0  
 VoltDiff(S2\_Volt,1,mV5000,2,True,0,\_60Hz,1,0)  
 If S2\_Volt > 4900 Then TTS2 = 1 Else TTS2 = 0  
 VoltDiff(S3\_Volt,1,mV5000,3,True,0,\_60Hz,1,0)  
 If S3\_Volt > 4900 Then TTS3 = 1 Else TTS3 = 0  
 VoltDiff(S4\_Volt,1,mV5000,4,True,0,\_60Hz,1,0)  
 If S4\_Volt > 4900 Then TTS4 = 1 Else TTS4 = 0  
 VoltDiff(S5\_Volt,1,mV5000,5,True,0,\_60Hz,1,0)  
 If S5\_Volt > 4900 Then TTS5 = 1 Else TTS5 = 0  
 VoltDiff(S6\_Volt,1,mV5000,6,True,0,\_60Hz,1,0)  
 If S6\_Volt > 4900 Then TTS6 = 1 Else TTS6 = 0

'Check if current sensor status (wet/dry) equals that from last scan. If not, set "switchDepth" to current PT reading.

If TTS1 <> Last\_S1 Then S1\_switchDepth=TTW1  
 If TTS2 <> Last\_S2 Then S2\_switchDepth=TTW2  
 If TTS3 <> Last\_S3 Then S3\_switchDepth=TTW3

```
If TTS4 <> Last_S4 Then S4_switchDepth=TTW4  
If TTS5 <> Last_S5 Then S5_switchDepth=TTW5  
If TTS6 <> Last_S6 Then S6_switchDepth=TTIT
```

```
'Set "Last value" to the current value to be used next scan.
```

```
Last_S1=TTS1
```

```
Last_S2=TTS2
```

```
Last_S3=TTS3
```

```
Last_S4=TTS4
```

```
Last_S5=TTS5
```

```
Last_S6=TTS6
```

```
'Call Data Tables and Store Data
```

```
CallTable(TT_DATA)
```

```
NextScan
```

```
EndProg
```

## Appendix D-2: Wiring for Pressure Transducers and Sensors in CR1000

**Table D.1 - Treatment train CR1000 wiring list**

<i>Voltage Differential Channels</i>		<i>Wire Color</i>
1	H Sensor 1	Green
	L Sensor 1	White
g		
2	H Sensor 2	Green
	L Sensor 2	White
g		
3	H Sensor 3	Green
	L Sensor 3	White
g		
4	H Sensor 4	Green
	L Sensor 4	White
g		
5	H Sensor 5	Green
	L Sensor 5	White
g		
<i>Pulse Port Channels</i>		<i>Wire Color</i>
1	P1	
	g Pressure Transducers 1-6	Yellow
2	P2	
	g Pressure Transducers 1-6	Clear
<i>Switched Voltage Excitation</i>		<i>Wire Color</i>
1	EX1	
	g Pressure Transducers 1-6	Blue
<i>Comm Channels</i>		<i>Wire Color</i>
Com1	C1 Pressure Transducers 1-2	White
	C2	
Com2	C3 Pressure Transducers 3-4	White
	C4	
G		
Com3	C5 Pressure Transducers 5-6	White
	C6	
<i>Power Out Channels</i>		<i>Wire Color</i>
G	empty	
5V	Sensors 1-6	Green
G	empty	
SW-12	empty	
G	Pressure Transducers 1-6	Black
12V	Pressure Transducers 1-6	Red
12V	Sensors 1-6	Red
G	Sensors 1-6	Black

## Appendix E: XT-1000 Calibration Method

The XT-1000 is a high accuracy magnetostrictive level sensor. The sensor requires setup with the CR1000 with the code included in the treatment train's instrumentation file in the Villanova database. The max depth must be determined based on the length the magnetic ball is allowed to move up and down the probe. The program should then output a relatively accurate depth reading if the probe is placed in water and the ball is allowed to float up and down. After following the factory instructions on measuring the sensor's span of the 4-20 mA output (a copy of the user manual is available in the treatment train's directory at Villanova or online), further calibration is necessary.

With the same code running, hand measurements should be recorded for the depth of water in some sort of container (bottom of container to top surface of water) and the corresponding mill volts being displayed by the XT-1000. Depth readings should be ignored at this point. At least 6 points should be collected from this procedure and a graph of measured depth versus mV should be created and fitted with a linear trendline. The R squared from the graph should be very close to 1. The equation of the linear line will then be used as the equation for the output of depth in the code for the CR1000. The following code is an example from a test on a sample XT-1000. The XT-1000 was plugged into the third differential channel in this example.

*'This statement should keep the public variables (calibration coefs. In memory after power down.*

*PreserveVariables*

*'Declare Data Variables*

*Public Batt\_Volt*

*Public xt1000voltage*

*Public depth*

*Dim X, resistance*

*'Use inches for these numbers*

```

Const maxdepth=4.7575

'Declare units

Units depth=inches

'Define Data Tables

'Create the DATA tables

DataTable(LEVEL_DATA,True,-1)

  DataInterval(0,5,Min,10)

  Average(1,xt1000voltage,FP2,False)

  Average(1,depth,FP2,False)

EndTable

'Define Custom Menu for the keyboard display in the white weather box on site

DisplayMenu("Lab Level Sensors",-2)

  SubMenu("Current Data")

    DisplayValue("xt1000voltage",xt1000voltage)

    DisplayValue("depth",depth)

  EndSubMenu

EndMenu

'Main Program

BeginProg

'20 second scan rate

Scan(10,Sec,1,0)

'Default Datalogger Battery Voltage measurement Batt_Volt:

Battery(Batt_Volt)

'Gems XT-1000: Diff channel 3

'Diff H – signal wire AND resistor wire (220 ohm)

```

*'Diff L – resistor wire AND extra short length of wire*

*'G – extra short length of wire*

*VoltDiff(xt1000voltage,1,mV5000,3,True,0,\_60Hz,1,0)*

*depth=((xt1000voltage\*.00133)+.29255)*

*'Call Data Tables and Store Data*

*CallTable(LEVEL\_DATA)*

*NextScan*

*EndProg*

## Appendix F-1: Infiltration Trench Individual Storm Graphs

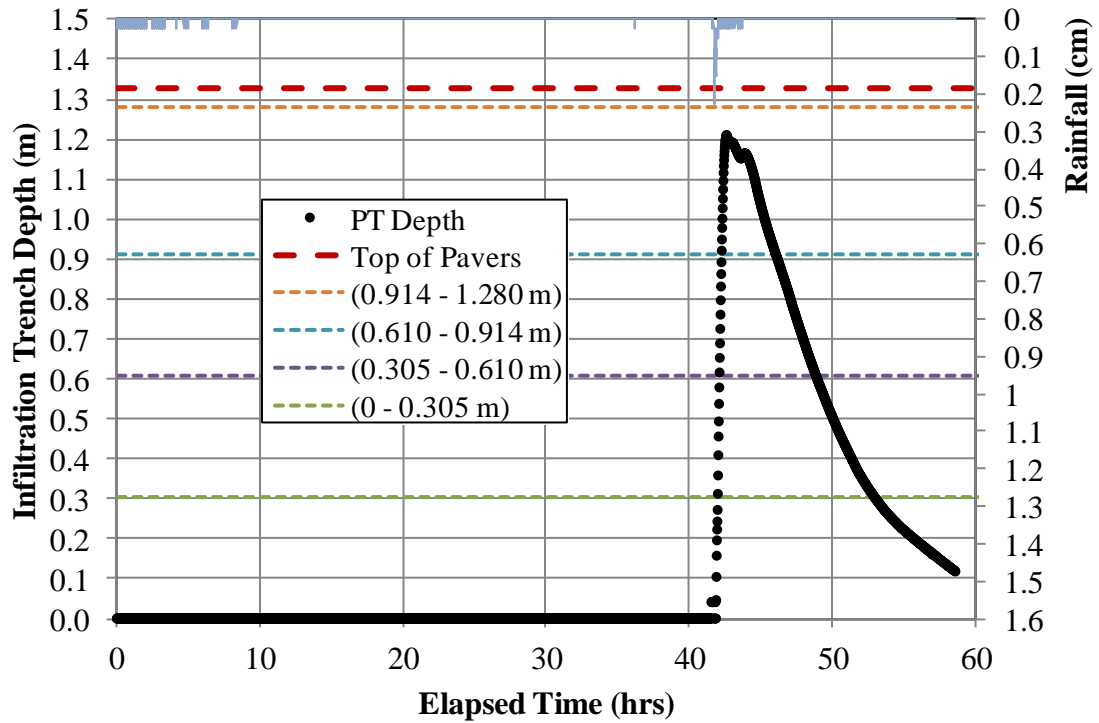


Figure F.1 - July 16, 2012 pressure transducer data

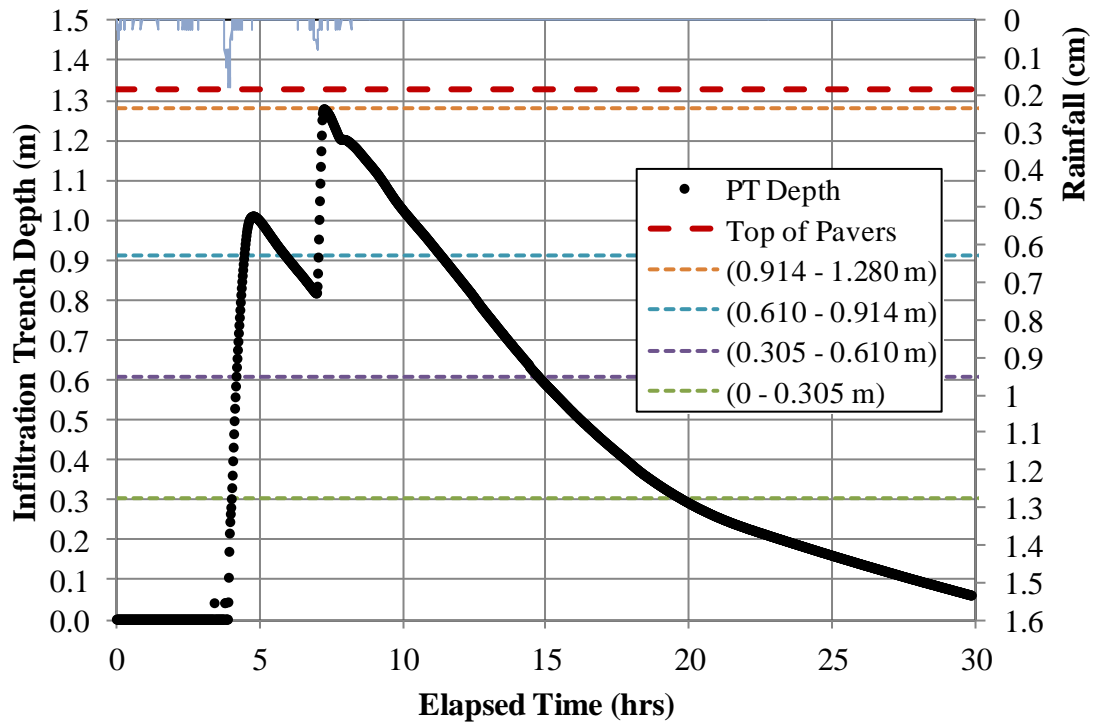


Figure F.2 - July 20, 2012 pressure transducer data

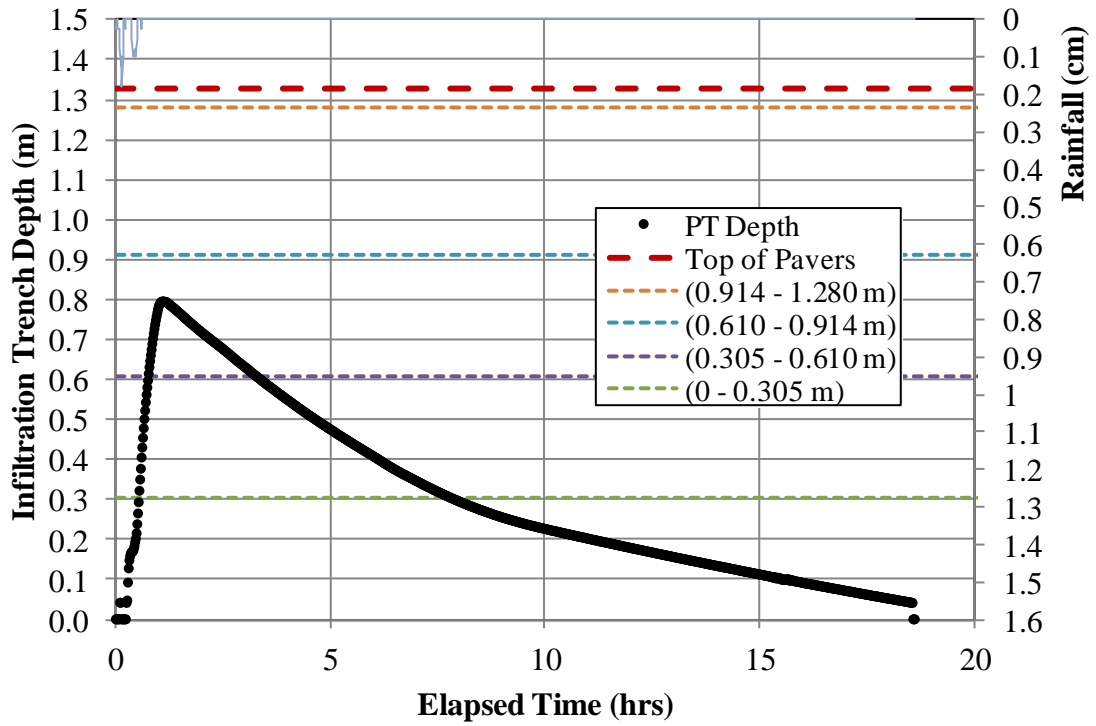


Figure F.3 - July 28, 2012 pressure transducer data

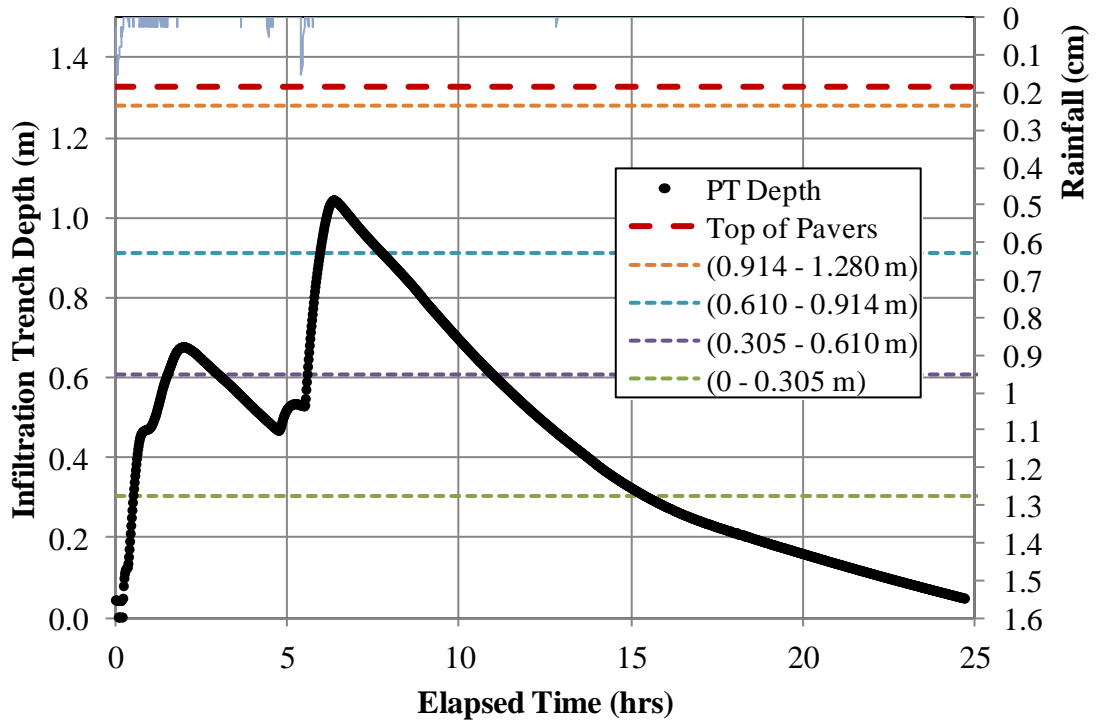


Figure F.4 - August 5, 2012 pressure transducer data

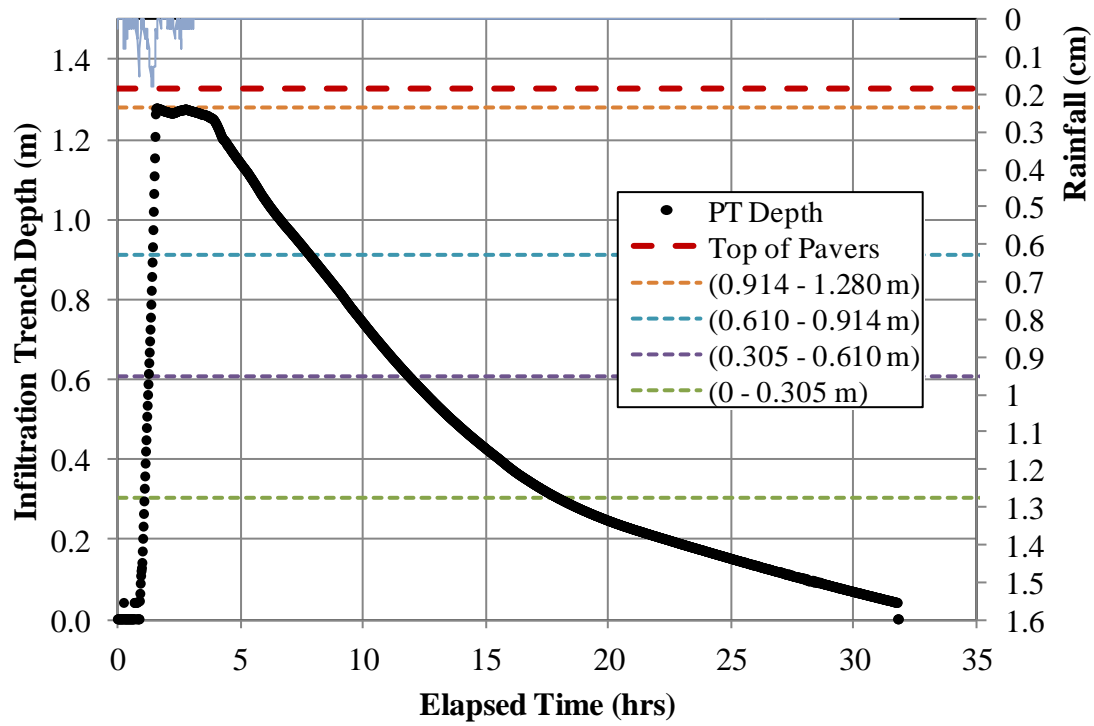


Figure F.5 - August 10, 2012 pressure transducer data

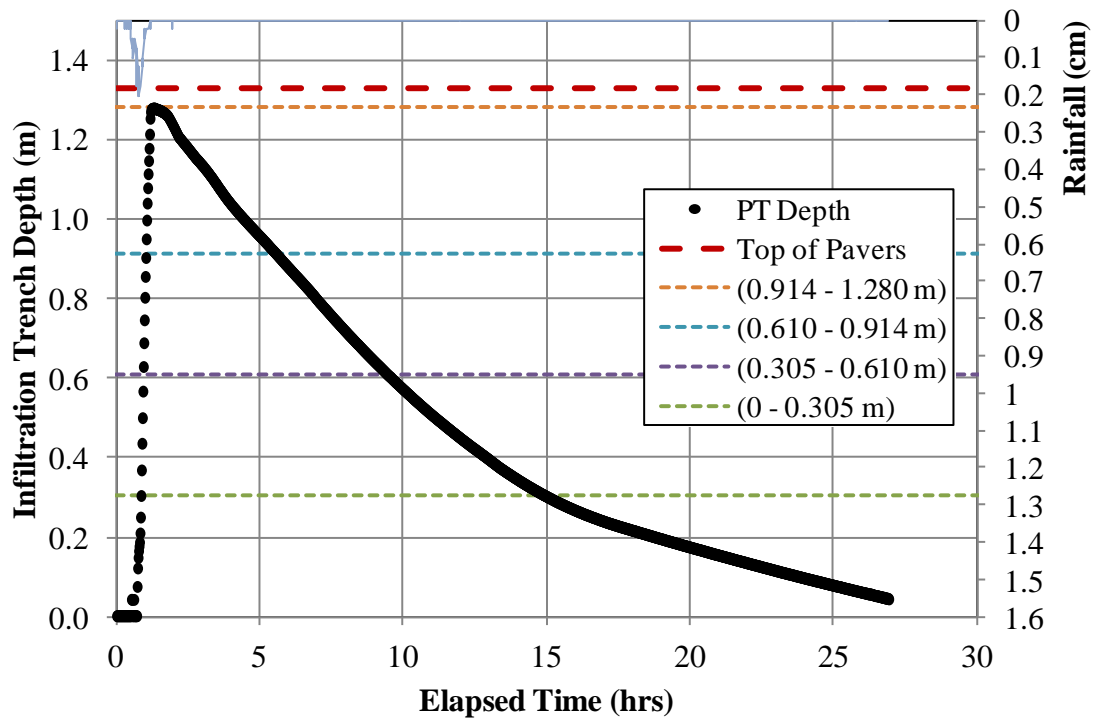


Figure F.6 - August 14, 2012 pressure transducer data

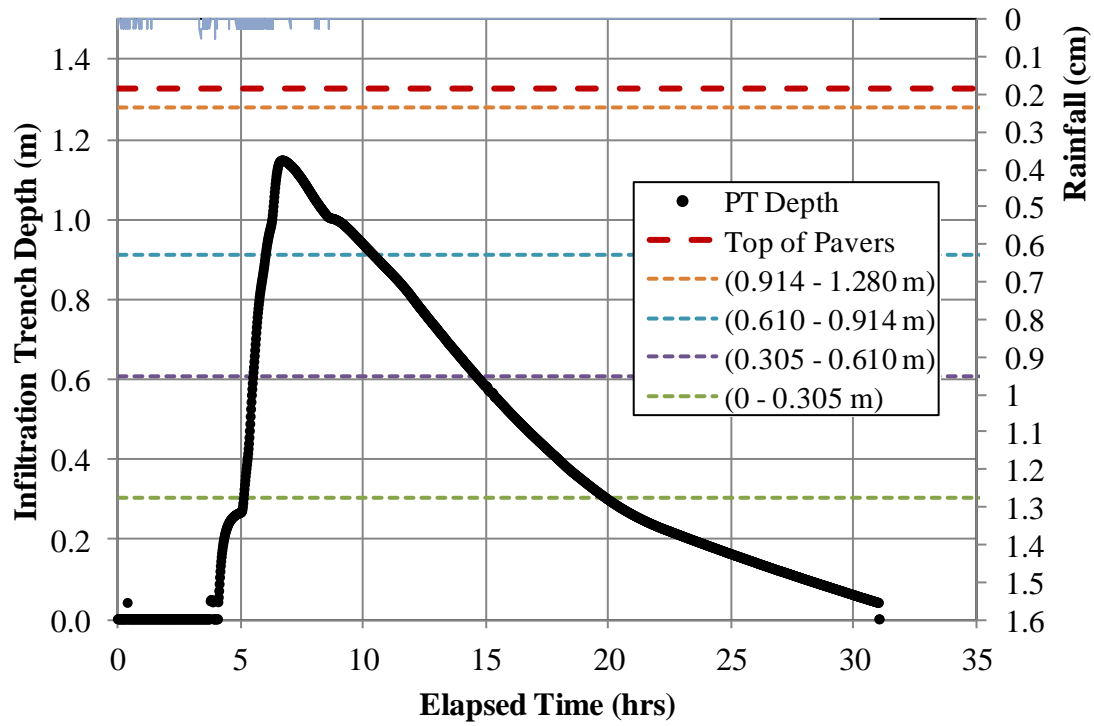


Figure F.7 - August 18, 2012 pressure transducer data

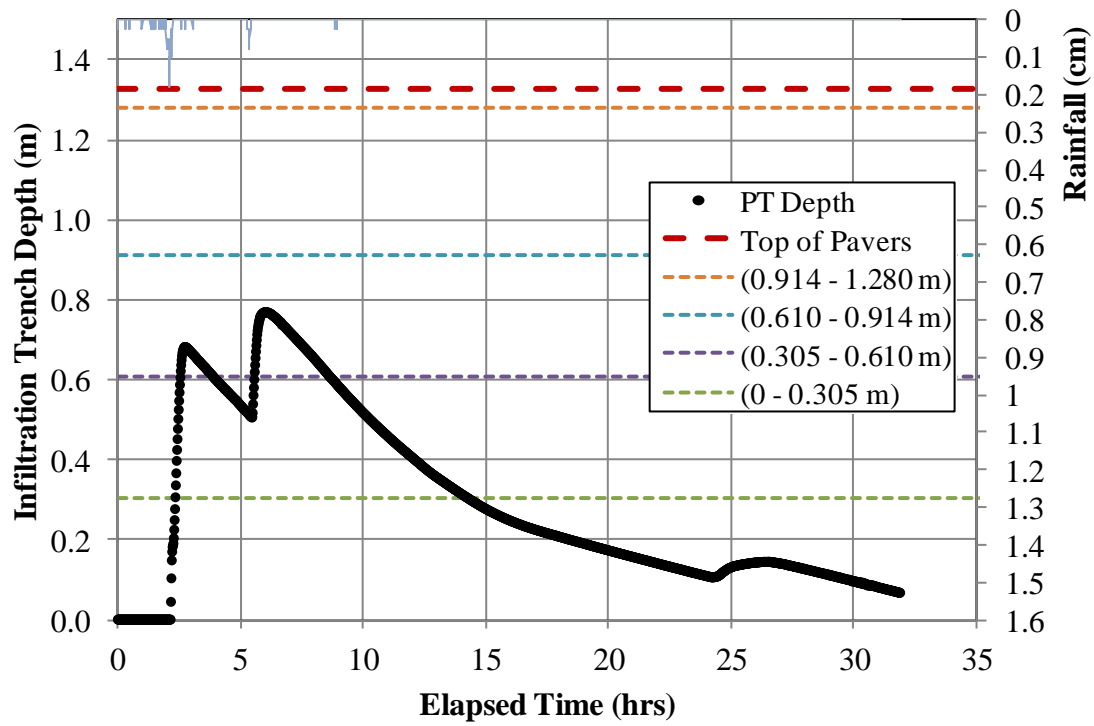


Figure F.8 - August 27, 2012 pressure transducer data

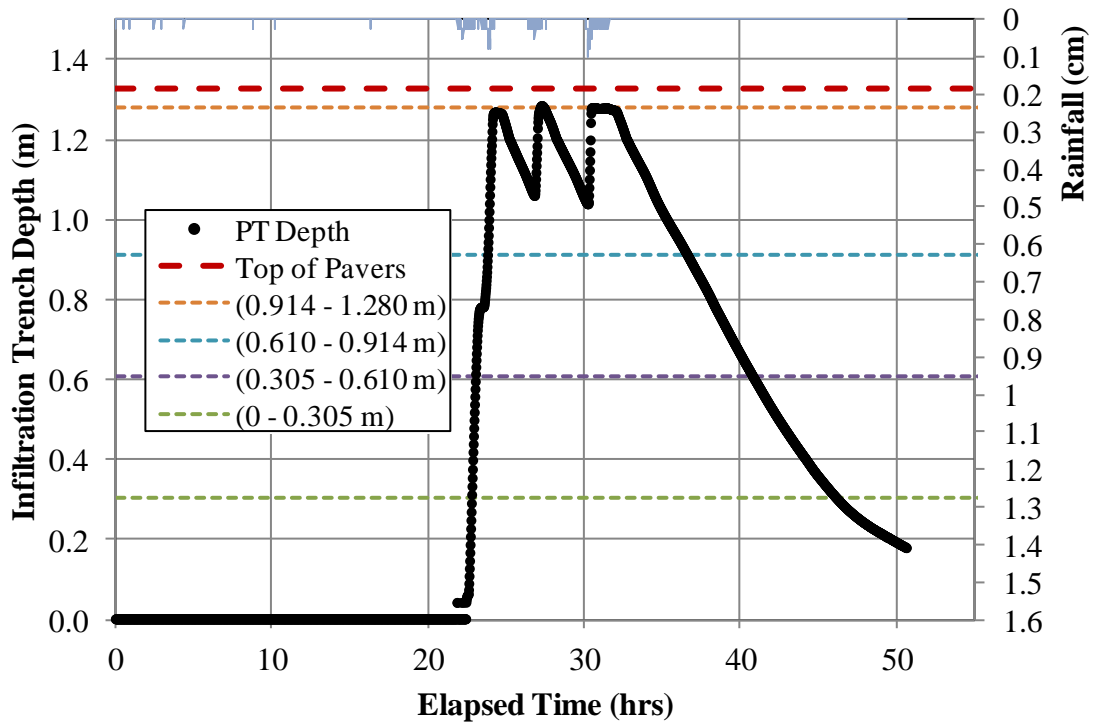


Figure F.9 - September 2, 2012 pressure transducer data

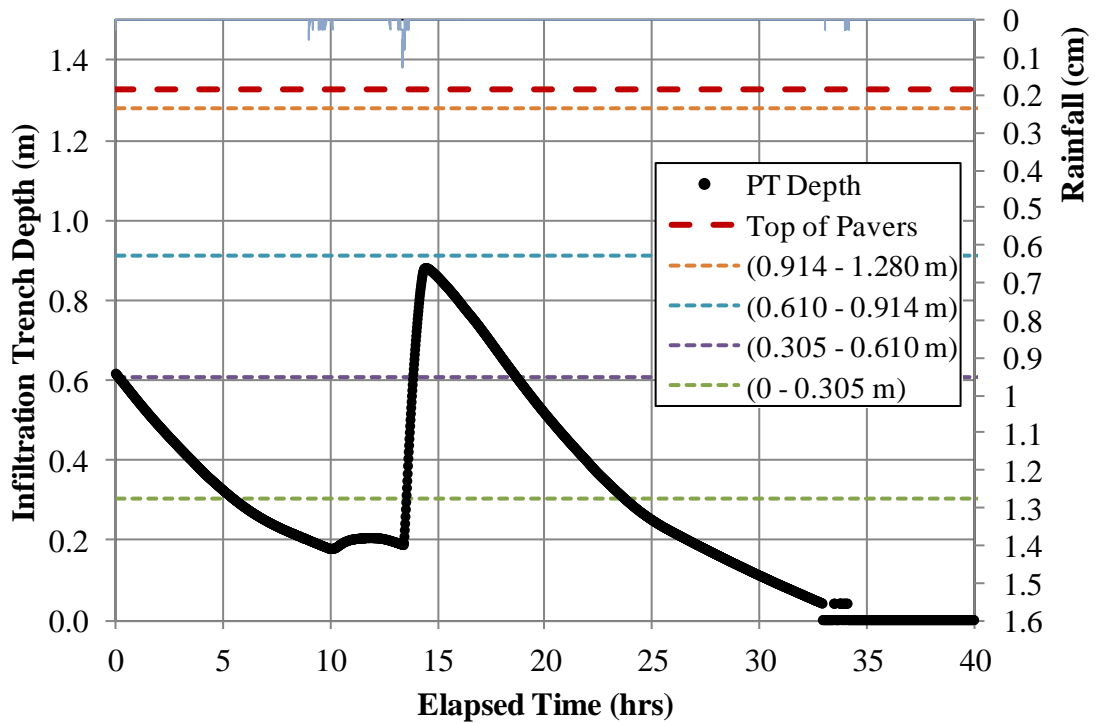


Figure F.10 - September 4, 2012 pressure transducer data

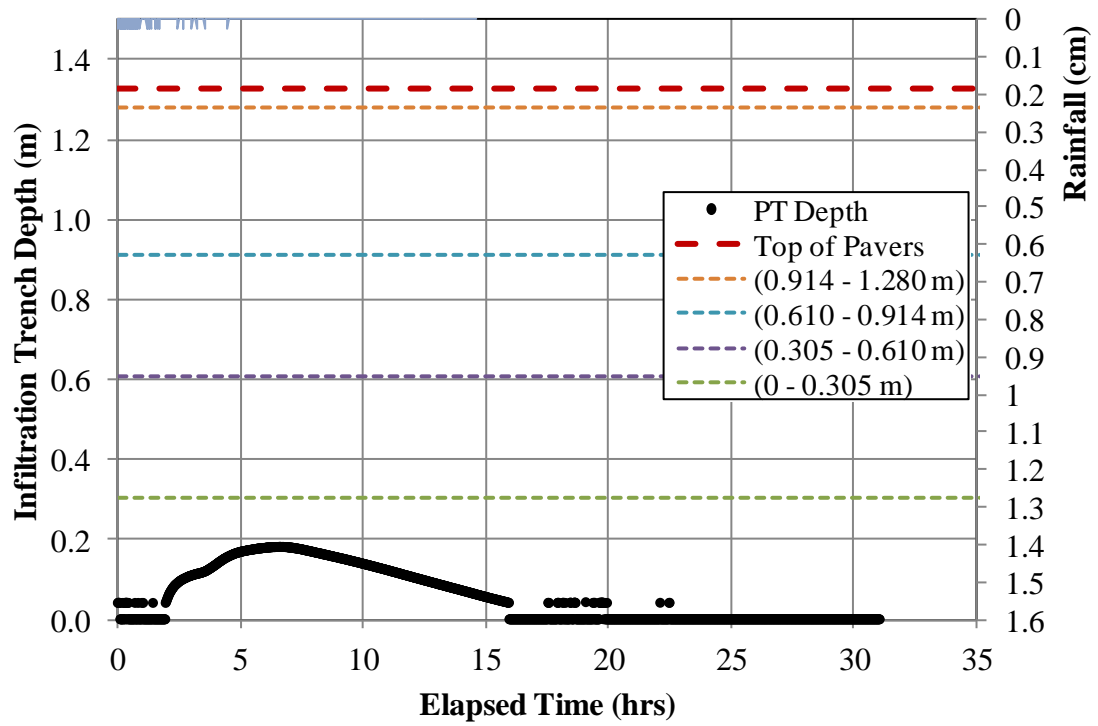


Figure F.11 - September 8, 2012 pressure transducer data

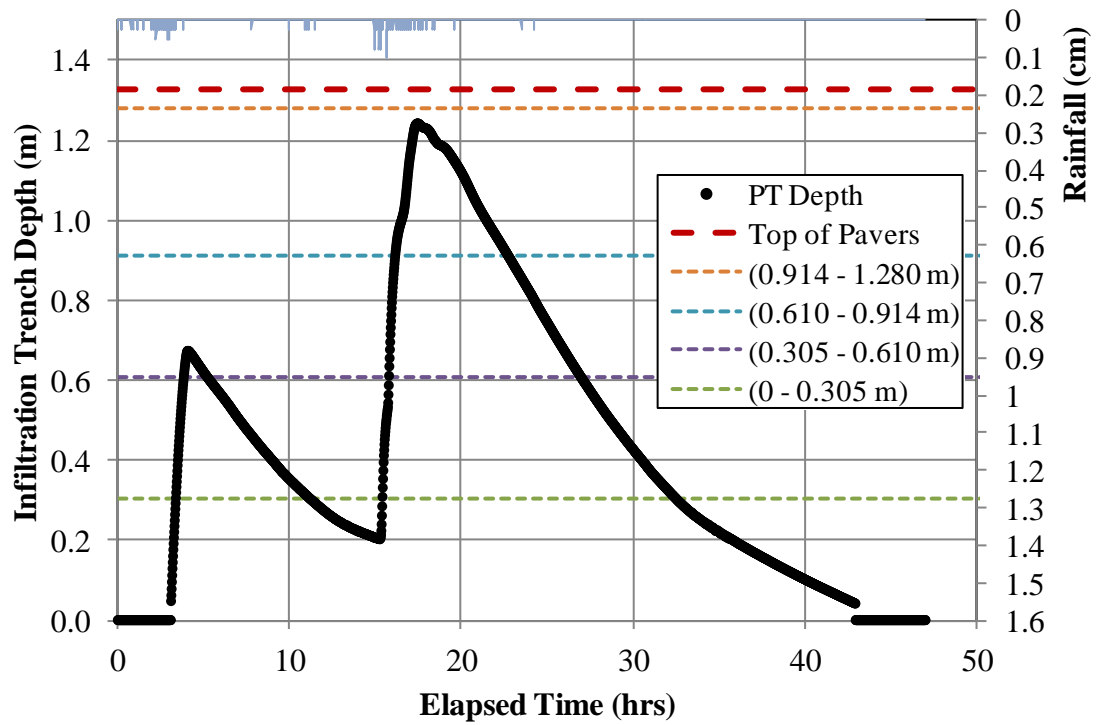


Figure F.12 - September 18, 2012 pressure transducer data

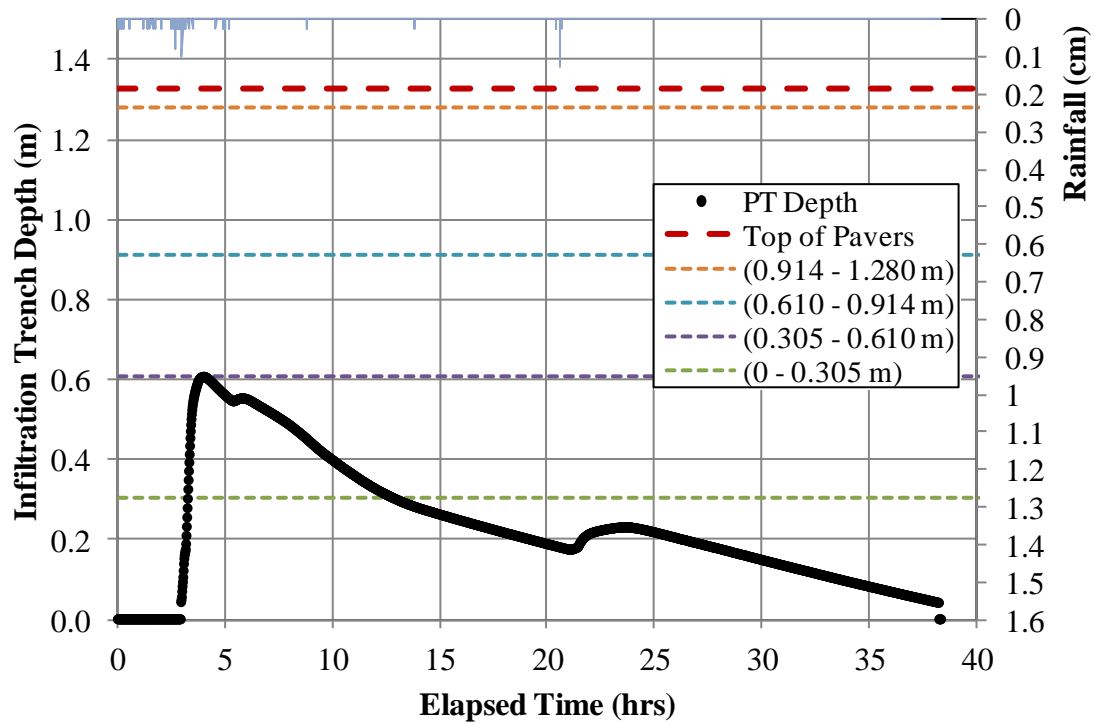


Figure F.13 - October 2, 2012 pressure transducer data

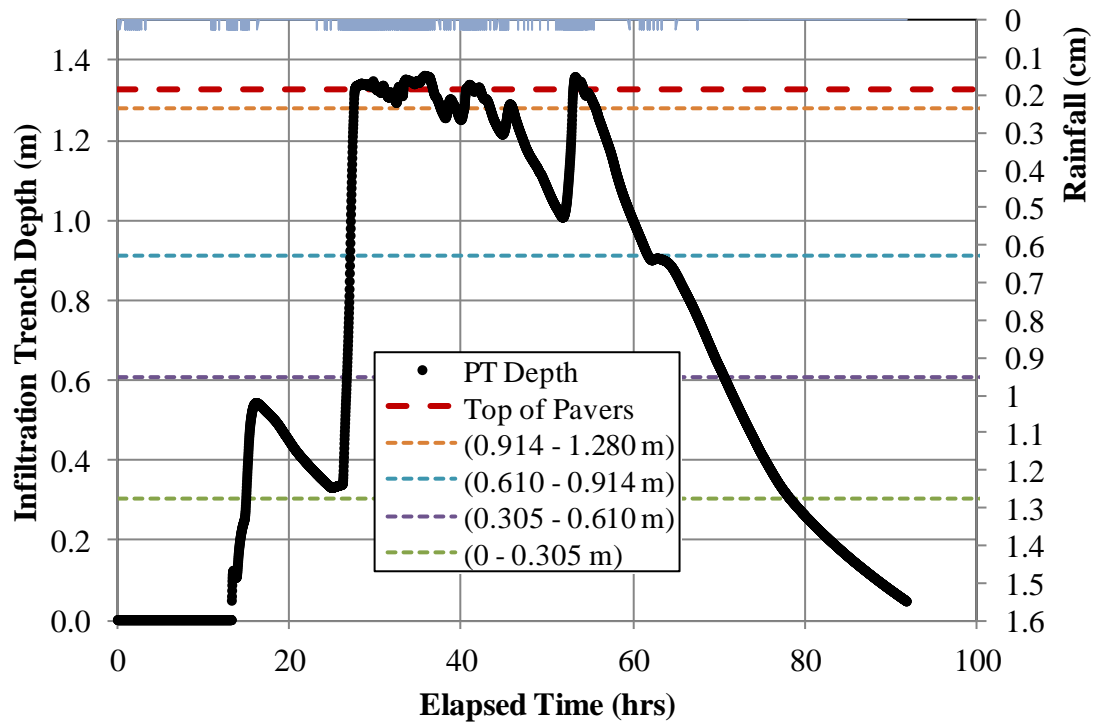


Figure F.14 - October 28, 2012 pressure transducer data

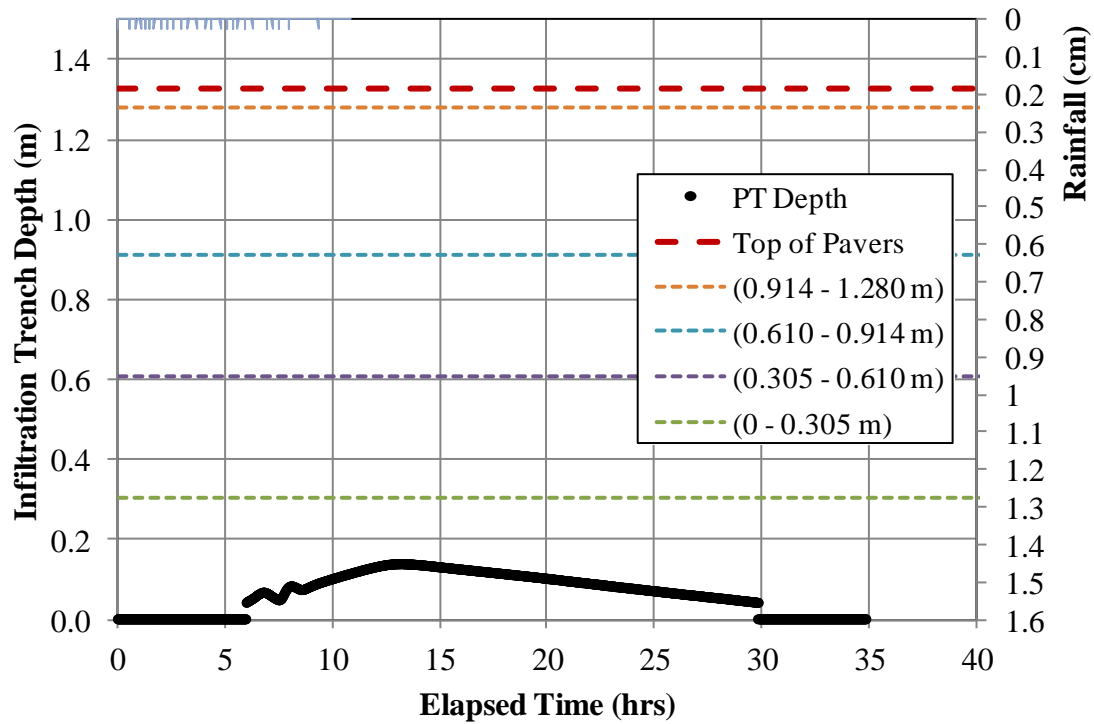


Figure F.15 - November 7, 2012 pressure transducer data

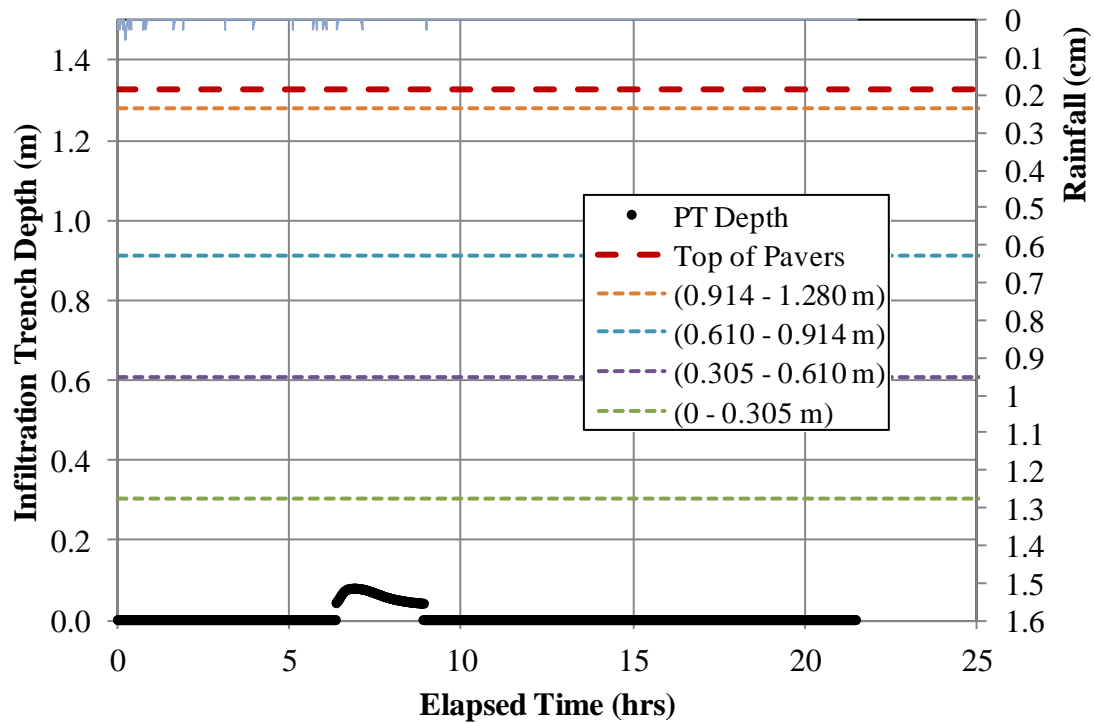


Figure F.16 - November 13, 2012 pressure transducer data

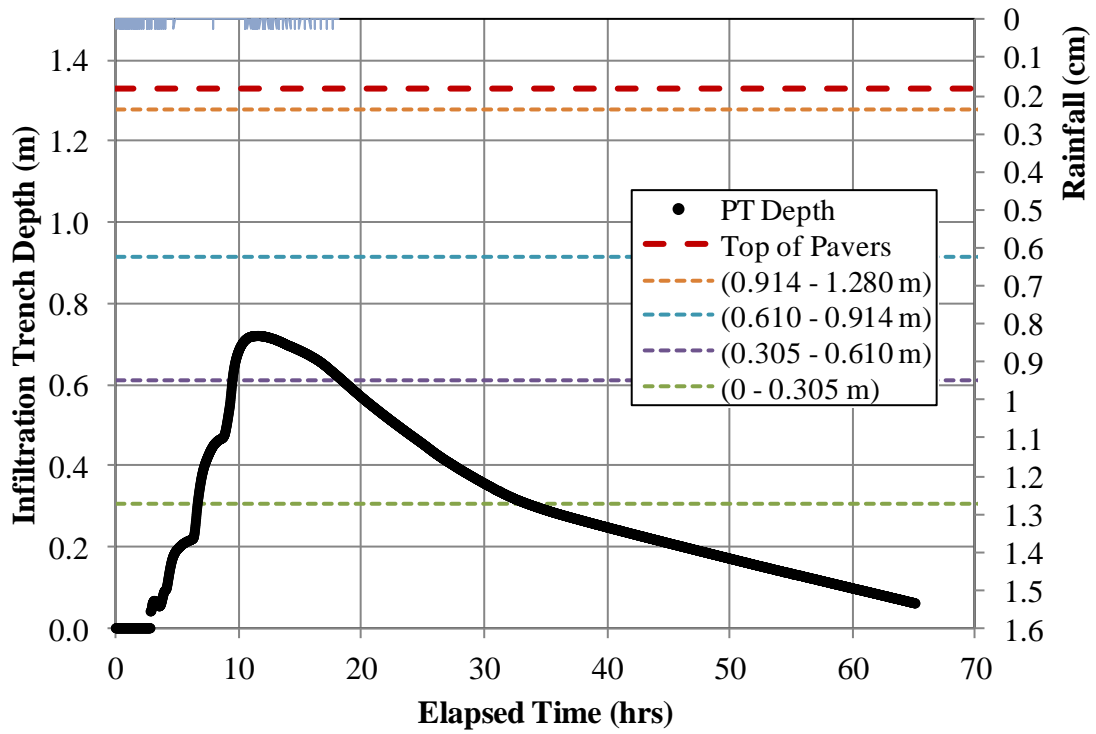


Figure F.17 - November 27, 2012 pressure transducer data

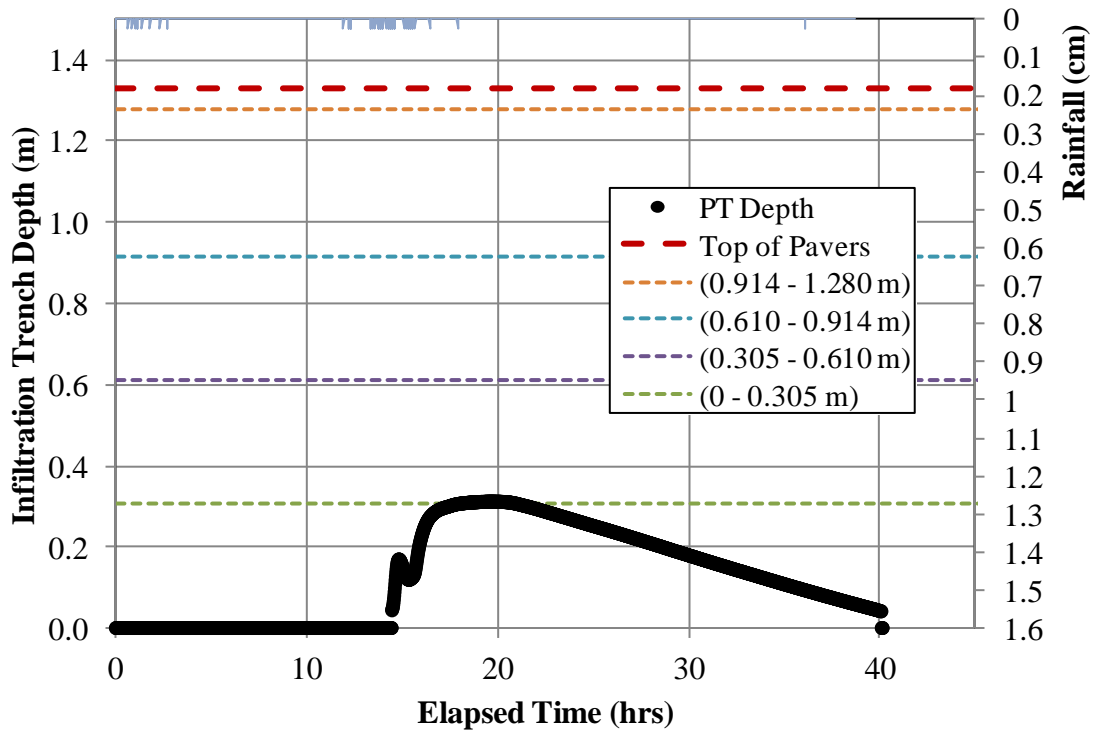


Figure F.18 - December 8, 2012 pressure transducer data

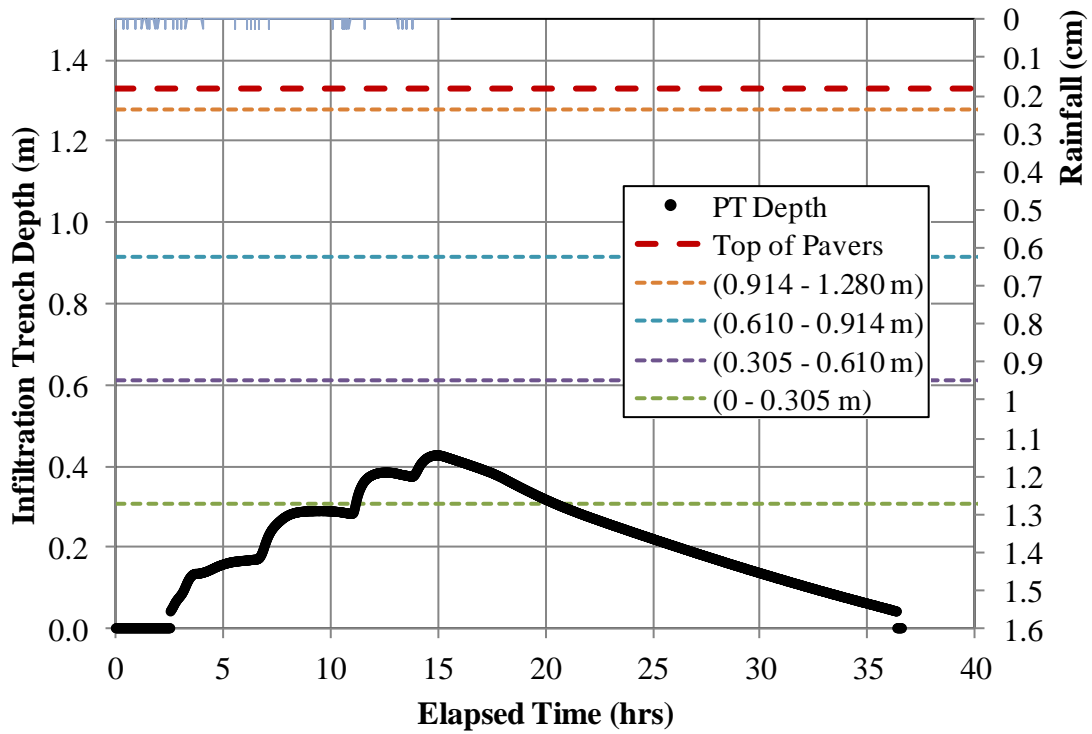


Figure F.19 - December 9, 2012 pressure transducer data

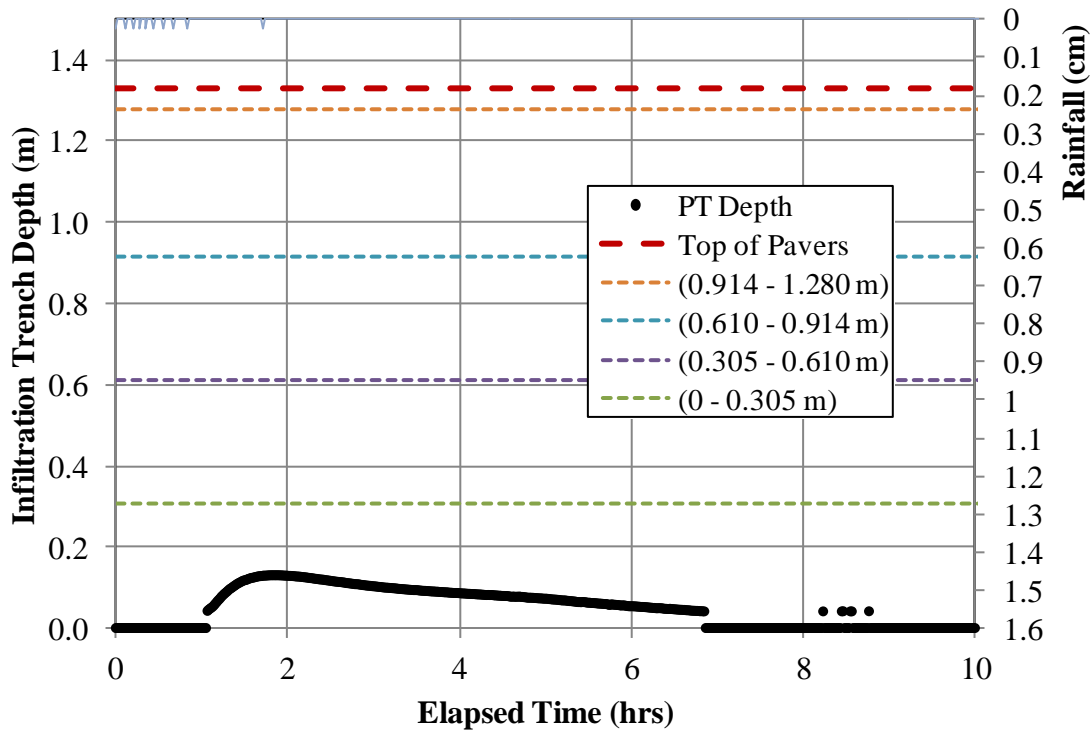


Figure F.20 - December 11, 2012 pressure transducer data

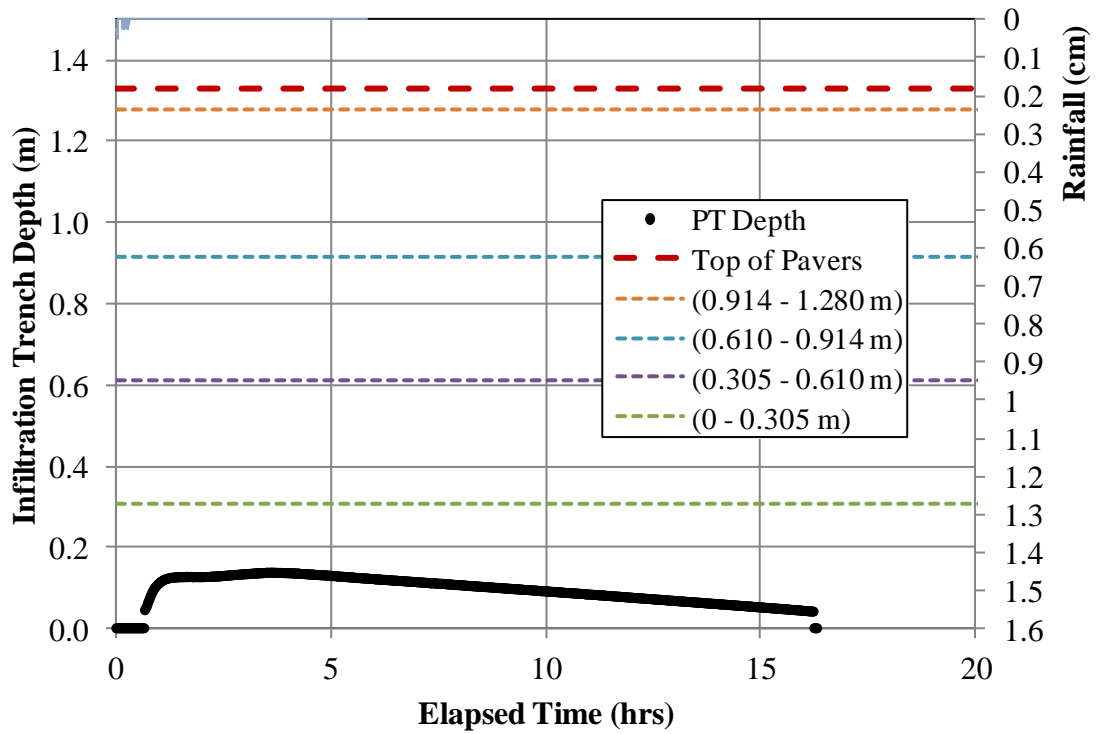


Figure F.21 - December 18, 2012 pressure transducer data

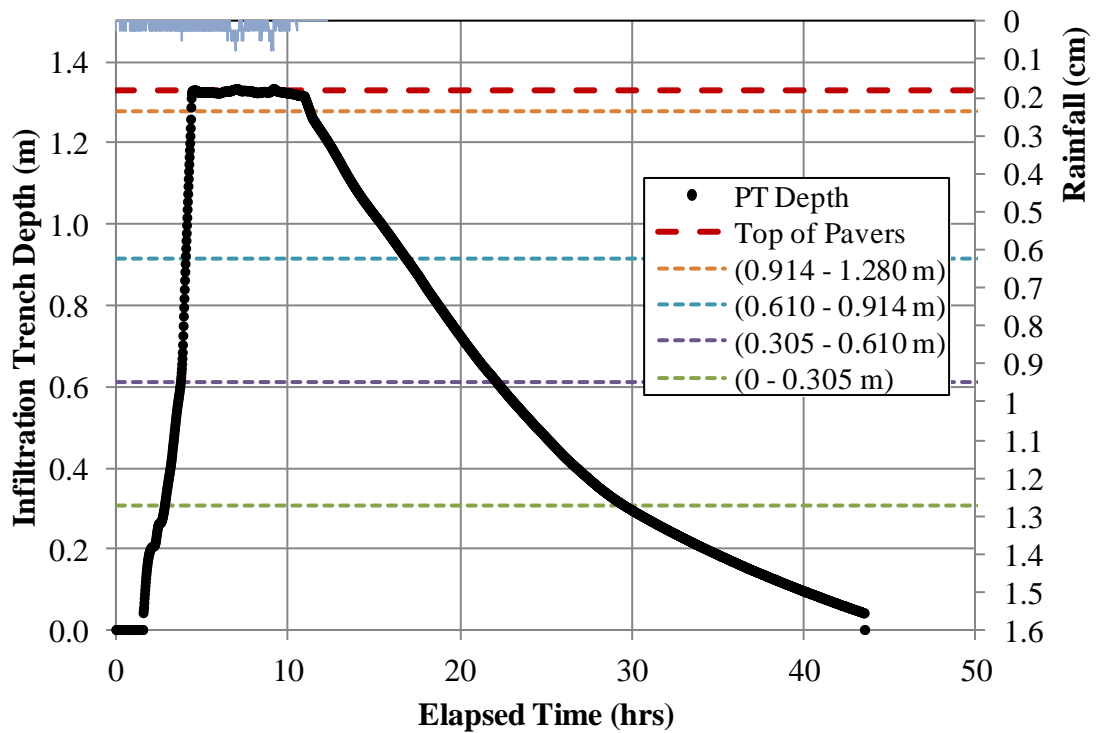


Figure F.22 - December 20, 2012 pressure transducer data

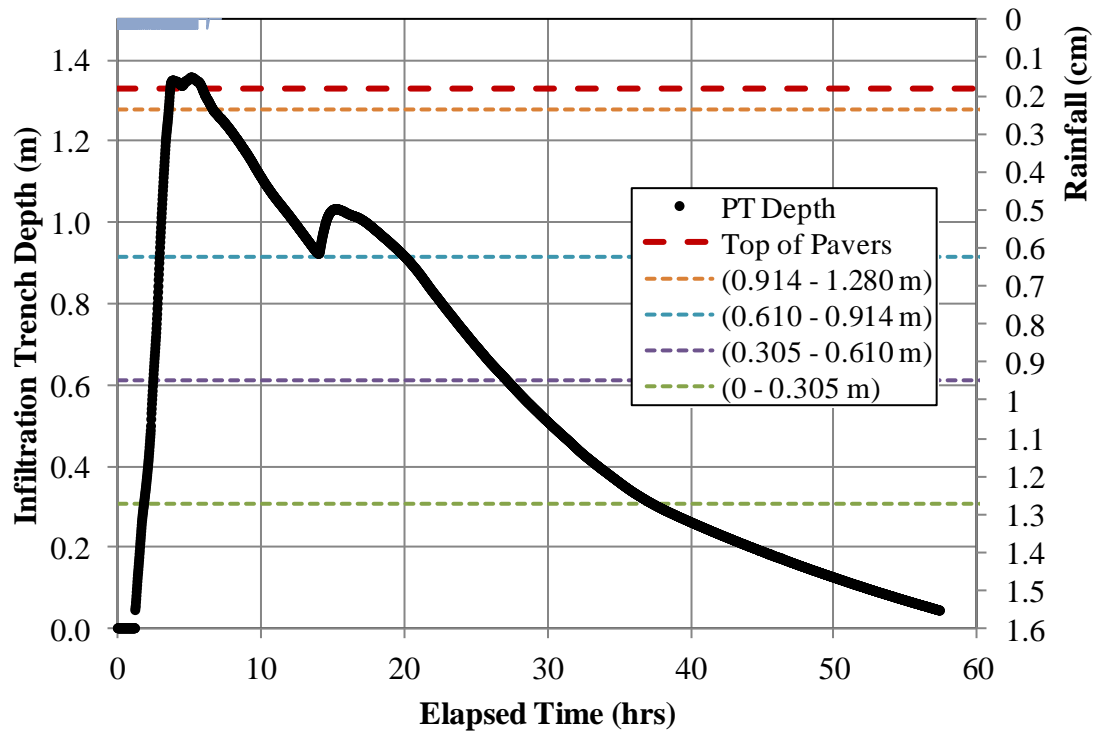


Figure F.23 - December 26, 2012 pressure transducer data

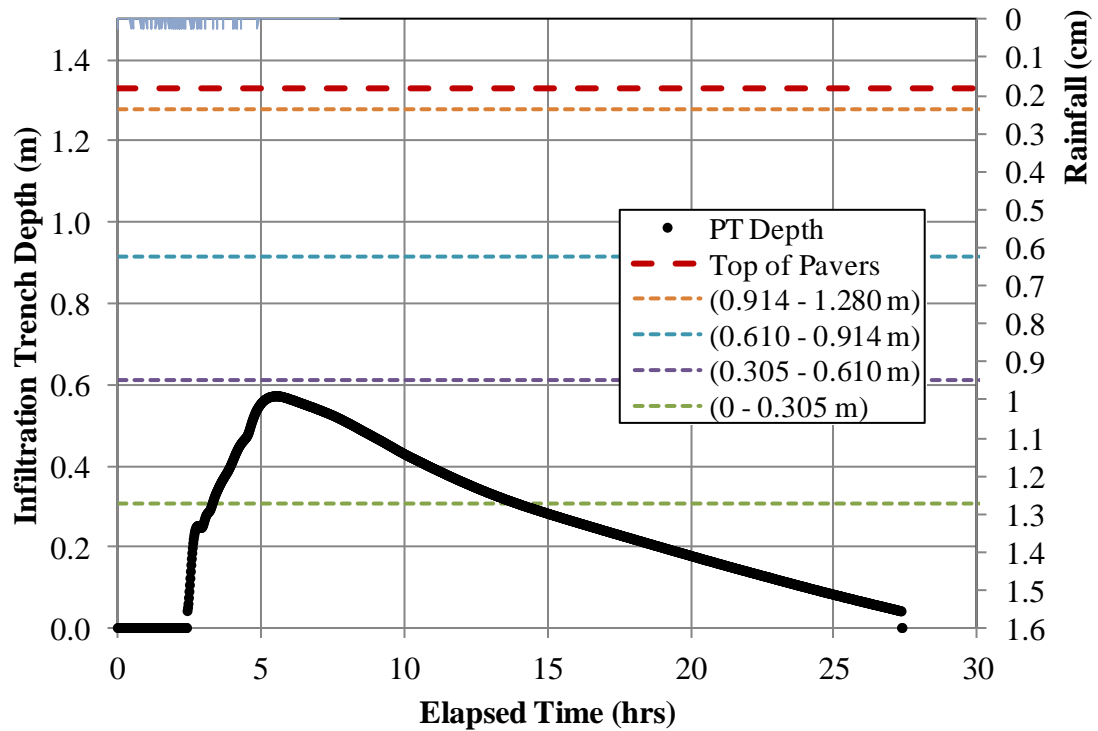


Figure F.24 - January 11, 2013 pressure transducer data

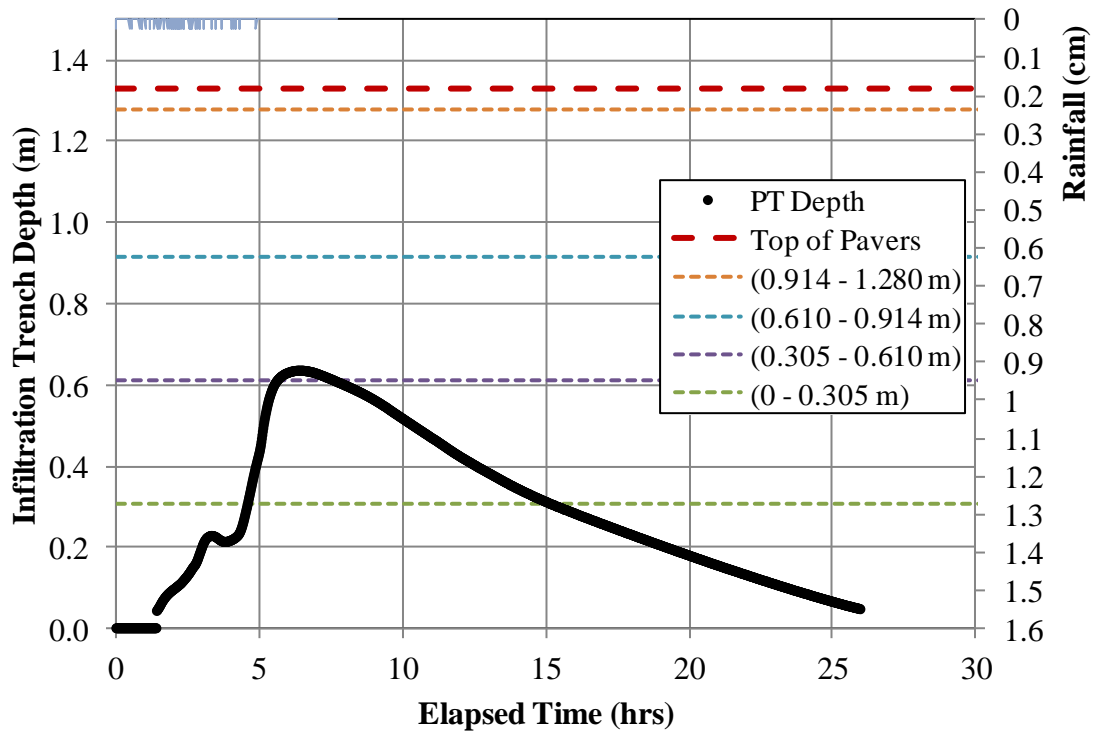


Figure F.25 - January 14, 2013 pressure transducer data

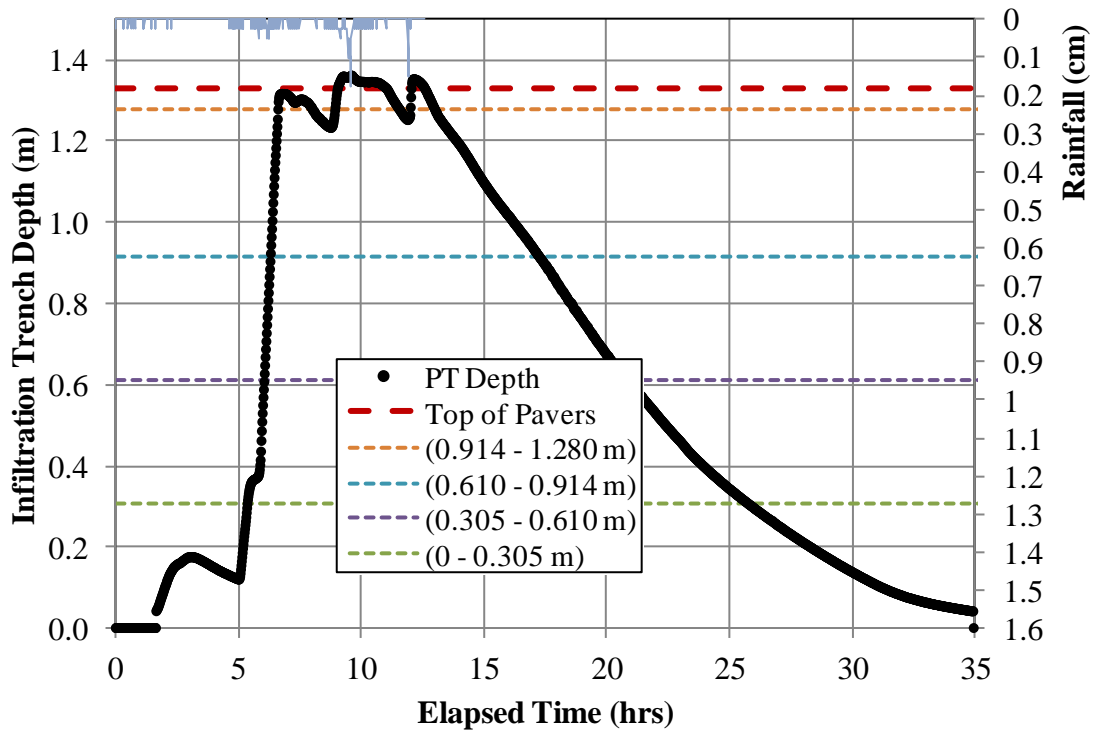


Figure F.26 - January 30, 2013 pressure transducer data

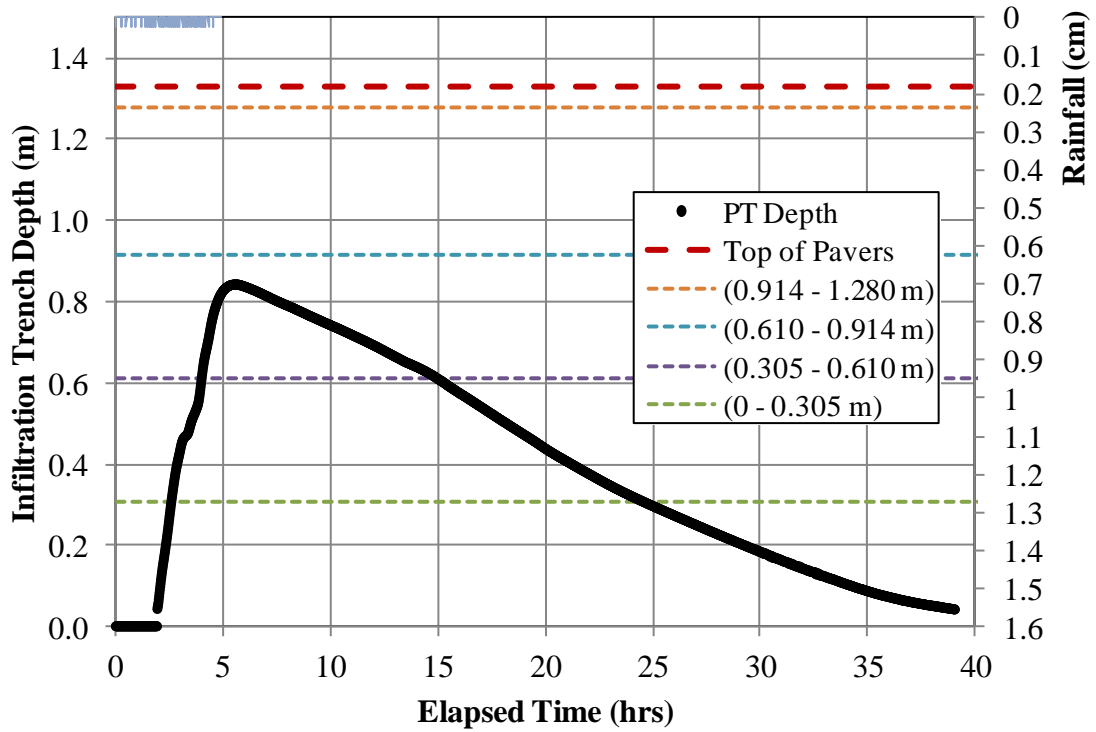


Figure F.27 - February 11, 2013 pressure transducer data

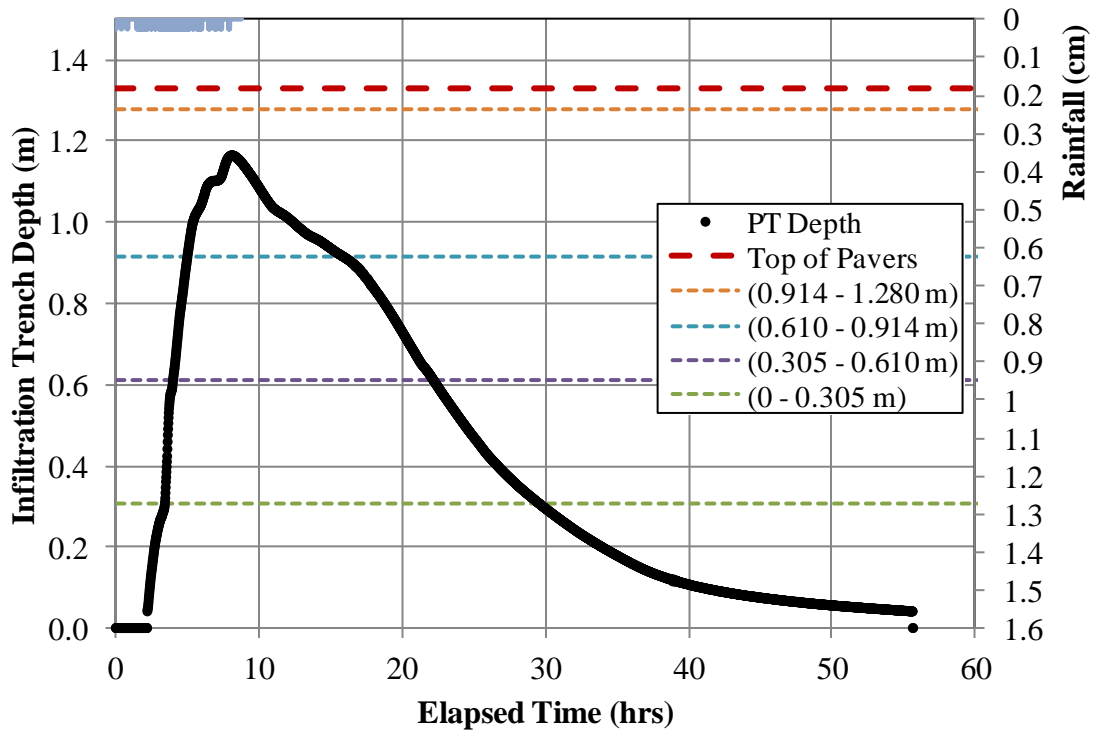


Figure F.28 - February 26, 2013 pressure transducer data

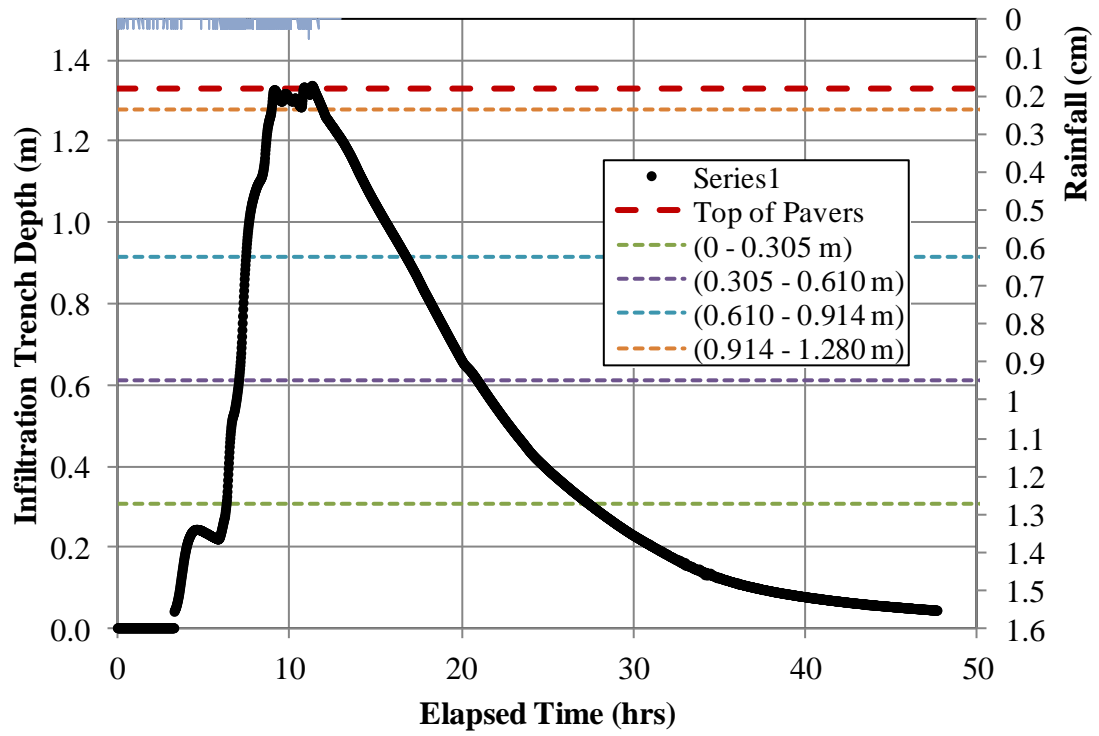


Figure F.29 - March 12, 2013 pressure transducer data

## Appendix F-2: Rainfall and Time before Depth Occurs in IT

Table F.1 - Rainfall volume and amount of time before IT depth occurs

Storm	Rainfall Before IT Depth (cm)	Time from first .0254 cm rain to Vol in IT (min / hours)	
7/16	1.47	2495	41.58
7/20	0.51	226	3.77
7/28	0.74	14	0.23
8/5	1.04	14	0.23
8/10	0.27	48	0.80
8/14	1.04	43	0.72
8/18	0.91	247	4.12
8/27	1.35	131	2.18
9/2	0.99	1349	22.48
9/4	0.33	605	10.08
9/8	0.73	119	1.98
9/18	1.22	187	3.12
10/2	0.71	178	2.97
10/28	0.84	798	13.30
11/7	0.51	361	6.02
11/13	0.56	383	6.38
11/27	0.64	171	2.85
12/8	0.69	869	14.48
12/9	0.25	154	2.57
12/11	0.23	65	1.08
12/18	0.23	41	0.68
12/20	0.43	96	1.60
12/26	0.58	74	1.23
1/11	0.58	147	2.45
1/14	0.28	86	1.43
1/30	0.25	100	1.67
2/11	0.33	117	1.95
2/26	0.33	134	2.23
3/12	0.41	199	3.32

### Appendix F-3: Recession and Infiltration Rate Raw Data Table and Calculations

Table F.1 - Recession and infiltration rates and data

RANGE (m)	Height (m)	DATE	Pt 1 (min / m)		Pt 2 (min / m)		Recession Rate (m/min)	Recession Rate (cm/hr)	Rate (m <sup>3</sup> /hr)	Area (m <sup>2</sup> )	Infiltration Rate (m/hr)	Infiltration Rate (cm/hr)	Rain (cm)	MAX PT (m)
0.914-1.280	1.280	16-Jul	169	1.146	251	0.944	0.0025	<b>14.81</b>	0.80	17.88	0.0450	<b>4.50</b>	3.96	1.170
0.610-0.914	0.914	16-Jul	271	0.906	416	0.639	0.0018	<b>11.01</b>	0.60	14.32	0.0418	<b>4.18</b>	3.96	
0.305-0.610	0.610	16-Jul	430	0.615	632	0.331	0.0014	<b>8.43</b>	0.46	11.36	0.0403	<b>4.03</b>	3.96	
0-0.305	0.305	16-Jul	672	0.291	1015	0.091	0.0006	<b>3.51</b>	0.19	8.40	0.0227	<b>2.27</b>	3.96	
0.914-1.280	1.280	20-Jul	444	1.237	654	0.920	0.0015	<b>9.06</b>	0.49	17.88	0.0275	<b>2.75</b>	3.15	1.238
0.610-0.914	0.914	20-Jul	660	0.912	850	0.628	0.0015	<b>8.94</b>	0.49	14.32	0.0339	<b>3.39</b>	3.15	
0.305-0.610	0.610	20-Jul	874	0.592	1099	0.336	0.0011	<b>6.84</b>	0.37	11.36	0.0327	<b>3.27</b>	3.15	
0-0.305	0.305	20-Jul	1184	0.267	1732	0.042	0.0004	<b>2.46</b>	0.13	8.40	0.0159	<b>1.59</b>	3.15	
0.610-0.914	0.914	28-Jul	205	0.755	290	0.636	0.0014	<b>8.41</b>	0.46	14.32	0.0319	<b>3.19</b>	1.35	0.755
0.305-0.610	0.610	28-Jul	313	0.601	541	0.324	0.0012	<b>7.31</b>	0.40	11.36	0.0350	<b>3.50</b>	1.35	
0-0.305	0.305	28-Jul	632	0.246	1149	0.035	0.0004	<b>2.44</b>	0.13	8.40	0.0158	<b>1.58</b>	1.35	
0.914-1.280	1.280	5-Aug	1426	0.994	1471	0.920	0.0017	<b>9.92</b>	0.54	17.88	0.0301	<b>3.01</b>	2.36	1.003
0.610-0.914	0.914	5-Aug	1481	0.902	1662	0.615	0.0016	<b>9.53</b>	0.52	14.32	0.0362	<b>3.62</b>	2.36	
0.305-0.610	0.610	5-Aug	1664	0.581	1884	0.334	0.0011	<b>6.74</b>	0.37	11.36	0.0323	<b>3.23</b>	2.36	
0-0.305	0.305	5-Aug	1918	0.300	2034	0.213	0.0008	<b>4.51</b>	0.25	8.40	0.0292	<b>2.92</b>	2.36	
0.914-1.280	1.280	10-Aug	204	1.217	407	0.926	0.0014	<b>8.59</b>	0.47	17.88	0.0261	<b>2.61</b>	5.59	1.237
0.610-0.914	0.914	10-Aug	419	0.911	649	0.619	0.0013	<b>7.62</b>	0.41	14.32	0.0289	<b>2.89</b>	5.59	
0.305-0.610	0.610	10-Aug	670	0.596	980	0.311	0.0009	<b>5.53</b>	0.30	11.36	0.0265	<b>2.65</b>	5.59	
0-0.305	0.305	10-Aug	1001	0.297	1875	0.005	0.0003	<b>2.01</b>	0.11	8.40	0.0130	<b>1.30</b>	5.59	
0.914-1.280	1.280	14-Aug	133	1.208	304	0.937	0.0016	<b>9.52</b>	0.52	17.88	0.0289	<b>2.89</b>	3.68	1.236
0.610-0.914	0.914	14-Aug	336	0.912	550	0.613	0.0014	<b>8.37</b>	0.45	14.32	0.0317	<b>3.17</b>	3.68	
0.305-0.610	0.610	14-Aug	567	0.593	835	0.323	0.0010	<b>6.04</b>	0.33	11.36	0.0289	<b>2.89</b>	3.68	
0-0.305	0.305	14-Aug	871	0.295	1568	0.018	0.0004	<b>2.39</b>	0.13	8.40	0.0155	<b>1.55</b>	3.68	
0.914-1.280	1.280	18-Aug	1669	1.104	1832	0.925	0.0011	<b>6.61</b>	0.36	17.88	0.0201	<b>2.01</b>	2.01	1.108
0.610-0.914	0.914	18-Aug	1849	0.907	2096	0.614	0.0012	<b>7.11</b>	0.39	14.32	0.0270	<b>2.70</b>	2.01	
0.305-0.610	0.610	18-Aug	2103	0.607	2359	0.337	0.0011	<b>6.32</b>	0.34	11.36	0.0302	<b>3.02</b>	2.01	
0-0.305	0.305	18-Aug	2389	0.312	2857	0.063	0.0005	<b>3.18</b>	0.17	8.40	0.0206	<b>2.06</b>	2.01	
0.610-0.914	0.914	27-Aug	709	0.728	803	0.635	0.0010	<b>5.91</b>	0.32	14.32	0.0224	<b>2.24</b>	2.49	0.729
0.305-0.610	0.610	27-Aug	827	0.608	1137	0.305	0.0010	<b>5.85</b>	0.32	11.36	0.0280	<b>2.80</b>	2.49	
0-0.305	0.305	27-Aug	1140	0.303	2177	0.045	0.0002	<b>1.50</b>	0.08	8.40	0.0097	<b>0.97</b>	2.49	

Table F.2 - Recession and infiltration rates and data (continued)

RANGE (m)	Height (m)	DATE	Pt 1 (min / m)	Pt 2 (min / m)	Recession Rate (m/min)	Recession Rate (cm/hr)	Rate (m <sup>3</sup> /hr)	Area (m <sup>2</sup> )	Infiltration Rate (m/hr)	Infiltration Rate (cm/hr)	Rain (cm)	MAX PT (m)
0.914-1.280	1.280	2-Sep	169 1.223	289 1.026	0.0016	<b>9.86</b>	0.54	17.88	0.0300	<b>3.00</b>	4.70	1.244
0.914-1.280	1.280	2-Sep	340 1.228	500 0.998	0.0014	<b>8.63</b>	0.47	17.88	0.0262	<b>2.62</b>	4.70	
0.914-1.280	1.280	2-Sep	613 1.227	838 0.923	0.0014	<b>8.11</b>	0.44	17.88	0.0247	<b>2.47</b>	4.70	
0.610-0.914	0.914	2-Sep	852 0.907	1092 0.617	0.0012	<b>7.25</b>	0.39	14.32	0.0275	<b>2.75</b>	4.70	
0.306-0.610	0.610	2-Sep	1108 0.598	1391 0.313	0.0010	<b>6.04</b>	0.33	11.36	0.0289	<b>2.89</b>	4.70	
0-0.305	0.305	2-Sep	1408 0.300	1725 0.138	0.0005	<b>3.06</b>	0.17	8.40	0.0198	<b>1.98</b>	4.70	
0.610-0.914	0.914	4-Sep	1 0.770	120 0.623	0.0012	<b>7.41</b>	0.40	14.32	0.0281	<b>2.81</b>	1.32	0.840
0.305-0.610	0.610	4-Sep	135 0.605	428 0.310	0.0010	<b>6.04</b>	0.33	11.36	0.0289	<b>2.89</b>	1.32	
0-0.305	0.305	4-Sep	445 0.297	781 0.144	0.0005	<b>2.73</b>	0.15	8.40	0.0177	<b>1.77</b>	1.32	
0-0.305	0.305	8-Sep	1433 0.140	1973 0.001	0.0003	<b>1.54</b>	0.08	8.40	0.0100	<b>1.00</b>	0.90	0.141
0.914-1.280	1.280	18-Sep	1109 1.201	1362 0.941	0.0010	<b>6.18</b>	0.34	17.88	0.0188	<b>1.88</b>	3.18	1.202
0.610-0.914	0.914	18-Sep	1403 0.893	1629 0.620	0.0012	<b>7.24</b>	0.39	14.32	0.0275	<b>2.75</b>	3.18	
0.305-0.610	0.610	18-Sep	1656 0.590	1919 0.333	0.0010	<b>5.87</b>	0.32	11.36	0.0281	<b>2.81</b>	3.18	
0-0.305	0.305	18-Sep	1967 0.294	2624 0.005	0.0004	<b>2.64</b>	0.14	8.40	0.0171	<b>1.71</b>	3.18	
		26-Sep	- -	- -	-	-	-	-	-	-	0.84	0.000
0.305-0.610	0.610	2-Oct	835 0.557	1258 0.308	0.0006	<b>3.54</b>	0.19	11.36	0.0169	<b>1.69</b>	1.55	0.566
0-0.305	0.305	2-Oct	1272 0.300	1837 0.135	0.0003	<b>1.76</b>	0.10	8.40	0.0114	<b>1.14</b>	1.55	
0-0.305	0.305	2-Oct	2037 0.186	2861 0.004	0.0002	<b>1.33</b>	0.07	8.40	0.0086	<b>0.86</b>	1.55	
0.305-0.610	0.610	28-Oct	1244 0.496	1683 0.309	0.0004	<b>2.56</b>	0.14	11.36	0.0122	<b>1.22</b>	11.00	1.321
0.914-1.280	1.280	28-Oct	3022 1.220	3349 0.969	0.0008	<b>4.60</b>	0.25	17.88	0.0140	<b>1.40</b>	11.00	
0.914-1.280	1.280	29-Oct	3565 1.257	3886 0.927	0.0010	<b>6.17</b>	0.34	17.88	0.0188	<b>1.88</b>	11.00	
0.610-0.914	0.914	29-Oct	3939 0.881	4418 0.619	0.0005	<b>3.28</b>	0.18	14.32	0.0124	<b>1.24</b>	11.00	
0.305-0.610	0.610	29-Oct	4444 0.599	4848 0.313	0.0007	<b>4.25</b>	0.23	11.36	0.0203	<b>2.03</b>	11.00	
0-0.305	0.305	29-Oct	4875 0.297	5732 0.014	0.0003	<b>1.99</b>	0.11	8.40	0.0129	<b>1.29</b>	11.00	
0-0.305	0.305	7-Nov	567 0.039	638 0.010	0.0004	<b>2.45</b>	0.13	8.40	0.0158	<b>1.58</b>	0.66	0.098
0-0.305	0.305	13-Nov	1598 0.097	2548 0.004	0.0001	<b>0.59</b>	0.03	8.40	0.0038	<b>0.38</b>	0.64	0.039
0.610-0.914	0.914	27-Nov	1064 0.680	1319 0.628	0.0002	<b>1.23</b>	0.07	14.32	0.0047	<b>0.47</b>	1.55	0.680
0.305-0.610	0.610	27-Nov	1391 0.602	2095 0.335	0.0004	<b>2.28</b>	0.12	11.36	0.0109	<b>1.09</b>	1.55	
0-0.305	0.305	27-Nov	2258 0.290	2815 0.201	0.0002	<b>0.96</b>	0.05	8.40	0.0062	<b>0.62</b>	1.55	
0-0.305	0.305	8-Dec	430 0.270	1501 0.023	0.0002	<b>1.38</b>	0.08	8.40	0.0089	<b>0.89</b>	0.97	0.271

**Table F.2 - Recession and infiltration rates and data (continued)**

<b>RANGE (m)</b>	<b>Height (m)</b>	<b>DATE</b>	<b>Pt 1 (min / m)</b>		<b>Pt 2 (min / m)</b>		<b>Recession Rate (m/min)</b>	<b>Recession Rate (cm/hr)</b>	<b>Rate (m<sup>3</sup>/hr)</b>	<b>Area (m<sup>2</sup>)</b>	<b>Infiltration Rate (m/hr)</b>	<b>Infiltration Rate (cm/hr)</b>	<b>Rain (cm)</b>	<b>MAX PT (m)</b>
0.305-0.610	0.610	9-Dec	1412	0.386	1629	0.311	0.0003	<b>2.07</b>	0.11	11.36	0.0099	<b>0.99</b>	0.81	0.386
0-0.305	0.305	9-Dec	1656	0.298	2630	0.015	0.0003	<b>1.74</b>	0.09	8.40	0.0113	<b>1.13</b>	0.81	
0-0.305	0.305	11-Dec	413	0.088	656	0.012	0.0003	<b>1.87</b>	0.10	8.40	0.0121	<b>1.21</b>	0.25	0.090
0-0.305	0.305	18-Dec	194	0.097	896	0.008	0.0001	<b>0.76</b>	0.04	8.40	0.0049	<b>0.49</b>	0.23	0.097
0.914-1.280	1.280	20-Dec	562	1.275	874	0.925	0.0011	<b>6.73</b>	0.37	17.88	0.0205	<b>2.05</b>	7.54	1.293
0.610-0.914	0.914	20-Dec	895	0.905	1181	0.621	0.0010	<b>5.95</b>	0.32	14.32	0.0226	<b>2.26</b>	7.54	
0.305-0.610	0.610	20-Dec	1200	0.604	1588	0.316	0.0007	<b>4.45</b>	0.24	11.36	0.0213	<b>2.13</b>	7.54	
0-0.305	0.305	20-Dec	1616	0.301	2500	0.007	0.0003	<b>2.00</b>	0.11	8.40	0.0129	<b>1.29</b>	7.54	
0.914-1.280	1.280	26-Dec	281	1.296	697	0.939	0.0009	<b>5.14</b>	0.28	17.88	0.0156	<b>1.56</b>	2.79	1.317
0.610-0.914	0.914	26-Dec	1077	0.907	1490	0.615	0.0007	<b>4.24</b>	0.23	14.32	0.0161	<b>1.61</b>	2.79	
0.305-0.610	0.610	26-Dec	1513	0.601	2054	0.310	0.0005	<b>3.23</b>	0.18	11.36	0.0154	<b>1.54</b>	2.79	
0-0.305	0.305	26-Dec	2085	0.297	3316	0.014	0.0002	<b>1.38</b>	0.08	8.40	0.0089	<b>0.89</b>	2.79	
0.305-0.610	0.610	11-Jan	413	0.530	805	0.314	0.0006	<b>3.31</b>	0.18	11.36	0.0158	<b>1.58</b>	0.99	0.531
0-0.305	0.305	11-Jan	843	0.295	1601	0.033	0.0003	<b>2.07</b>	0.11	8.40	0.0134	<b>1.34</b>	0.99	
0.305-0.610	0.610	14-Jan	498	0.593	924	0.312	0.0007	<b>3.96</b>	0.22	11.36	0.0190	<b>1.90</b>	0.94	0.595
0-0.305	0.305	14-Jan	948	0.297	1564	0.036	0.0004	<b>2.54</b>	0.14	8.40	0.0164	<b>1.64</b>	0.94	
0.914-1.280	1.280	30-Jan	803	1.251	1032	0.919	0.0015	<b>8.70</b>	0.47	17.88	0.0265	<b>2.65</b>	4.78	1.321
0.610-0.914	0.914	30-Jan	1040	0.909	1238	0.622	0.0015	<b>8.70</b>	0.47	14.32	0.0330	<b>3.30</b>	4.78	
0.305-0.610	0.610	30-Jan	1249	0.608	1519	0.311	0.0011	<b>6.60</b>	0.36	11.36	0.0316	<b>3.16</b>	4.78	
0-0.305	0.305	30-Jan	1532	0.300	1972	0.033	0.0006	<b>3.65</b>	0.20	8.40	0.0236	<b>2.36</b>	4.78	
0.610-0.914	0.914	11-Feb	374	0.795	811	0.614	0.0004	<b>2.49</b>	0.14	14.32	0.0094	<b>0.94</b>	1.04	0.802
0.305-0.610	0.610	11-Feb	827	0.607	1369	0.316	0.0005	<b>3.22</b>	0.18	11.36	0.0154	<b>1.54</b>	1.04	
0-0.305	0.305	11-Feb	1399	0.302	2168	0.032	0.0004	<b>2.11</b>	0.11	8.40	0.0137	<b>1.37</b>	1.04	
0.914-1.280	1.280	26-Feb	529	1.115	859	0.918	0.0006	<b>3.59</b>	0.20	17.88	0.0109	<b>1.09</b>	1.47	1.125
0.610-0.914	0.914	26-Feb	876	0.912	1291	0.615	0.0007	<b>4.29</b>	0.23	14.32	0.0163	<b>1.63</b>	1.47	
0.305-0.610	0.610	26-Feb	1305	0.604	1702	0.309	0.0007	<b>4.45</b>	0.24	11.36	0.0213	<b>2.13</b>	1.47	
0-0.305	0.305	26-Feb	1715	0.303	2609	0.044	0.0003	<b>1.74</b>	0.09	8.40	0.0112	<b>1.12</b>	1.47	
0.914-1.280	1.280	12-Mar	689	1.289	974	0.920	0.0013	<b>7.76</b>	0.42	17.88	0.0236	<b>2.36</b>	3.00	1.297
0.610-0.914	0.914	12-Mar	985	0.907	1209	0.615	0.0013	<b>7.81</b>	0.42	14.32	0.0296	<b>2.96</b>	3.00	
0.305-0.610	0.610	12-Mar	1219	0.606	1575	0.308	0.0008	<b>5.03</b>	0.27	11.36	0.0241	<b>2.41</b>	3.00	
0-0.305	0.305	12-Mar	1584	0.302	2376	0.039	0.0003	<b>1.99</b>	0.11	8.40	0.0129	<b>1.29</b>	3.00	

## Appendix G: Inflow, Overflow, and Capture Volumes

Table G.1 - Rainfall volume, duration and intensity, and treatment train inflow, overflow, and capture volumes

Date	Duration (hrs)	Rain (cm)	Total Intensity (cm/hr)	TT Inflow Volume (m <sup>3</sup> )	Overflow Volume (m <sup>3</sup> )	Capture Volume (m <sup>3</sup> )	% Capture
7/16/12	43.80	3.96	0.090	35.87		35.87	100%
7/20/12	7.43	3.15	0.424	28.32		28.32	100%
7/28/12	0.60	1.35	2.244	11.56		11.56	100%
8/5/12	12.83	2.36	0.184	21.00		21.00	100%
<b>8/10/12</b>	<b>3.05</b>	<b>5.59</b>	<b>1.832</b>	<b>50.97</b>	<b>0.63</b>	<b>50.34</b>	<b>99%</b>
8/14/12	16.03	3.68	0.230	33.27		33.27	100%
8/18/12	8.60	2.01	0.233	17.70		17.70	100%
8/27/12	18.96	2.49	0.131	22.18		22.18	100%
<b>9/2/12</b>	<b>31.58</b>	<b>4.70</b>	<b>0.149</b>	<b>42.71</b>	<b>0.83</b>	<b>41.88</b>	<b>98%</b>
9/4/12	34.15	1.32	0.039	11.33		11.33	100%
9/8/12	4.48	0.89	0.198	7.32		7.32	100%
9/18/12	23.69	3.18	0.134	28.55		28.55	100%
10/2/12	20.67	1.55	0.075	13.45		13.45	100%
<b>10/28/12</b>	<b>66.96</b>	<b>11.00</b>	<b>0.164</b>	<b>101.23</b>	<b>1.78</b>	<b>99.45</b>	<b>98%</b>
11/7/12	9.33	0.66	0.071	5.19		5.19	100%
11/13/12	8.98	0.64	0.071	4.96		4.96	100%
11/27/12	17.65	1.55	0.088	13.45		13.45	100%
12/8/12	36.10	0.97	0.027	8.02		8.02	100%
12/9/12	13.83	0.81	0.059	6.61		6.61	100%
12/11/12	1.72	0.25	0.148	1.42		1.42	100%
12/18/12	0.28	0.23	0.807	1.18		1.18	100%
<b>12/20/12</b>	<b>10.48</b>	<b>7.54</b>	<b>0.720</b>	<b>69.14</b>	<b>2.07</b>	<b>67.07</b>	<b>97%</b>
<b>12/26/12</b>	<b>6.30</b>	<b>2.79</b>	<b>0.443</b>	<b>25.01</b>	<b>0.47</b>	<b>24.55</b>	<b>98%</b>
1/11/13	4.88	0.99	0.203	8.26		8.26	100%
1/14/13	5.92	0.94	0.159	7.79		7.79	100%
<b>1/30/13</b>	<b>11.98</b>	<b>4.78</b>	<b>0.398</b>	<b>43.42</b>	<b>2.37</b>	<b>41.05</b>	<b>95%</b>
2/11/13	4.55	1.04	0.229	8.73		8.73	100%
2/26/13	7.90	1.47	0.186	12.74		12.74	100%
<b>3/12/13</b>	<b>11.65</b>	<b>3.00</b>	<b>0.257</b>	<b>26.90</b>	<b>0.34</b>	<b>26.56</b>	<b>99%</b>

## Appendix H: Volume into the Treatment Train and Infiltration Trench

**Table H.1 - Rainfall characteristics and volume of stormwater to the TT and into the IT**

Storm	Rain (cm)	Time of water in trench (hrs)	Recession (cm/hr)	Area (m <sup>2</sup> )	VIT <sub>R</sub> (m <sup>3</sup> )	Infiltration (cm/hr)	MAX PT (m)	Area (m <sup>2</sup> )	VIT <sub>I</sub> (m <sup>3</sup> )	V to TT (m <sup>3</sup> )	V in IT / V to TT (R)	V in IT / V to TT (I)
7/16	3.96	16.72	9.44	5.43	<b>8.58</b>	3.75	1.17	11.42	<b>7.15</b>	35.87	0.24	0.20
7/20	3.15	24.40	6.82	5.43	<b>9.05</b>	2.75	1.24	11.75	<b>7.89</b>	28.32	0.32	0.28
7/28	1.35	15.65	6.05	5.43	<b>5.15</b>	2.76	0.75	9.40	<b>4.05</b>	11.56	0.45	0.35
8/5	2.36	22.52	7.67	5.43	<b>9.39</b>	3.19	1.00	10.61	<b>7.63</b>	21.00	0.45	0.36
8/10	5.59	27.52	5.94	5.43	<b>8.88</b>	2.36	1.24	11.74	<b>7.63</b>	50.97	0.17	0.15
8/14	3.68	23.38	6.58	5.43	<b>8.36</b>	2.63	1.24	11.74	<b>7.21</b>	33.27	0.25	0.22
8/18	2.01	24.28	5.81	5.43	<b>7.66</b>	2.45	1.11	11.11	<b>6.61</b>	17.70	0.43	0.37
8/27	2.49	28.20	4.42	5.43	<b>6.78</b>	2.00	0.73	9.27	<b>5.24</b>	22.18	0.31	0.24
9/2	4.70	28.23	7.16	5.43	<b>10.98</b>	2.62	1.24	11.77	<b>8.70</b>	42.71	0.26	0.20
9/4	1.32	20.68	5.39	5.43	<b>6.06</b>	2.49	0.84	9.81	<b>5.05</b>	11.33	0.54	0.45
9/8	0.89	10.93	1.54	5.43	<b>0.92</b>	1.00	0.14	6.41	<b>0.70</b>	7.32	0.13	0.10
9/18	3.18	37.23	5.48	5.43	<b>11.10</b>	2.29	1.20	11.57	<b>9.85</b>	28.55	0.39	0.35
10/2	1.55	31.10	2.21	5.43	<b>3.73</b>	1.23	0.57	8.48	<b>3.24</b>	13.45	0.28	0.24
10/28	11.00	75.70	3.81	5.43	<b>15.67</b>	1.51	1.32	12.15	<b>13.89</b>	101.23	0.15	0.14
11/7	0.66	15.37	2.45	5.43	<b>2.04</b>	1.58	0.10	6.20	<b>1.51</b>	5.19	0.39	0.29
11/13	0.64	2.42	0.59	5.43	<b>0.08</b>	0.38	0.04	5.92	<b>0.05</b>	4.96	0.02	0.01
11/27	1.55	58.07	1.49	5.43	<b>4.70</b>	0.73	0.68	9.04	<b>3.81</b>	13.45	0.35	0.28
12/8	0.97	21.62	1.38	5.43	<b>1.62</b>	0.89	0.27	7.05	<b>1.36</b>	8.02	0.20	0.17
12/9	0.81	30.10	1.91	5.43	<b>3.12</b>	1.06	0.39	7.61	<b>2.43</b>	6.61	0.47	0.37
12/11	0.25	2.32	1.87	5.43	<b>0.24</b>	1.21	0.09	6.16	<b>0.17</b>	1.42	0.17	0.12
12/18	0.23	9.17	0.76	5.43	<b>0.38</b>	0.49	0.10	6.20	<b>0.28</b>	1.18	0.32	0.24
12/20	7.54	38.30	4.78	5.43	<b>9.95</b>	1.93	1.29	12.01	<b>8.89</b>	69.14	0.14	0.13
12/26	2.79	51.08	3.50	5.43	<b>9.71</b>	1.40	1.32	12.13	<b>8.69</b>	25.01	0.39	0.35
1/11	0.99	21.80	2.69	5.43	<b>3.19</b>	1.46	0.53	8.31	<b>2.65</b>	8.26	0.39	0.32
1/14	0.94	22.38	3.25	5.43	<b>3.96</b>	1.77	0.59	8.62	<b>3.41</b>	7.79	0.51	0.44
1/30	4.78	29.60	6.91	5.43	<b>11.12</b>	2.87	1.32	12.15	<b>10.31</b>	43.42	0.26	0.24
2/11	1.04	32.78	2.61	5.43	<b>4.65</b>	1.28	0.80	9.63	<b>4.05</b>	8.73	0.53	0.46
2/26	1.47	39.87	3.52	5.43	<b>7.62</b>	1.49	1.12	11.20	<b>6.66</b>	12.74	0.60	0.52
3/12	3.00	34.67	5.65	5.43	<b>10.64</b>	2.25	1.30	12.03	<b>9.40</b>	26.90	0.40	0.35

## Appendix I: Storm Durations and Volumes

Table I.1 - Rainfall volumes and storm durations

Date	Duration (hrs)	Rain (cm)
7/16/12	43.80	3.96
7/20/12	7.43	3.15
7/28/12	0.60	1.35
8/5/12	12.83	2.36
<b>8/10/12</b>	<b>3.05</b>	<b>5.59</b>
8/14/12	16.03	3.68
8/18/12	8.60	2.01
8/27/12	18.96	2.49
<b>9/2/12</b>	<b>31.58</b>	<b>4.70</b>
9/4/12	34.15	1.32
9/8/12	4.48	0.89
9/18/12	23.69	3.18
10/2/12	20.67	1.55
<b>10/28/12</b>	<b>66.96</b>	<b>11.00</b>
11/7/12	9.33	0.66
11/13/12	8.98	0.64
11/27/12	17.65	1.55
12/8/12	36.10	0.97
12/9/12	13.83	0.81
12/11/12	1.72	0.25
12/18/12	0.28	0.23
<b>12/20/12</b>	<b>10.48</b>	<b>7.54</b>
<b>12/26/12</b>	<b>6.30</b>	<b>2.79</b>
1/11/13	4.88	0.99
1/14/13	5.92	0.94
<b>1/30/13</b>	<b>11.98</b>	<b>4.78</b>
2/11/13	4.55	1.04
2/26/13	7.90	1.47
<b>3/12/13</b>	<b>11.65</b>	<b>3.00</b>

**Appendix J: Rainfall Intensities ( $i_{1,2,3}$ ) vs. Rainfall Volumes**

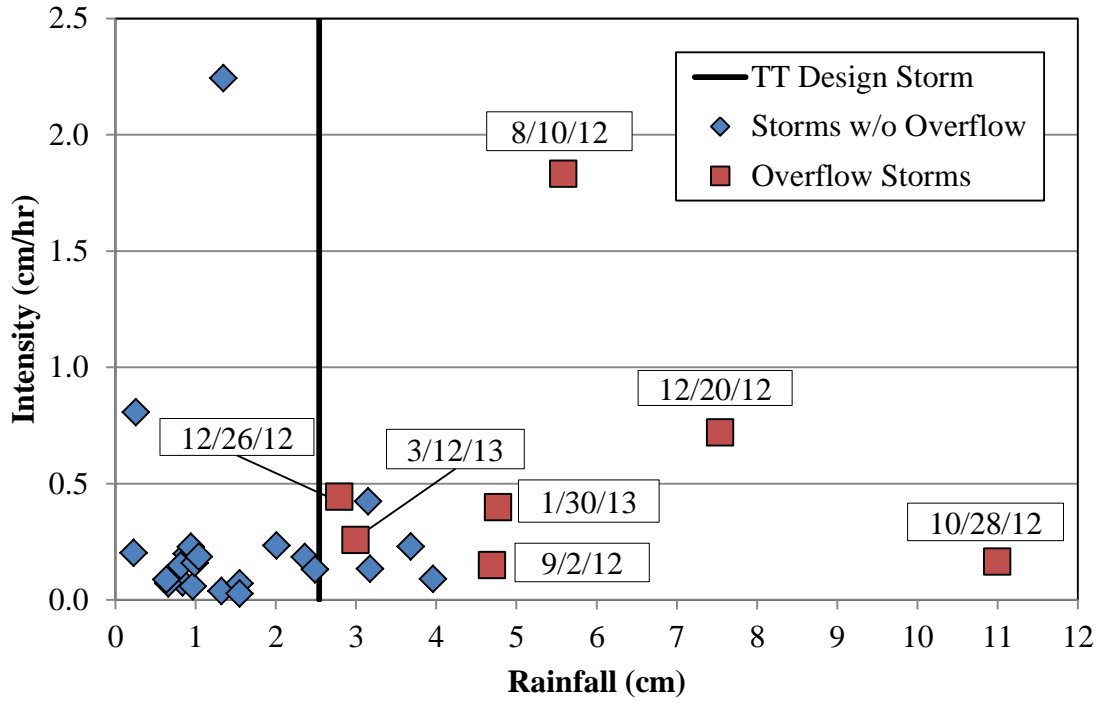


**Figure J.30 - Rainfall intensity ( $i_1$ ) vs. rainfall for each storm**

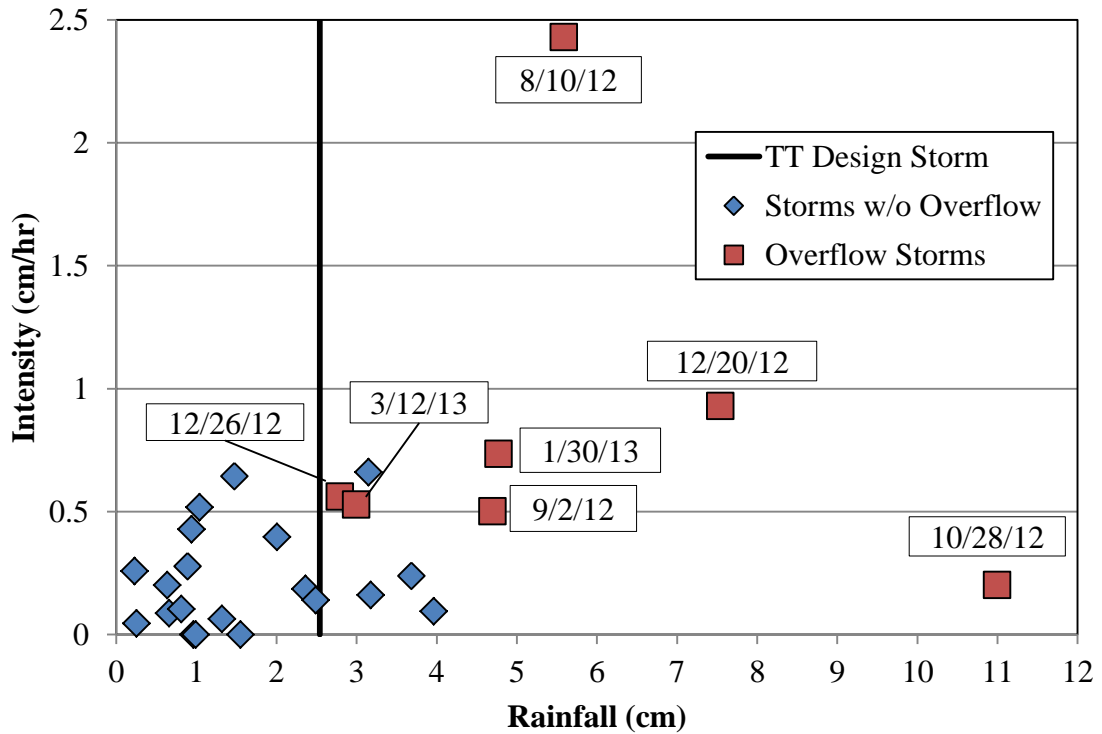


**Figure J.31 - Intensity ( $i_2$ ) vs. rainfall for each storm**

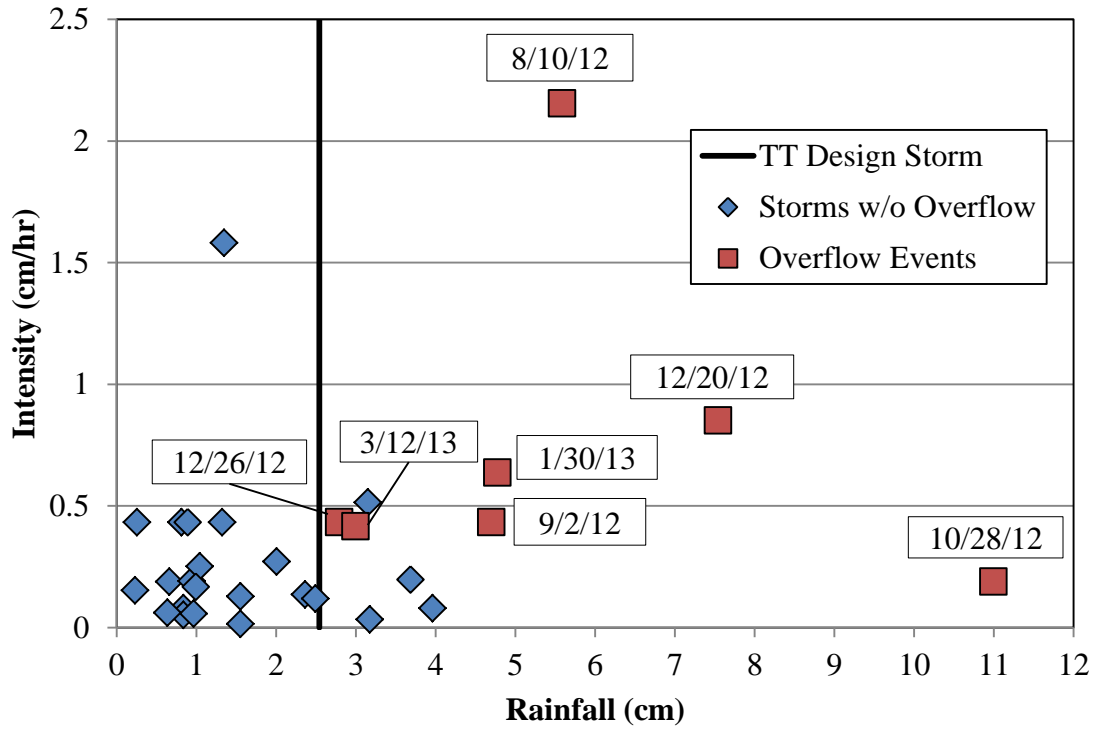


Figure J.32 - Intensity ( $i_3$ ) vs. rainfall for each storm